Nagra
Nationale
Genossenschaft
für die Lagerung
radioaktiver Abfälle

Cédra
Société coopérative
nationale
pour l'entreposage
de déchets radioactifs

Cisra
Società cooperativa
nazionale
per l'immagazzinamento
di scorie radioattive

TECHNICAL REPORT 83-27

GEOCHEMICAL AND ISOTOPE CHARACTERIZATION OF THE STRIPA GROUNDWATERS PROGRESS REPORT

L. CARLSSON
T. OLSSON
J. ANDREWS
J.-CH. FONTES
J.L. MICHELOT
K. NORDSTROM

FEBRUARY 1983

Parkstrasse 23 5401 Baden/Schweiz Telephon 056/20 55 11

Nagra
Nationale
Genossenschaft
für die Lagerung
radioaktiver Abfälle

Cédra
Société coopérative
nationale
pour l'entreposage
de déchets radioactifs

Cisra
Società cooperativa
nazionale
per l'immagazzinamento
di scorie radioattive

TECHNICAL REPORT 83-27

GEOCHEMICAL AND ISOTOPE CHARACTERIZATION OF THE STRIPA GROUNDWATERS PROGRESS REPORT

L. CARLSSON
T. OLSSON
J. ANDREWS
J.-CH. FONTES
J.L. MICHELOT
K. NORDSTROM

FEBRUARY 1983

Parkstrasse 23 5401 Baden/Schweiz Telephon 056/20 55 11

Das Stripa-Projekt ist ein Projekt der Nuklearagentur der OECD. Unter internationaler Beteiligung werden von 1980-84 Forschungsarbeiten in einem unterirdischen Felslabor in Schweden durchgeführt. Diese sollen die Kenntnisse auf folgenden Gebieten erweitern:

- hydrogeologische und geochemische Messungen in Bohrlöchern
- Ausbreitung des Grundwassers und Transport von Radionukliden durch Klüfte im Gestein
- Chemische Zusammensetzung des Grundwassers in grosser Tiefe
- Verhalten von Materialien, welche zur Abdichtung von Endlagern eingesetzt werden sollen

Seitens der Schweiz beteiligt sich die Nagra an diesen Untersuchungen.

The Stripa Project is organized as an autonomous project of the Nuclear Energy Agency of the OECD. In the period from 1980-84 an international cooperative programme of investigations is being carried out in an underground rock laboratory in Sweden. The aim of the work is to improve our knowledge in the following areas:

- hydrogeological and geochemical measurement methods in boreholes
- flow of groundwater and transport of radionuclides in fissured rock
- geochemistry of groundwater at great depths
- behaviour of backfill material in a real geological environment

Switzerland is represented in the Stripa Project by Nagra.

Le projet Stripa est un projet autonome de l'Agence pour l'Energie Nucléaire de l'OCDE. Il s'agit d'un programme de recherche avec participation internationale qui sera effectué entre 1980 et 1984 dans un laboratoire souterrain en Suède. Le but de ces travaux est d'améliorer et d'étendre les connaissances dans les domaines suivants:

- mesures hydrogéologiques et géochimiques dans les trous de forage
- écoulement des eaux souterraines et transport des radionucléides dans les roches fracturées
- chimie des eaux souterraines à grande profondeur
- comportement dans un environnement réel des matériaux de bourrage pour dépôts de déchets radioactifs

La Suisse est représentée dans le projet Stripa par la Cédra.

GEOCHEMICAL AND ISOTOPE CHARACTERIZATION OF THE STRIPA GROUNDWATERS - PROGRESS REPORT

Leif Carlsson
Swedish Geological, Göteborg, Sweden

Tommy Olsson
Geological Survey of Sweden, Uppsala, Sweden

John Andrews
University of Bath, Bath, UK

Jean-Charles Fontes
Universite, Paris-Sud, Paris, France

Jean L. Michelot
Universite, Paris-Sud, Paris, France

Kirk Nordstrom
United States Geological Survey, Menlo Park, USA

February 1983

CONTENTS

ABSTRACT

This progress report contains the recent results of the hydrogeochemical program, a part of the hydrogeological investigations at the Stripa test site. A considerable number of groundwater samples have been collected and analyzed for major dissolved cations, anions, trace elements, stable isotopes, radioisotopes and dissolved gases to depths approaching 900 m. This report presents (1) the background geology and hydrogeology (2) major and trace element characteristics of the deep groundwaters (3) major radioelement characteristics and inert gases (4) stable isotopes of water and dissolved sulfate and (5) preliminary interpretations of the groundwater chemistry trends. As the studies at Stripa are still in progress, all interpretations are considered tentative and preliminary. Any conclusions drawn may be modified as a consequence of continued sampling and analysis.

1 GEOLOGICAL AND HYDROGEOLOGICAL CHARACTERIZATION OF THE STRIPA GRANITE

1.1 GENERAL

Hydrogeological investigations in boreholes is one of the main programs included in the current Stripa Project. The purpose of these investigations are as follows:

1. Methodology development for hydrogeological and hydrogeochemical investigations in subsurface, nearly horizontal and vertical boreholes.

2. Instrumentation and equipment development in subsurface, nearly horizontal and vertical boreholes.

3. Hydraulic, chemical and isotopic characterization of the Stripa granite and groundwaters.

The work is carried out according to the defined program presented by Carlsson, et al (1981). During autumn 1981, the program was modified due to results from the drilling of borehole V1. The present program diverges from that originally defined in that sense that it has been expanded by the inclusion of a second vertical borehole - V2. The vertical hole V1 was terminated at its present length of 505 m. This modification gives a test lay-out which is more suitable to the actual geological conditions obtained in the test area. Thus the continued investigations are made

in the following four boreholes:

V1, a 505 m deep vertical borehole
V2, a 822 m deep vertical borehole
N1, a 300 m long subhorizontal borehole
E1, a 300 m long subhorizontal borehole

In the vertical holes, priority was given to the hydrogeochemical studies and a minor program for the hydraulic testing will follow the hydrogeochemistry. The program for hydrogeochemical sampling, analyses and evaluation was also slightly been revised. The investigations are performed by the Principal Investigators. A group consisting of experts in the field is formed to advise and to make analyses and interpretations in the hydrogeochemistry. The members in the group are:

John Andrews	UK
Erik Eriksson	Sweden
Ted Florkowski	IAEA
Jean-Charles Fontes	France
Peter Fritz	Canada
Heinz Loosli	Switzerland
Heribert Moser	West Germany
Kirk Nordstrom	USA

This report presents the progress with the hydrogeochemical program, analytical results and preliminary interpretations based on the chemical data obtained so far.

1.2 TEST SITES

The program for hydrogeological investigations in boreholes is carried out at two specific test sites down in the mine. At the SGU-site, which is the main site, three boreholes were drilled, one

vertical (V1) and two subhorizontal (N1 and E1). This site is located at the 360 m level. A fourth vertical borehole was drilled from a second site at the 410 m level. This borehole is the old borehole Dbh V1 made during the SAC-period and presently deepened down to a total depth of 822 m i.e. 1230 m below the ground surface. The locations of these sites and boreholes are shown in Figure 1.1.Data on the boreholes is given in Table 1.1. In addition to these boreholes a number of other holes in the SAC-area were used for minor tests and water sampling. Water sampling was also

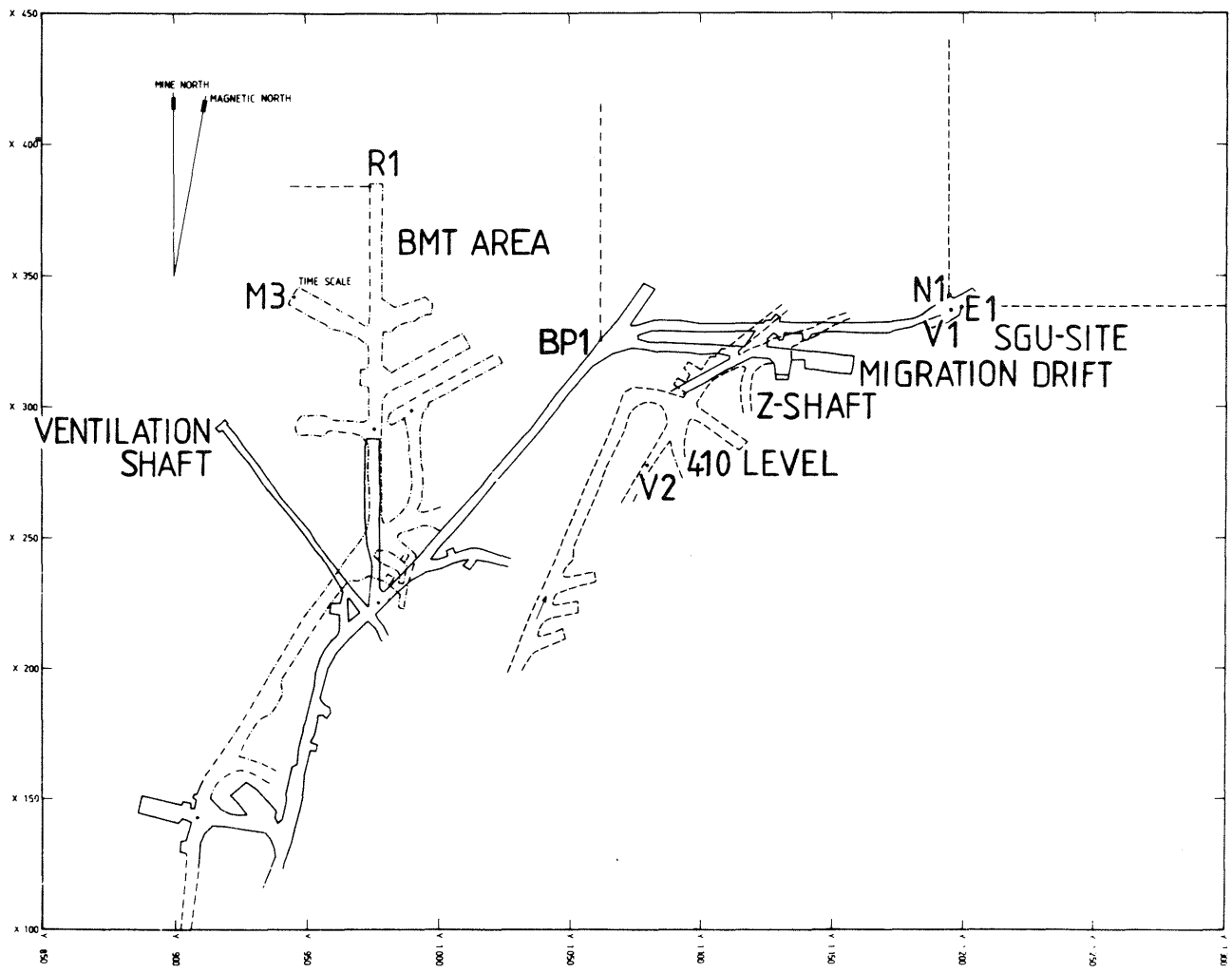

Figure 1.1 The investigation areas in the Stripa Mine with the boreholes used for water sampling.

conducted in private wells at the surface and from surface water schemes.

Table 1.1. Data on the main boreholes included in the hydrogeological program.

Bh no	Diameter	Collar coordinates			Length
	mm	X	Y	Z	m
V1	76	336.8	1195.7	356.7	505.9
V2	56	270	1075	407.7	822.0
N1	76	342.2	1194.6	355.5	300
E1	76	338.4	1199.7	355.7	300

1.3 GEOLOGY

1.3.1 Lithology and petrology

The target rock for all investigations in the Stripa Mine is a rather small intrusive body of granite - Stripa granite, which predominantly is a grey to reddish, medium-grained granitic rock type of Precambrian age. The Stripa Granite occurs at the surface in a belt of older supracrustal rocks with structures striking mainly in a NE-SW direction. The Stripa granite is generally unfoliated, which indicates a relatively mild tectonism after its formation. The largely concordant nature of the granite is not uncommon. Many postorogenetic granites in the Stripa region have been mapped as elongated intrusions parallel to the structures of the supracrustal belts (Koark and Lundström 1979).

Leptite, a strongly metamorphosed sedimentary rock, normally of volcanic origin, is the dominant rock type in the supracrustal formation. The regional distribution of the different rock types

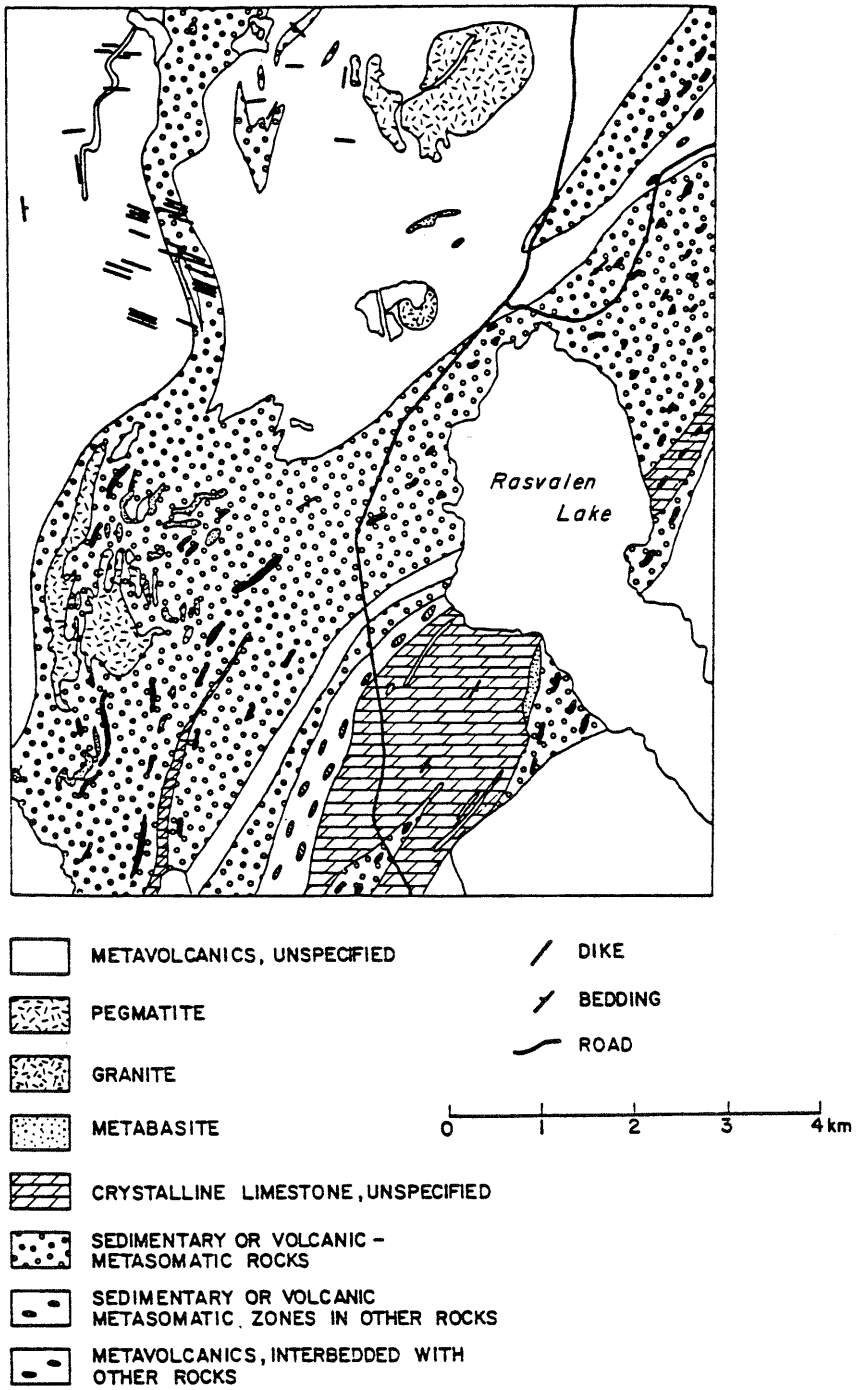

Figure 1.2 Geologic features of the Stripa area (Gale 1982).

is in a broad geologic context shown in Figure 1.2.

The main features of the configuration of the contact between the leptite syncline and the granite is illustrated in Figure 1.3, based on the data obtained from the mine workings and investigations in the SAC-program. The contact between the leptites and the granite is transected by the access drift to the hydrogeological test site at the 360 m level, approximately 300 m SSE from the ventilation shaft. The intrusive granite penetrates the metamorphic basement there as a thin veneer. In common the granite at the contact occurs partly as inclusions or dikes in the leptite. The granite surrounds the leptites in the Stripa syncline in the north-eastern part of the mine. The limits of the subsurface extension of the granite to SE is partly shown by the prospecting boreholes Pjt 3 and Pjt 3B as shown in the vertical section in Figure 1.3. This section is taken perpendicular to the contact, i.e l.in a NW-SE direction. The location of the section is indicated in Figure 1.4.

The petrology of the Stripra granite was studied by Olkiewicz, et al (1978, 1979), Koark and Lundström (1979) and Wollenberg, et al (1980). In the different reports the granite was named monzonite, monzogranite or granite, however, the term granite is used in the current report.

The matrix of the granite consists of approximately 34-45 volume-% of quartz, 35-40 % of partly sericitised plagioclase, 15-20 % of microcline and around 5 % of muscovite and biotite (altered to chlorite). Assessory opaque minerals, garnets and probably zircon also occur (Olkiewicz, et al 1979 and Wollenberg et al 1980).

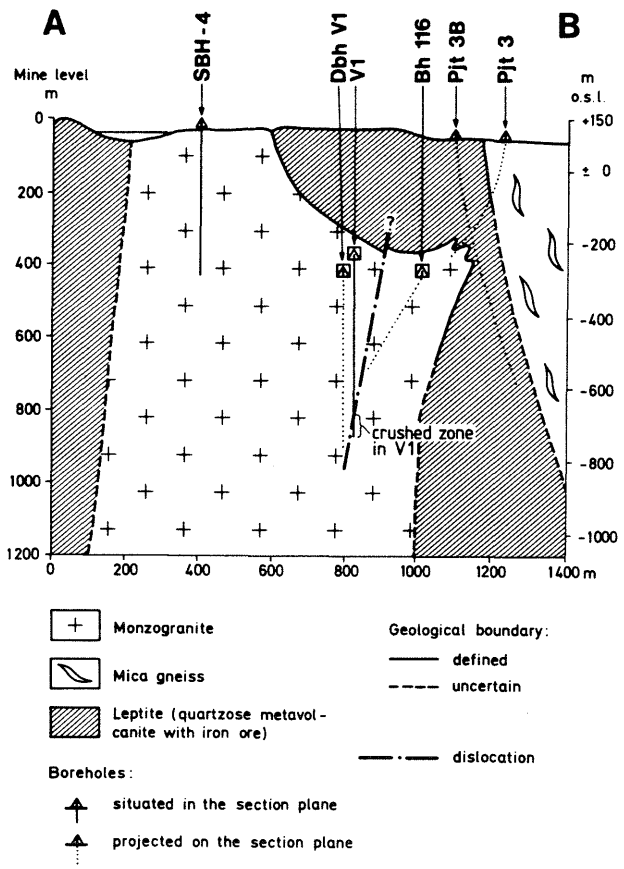

Figure 1.3 Vertical section through the investigation area. The location of the section is shown in Figure 4.

Oligoclase is the probable species of plagioclase present in the granite. Microcline is commonly perthitic or microperthitic. Commonly the microcline is interstitial to quartz and plagioclase (Wollenberg, et al 1980). Hematite is in some places dispersed as fine dust within the feldspar grains, particulary plagioclase, or along grain boundaries or cracks within the grains. The red colour in many of the granite samples is due to the occurence of hematite (Wollenberg, et al 1980). Veins of pegmatite and aplite are common in the granite.

A common texture of the Stripa granite is the abundance of fractures, both continous and discontinous on a microscopic scale. Even in relatively

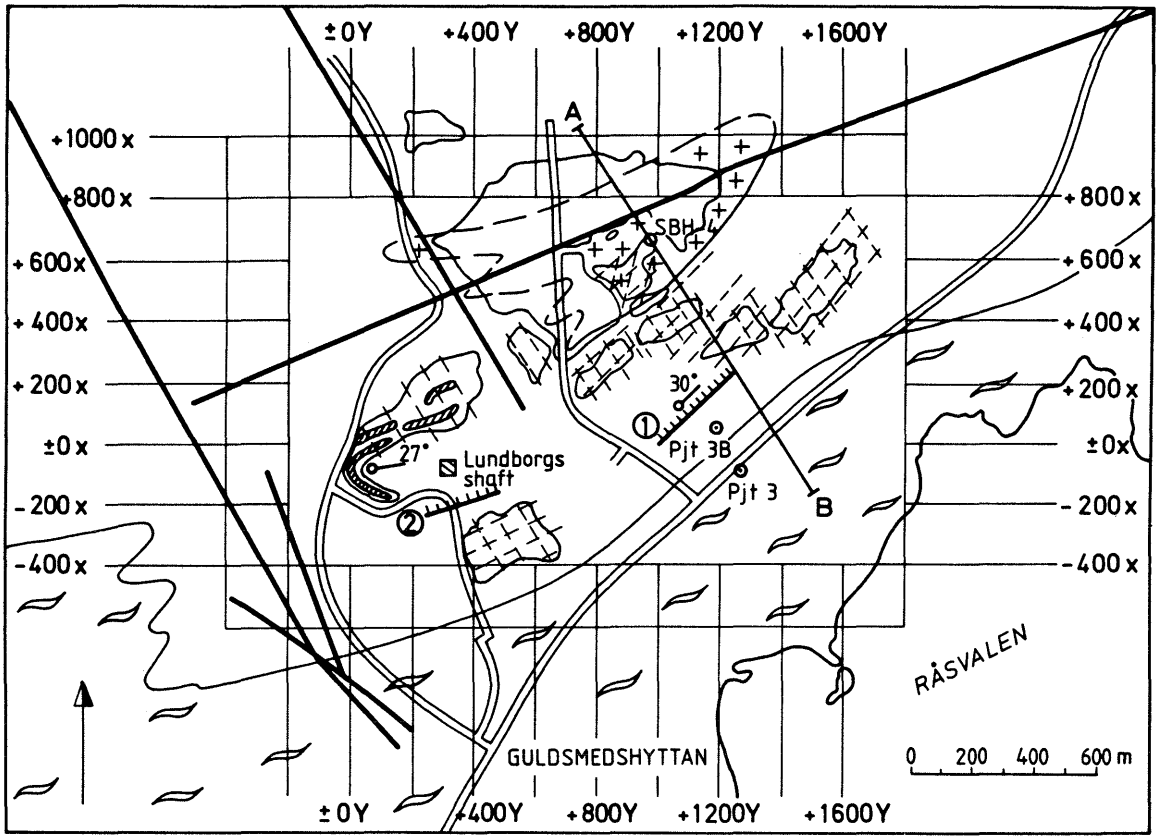

Monzogranite

Mica gneiss

Leptite with iron ore

Areas of exposed bedrock with predominating fracture pattern

① Dislocation at 410 m level

② Ottes - dislocation at 175 m level

⊙ SBH-4 Surface borehole

27° Synclinal axis of the leptite synform

A B Line of vertical section

+200 x Mine coordinates

Morphological lineament

Figure 1.4 Major structures in the Stripa area.

unfractured rock samples fine discontinous cracks within primary grains or along grain boundaries are common. These cracks are filled with intergrown chlorite and sericite or by quartz and feldspars and they frequently originate among primary

grains of the same minerals as those filling the cracks. This suggests that the crack fillings have not crystallized from fluids introduced from extraneous sources, but are due rather to remobilization and redeposition of primary components of the rock matrix (Wollenberg, et al 1980).

Another distinctive feature of the Stripa granite is the prevalence of cataclastic textures. Rather commonly there are evidences of movements along fracture surfaces or breccia zones as slickensides and fractures filled with a microscopically irresolvable clay-rich fault gouge and closing rounded fragments of granitic rock (Wollenberg, et al 1980).

Samples of Stripa granite and neighboring granitic rocks (Gusselby and Kloten massifs) were dated by potassium-helium method at the University of California, Berkeley (Wollenberg, et al 1980). The dates obtained were in millions of years 1691+-16, 1604+-14 and 1640+-44 for Stripa, Gusselby and Kloten respectively.

The leptite is usually a gray, red or grey-green to black, fine-grained foliated metamorphic rock (microschist) commonly cut by white or light green fractures. Mineralogically it is similar to the Stripa granite. Texturally, however, it does not resemble the granite, as it is finer, more even-grained and homogeneous. In detail, the leptite generally consist of a fine, even-grained mosaic of equant quartz with fewer plagioclase and microcline grains. Darker leptites generally contain more chlorite, at the expense of muscovite, than the lighter leptites, or they contain fewer porphyroblasts.

The contacts of leptite with Stripa granite was studied by Wollenberg, et al (1980) in thin sections. The contacts are generally sharp, possibly fault contacts. They show little sign of alteration such as might be expexted if the granite had intruded the leptite. The growths of sericite, or epidote-chlorite-filled fractures occur at the contact, in some places also opaque grains rich in uranium are associated with the contact.

Another variety of metamorphic rock at Stripa is a dark green fine-grained foliated rock rich in blue-green prismatic amphibole, usually logged as greenstone in core-logs. Texturally, it is a micro-schist like the more abundant leptite. However, its foliation is determined by amphibole prisms instead of chlorite and muscovite laths.

1.3.2 Radiogeology

The abundance of radioelements in the rocks was measured by Wollenberg, et al (1980). The fission-track radiographic method was used to determine the location and abundance of uranium in uncovered thin sections.

The Stripa granite is rather unique in its radio-element content, both in the abundance of elements and their ratios. Table 1.2 indicates the relatively high uranium and thorium contents of the granite, compared with other plutons in the region.

The measurements indicate that uranium is depleted in surface exposures of granite and leptite at Stripa, relative to its abundances in the same rock units underground.

Table 1.2 Radioelement contents (after Wollenberg et al 1980).

Rock type	No	Uranium ppm	Thorium ppm	Potassium %	Th/U
Stripa granite					
Surface	9	26.9±5.5	33.0±5.7	4.6±0.7	1.1±0.1
Underground	34	37.4±6.2	29.2±3.8	3.9±0.3	0.8±0.1
Leptite					
Surface	5	3.3±0.7	11.9±2.9	3.1±0.6	3.6±0.4
Underground	9	5.4±3.1	17.9±1.4	2.8±0.5	3.9±1.2
Regional rocks					
Granites	7	17.6±15.4	26.6±6.6	5.2±1.5	2.4±1.2
Metamorphic	5	6.1±1.5	14.6±8.7	2.5±1.1	2.6±1.9

In the Stripa granite, uranium is most highly concentrated in tiny opaque grains on the order of 50 micrometer in diameter, generally euhedral and in some places square in cross-section. These grains are usually found in chlorite, but also in muscovite-chlorite-sericite filled fractures, and even in cracks within quartz or feldspar. Usually the grains contain up to 5 % uranium, but concentrations up to 10-15 % have been observed (Wollenberg, et al 1980). Another locus of uranium concentration was observed in opaque grains with both a quartz-epidote-sericite-filled fracture on a contact between granite and leptite, and with fine carbonate-sericite stringers intersecting that contact on the granite side. Although the concentration of uranium is lower in these grains, on the order of 2 % U, the absolute abundance of uranium contained in them is greater.

Uranium is also found, in lower concentrations,

dispersed along chlorite-filled fractures without associated discrete grains. Concentrations are generally about 0.5 % or lower, but occasionally range up to 1.0 % uranium.

The Stripa leptite contains no appreciable discrete concentration of uranium either in the matrix or in a coarse epidote-filled fracture cutting it (Wollenberg, et al 1980). Uranium minerals were observed in chlorite-filled fractures cutting the iron ore at Stripa (Welin, 1964).

The heat production was calculated from the radio-elements of the Stripa pluton by Wollenberg, et al (1980). In table 1.3 the radiogenic heat production of the various rocks in the Stripa region are listed.

The Stripa granite averages 11.9 micro Watt per cubic meter. This should be compared with 2.8, considered to be the mean for granitic rocks (Heier and Rogers 1963) and 6.9 for the Bohus granite of southwestern Sweden (Landström, et al, in prep). The radiogenic heat production of the Stripa granite is four times that of the neighboring leptite and 1.75 times the heat production of other plutons in the region.

1.3.3 Fracturing of the Stripa granite

In Figure 1.4, the major structures in the Stripa area are visualized. The location of the section (Figure 1.3 above) is also included together with existing boreholes made from the ground surface. As regards the lineaments in the granite, it is seen that their direction generally is parallel to the syncline axis of the supracrustal formation.

Table 1.3 Radiogenic heat production of the rock in the Stripa region (Wollenberg, et al 1980).

Rock Type	No	Heat production μW/m
Stripa granite		
Surface	9	9.5
Underground	34	11.9
Leptite		
Surface	5	2.0
Underground	9	2.9
Regional rocks		
Granites	7	6.8
Metamorphic	5	2.8

The greater morphological lineaments diverges in direction from the syncline geometry, but may, however, also be governed by the configuration of the supracrustal rocks. Two dominant directions occur for the lineaments, i.e. ENE-WSW and NW-SE.

Based on both surface boreholes (SBH1 and SBH2) and subsurface holes (V1 and V2), the variation in frequency versus depth was studied. The variation with depth is shown in Figure 1.5. It must be noted that since V1 and V2 both are vertical, medium-steep and steep fractures will be underestimated. The fracture frequencies obtained in N1 and E1 are also included in the figure. These boreholes are more accurate measures of the steeply dipping fractures at the 360 m level.

A number of zones of fractured or crushed rock also exists in the granite. Normally these zones

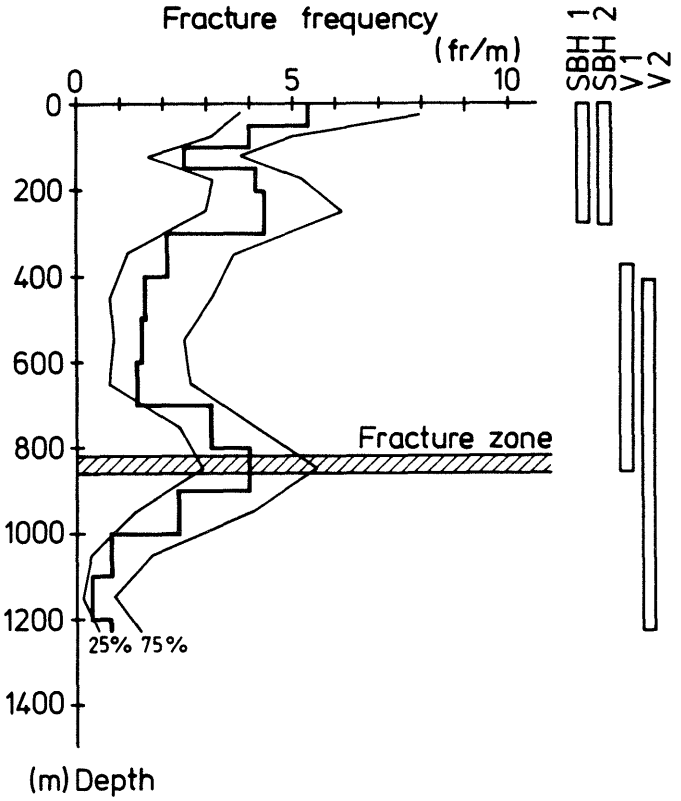

Figure 1.5 Fracture frequency versus depth based on core-logs from SBH1, SBH2, V1 and V2. The frequency is assumed to be log-normally distributed.

are thin, not exceeding 1 m in the cores, but a few zones are of several meters in thickness. A more extensive zone was found in the lowermost part of V1. Tectonically disturbed granite in the upper part of the borehole extends down to the 466 m depth and contains more widely spaced fracture zones and crushed zones usually less than 1 m in width. Fracturing tends to be more intense towards the bottom of this section, with a prominent increase in number of subvertical fractures.

A detailed compilation of fracturing is impractical for the strongly crushed part of the borehole (466 m down to the bottom of the borehole at 505 m). Totally 7.7 m of this section is disconnected or crushed to rubbles. The number of the fractures

in the crushed zone is partly based on an estimation (38 per cent from totally 510 fractures within this 40 m wide zone) and their dipping were not possible to establish. The fracture frequency was 12.9 fr/m in the zone to be compared to 1.5 fr/m for the rock mass above the zone.

The fracture zone in V1 has a high water inflow. The hydraulic conductivity is high in comparison to the rock mass and the zone is assumed to be of crucial importance for the groundwater system in the granite. However, the extension and orientation of the zone could be interpretaed according to different possibilities.

One of the possible interpretations of this zone is indicated in Figure 1.3. However, the zone was not found in V2 when this borehole was deepened down to a final depth of 820 m (1 230 m below ground surface). A cross-hole geohysical measurement was made between V1 and V2 and the result indicated that the major zone found in V1 was connected through three (possible four) minor zones intersected by V2. None of these zones showed, however, a fracturing in accordance with that found in V1.

Figure 1.6 shows a profile through the rock mass with the boreholes V1 and V2 in relation to the ore body. In this section a fracture zone found during the ore mapping is included. Its orientation is well defined in and around the ore body while its extension through V1 and V2 is hypothetical. The assumed extension is, however, indicated by the intense fracturing in the lowermost part of V1, but also of a somewhat more intense fracturing in the uppermost part of V2.

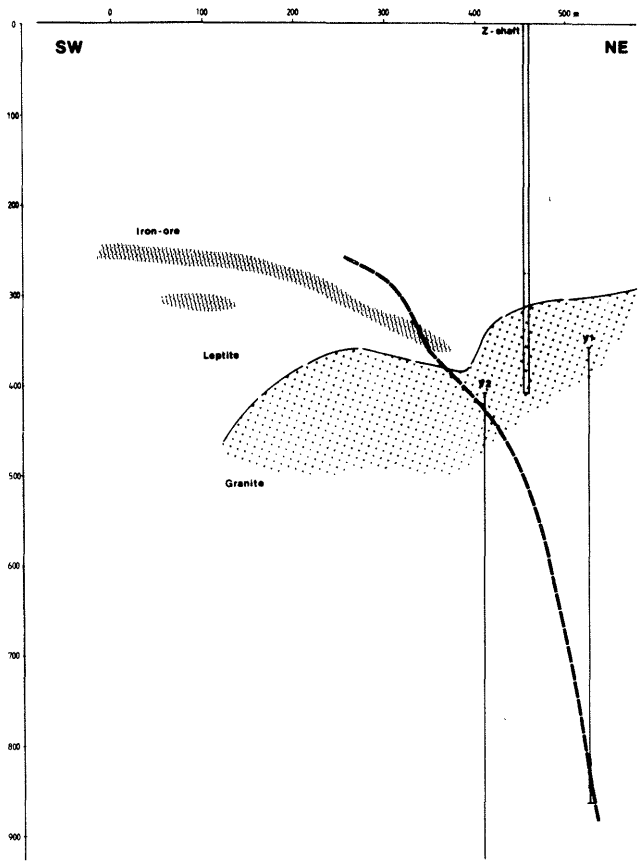

Figure 1.6 Vertical section through the investigation area.

This gives three probable explanations of the geometry of the fracture zone found in V1, none of which is more reliable than the others.

1. A zone striking N70E and dipping 60SE as indicated in Figure 1.3.

2. A zone striking NW-SE steeply dipping to NE as indicated in Figure 1.6.

3. The major zone is connected to V2 by a number of minor zones as indicated by geophysical measurements.

The actual interpretation may as well be a combination between any of the mentioned possibilities.

The mean fracture frequencies for the boreholes included in the hydrogeological program are given in Table 1.4.

Table 1.4 Fracture frequency in V1, V2, N1 and E1

Borehole	Fracture frequency
V1 (above the crushed zone)	1.5
V1 (crushed zone)	12.9
V2	2.1
N1	1.6
E1	4.7

Figure 1.7 shows a cumulative fracture diagram for V2 with regard to the dipping of the fractures. It is seen that medium steep fractures dominate while steeply dipping fractures have a low fracture frequency. Flat-lying fractures are in an intermediate position. This is in full agreement with the result obtained in V1 (Carlsson, et al 1981). It must be stressed that the vertical borehole V2 tends to underestimate vertical or steeply dipping fractures while sub-horizontal or flat-lying fractures are recorded with their actual frequency. With this in mind, it is clearly seen from Figure 1.7 that the steeply dipping fractures dominate and the relative frequency of these fractures increases with depth with a simultaneous decrease in flat-lying fractures. This is even more pronounced than illustrated in the figure owing to the variation in estimation depending on the dipping. The flat-lying fractures show a low frequency below approximately 400 m depth with 0.3 fr/m which decreases down to 0.1 fr/m in the lowermost 230 m. This condition indicates that medium steep or steep fractures dominate the fracture system at depth and the horizontal fracturing become more sparse.

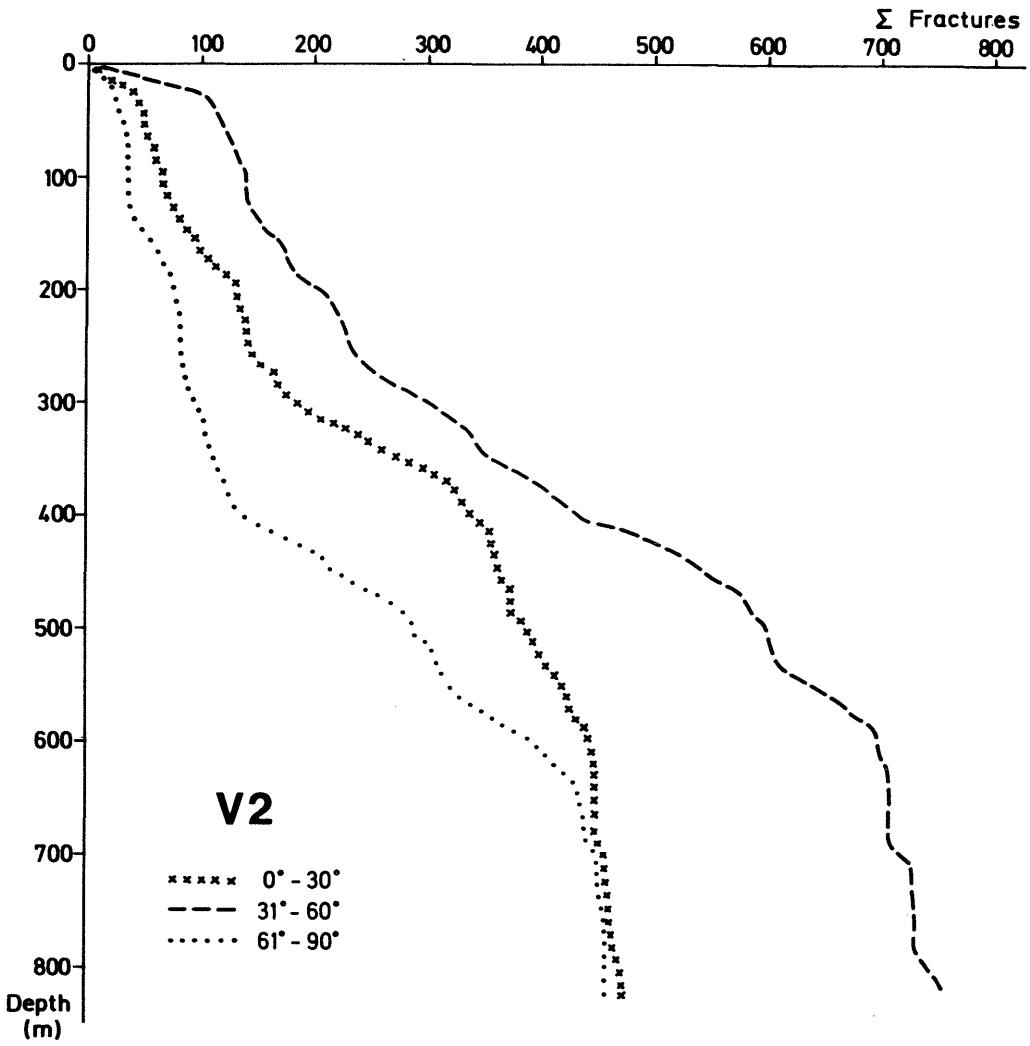

Figure 1.7 Cumulative fracture diagram for V2 with regard to dipping of the recorded fractures.

The fracture pattern which predominates in the rock mass at the SGU-site may be established by the fracture orientation data from the boreholes. The information from the boreholes N1 and E1 gives a rock mass dominated by steeply dipping fractures in N30E. Other fracture sets of importance are N30W and N10E, both steeply dipping. However, both of these boreholes are nearly horizontal, which indicates that flat-lying fractures will not be penetrated by the boreholes and consequently they will be underestimated. The vertical boreholes may serve as a tool to evaluate the existence of flat-lying fractures.

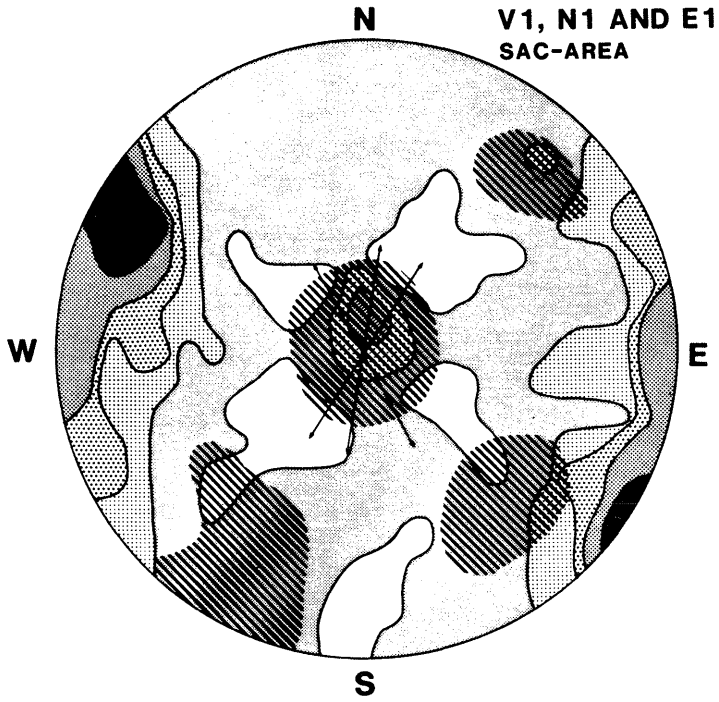

Figure 1.8 *Fracture sets obtained at the SGU-site and from the SAC-area (lined parts of the diagram). Semispherical projection, Schmidt net - lower hemisphere.*

Steep fractures dominate clearly the fracture pattern and make up as much as 40 per cent of all fractures in the rock mass adjacent to the SGU-site. Medium steep fractures makes up 31 per cent and the remaining 20 per cent are attributed to flat lying fractures. Thus it is possible to distinguish the following sets of fractures at the SGU-site.

1 N10E;80E
2 N30E;85E
3 N30W;90
4 Sub-horizontal;25

These sets are shown in the semispherical projection in Figure 1.8.

The obtained orientations from the SGU-area could be compared with the orientations found in the huge stock of fracture data which exists from the SAC-area (Wollenberg, et al 1980, Olkiewicz, et al 1979). In that area the following fracture sets were found:

1 NNW-SSE;60N
2 NW - SE;85NE
3 N65W;50SW
4 Horizontal

These sets are also included in Figure 1.8. As seen in the figure there is a difference between the fracturing at the SGU-site and at the SAC-area, but some resemblance may be found. The difference may be an effect of the sedimentary structures which could have effected the fracturing of the granite. This is also indicated in Figure 1.4. There seems to be a swing in orientation of the fracture system which probably is governed by the configuration of the leptite syncline. Closer to the contact between granite and leptite the fracturing is affected by the syncline, while at farther distances it seems to be more independent with increased upright and orthogonal fracturing of the granite.

1.3.4 Fracture fillings

All boreholes in the hydrogeological program show similar characteristics regarding the existing fractures. Detailed fracture logs are given in previous reports on the core logs (Carlsson, et al 1981, Carlsson et al 1982a and 1982b). The recorded fractures may be classified into on or of fine different groups;

1 Fractures with fresh, uneven surfaces
2 Open or sealed fractures
3 Small-scale shear zones
4 Brecciation and granulation of the granitic matrix
5 Quartz veins

Except for the fractures included in the first group, all other are characterized by the existence of coating minerals or weathering indications on the fracture surfaces. The fracture filling minerals were megascopically classified on the basis of colour, hardness and appearence of carbonates. As pointed out by Wollenberg, et al (1980), it is normal that different fracture filling minerals are intergrown in a varying combination which makes the megascopical classification somewhat uncertain. An extra check was therefore made by using X-ray diffraction on five samples taken from the V2 core.

The result of this test showed that the plagioclase mixing with epidote was much more common than expected. The conclusion which may be drawn from this result is that plagioclase in general have been underestimated.

Chlorite, which is the most common fracture filling mineral, is very dark, almost black, and much harder than normal due to mixing with epidote and plagioclase. Also, the epidote shows many types of colour variations in the green colour spectrum when mixed with plagioclase.

Sericite, commonly intergrown with chlorite, is nearly as common as chlorite. Next to chlorite (and sericite), calcite is the most common fracture filling mineral. Its occurrence ranges from fillings of hairline cracks and thin coatings

and intergrowns with other minerals to coarse crystals grown in the spacings of large fractures.

Epidote occurs commonly in fractures, veins and shear zones, which are sealed in the core, associated with quartz, chlorite and sericite. Other fracture filling minerals identified in the cores include pyrite, fluorite, iron oxides and zinc sulphide. The great majority of the fracture infillings are less than 1 mm in width.

Borehole V2 penetrates the mostly deep-seated rock mass and it was therefore of interest to study the variation in mineral coatings versus depth. The result of this study is summarized in Figure 1.9, where it is seen that the coating of chlorite and chlorite/calcite-mixing are about constant throughout the full length of the borehole. The most striking change with depth is that the calcite shows a marked decrease at 250 - 450 m depth with a simultaneous increase in epidote. Each of the chlorite, calcite and epidote coatings make up about 25 - 30 per cent of all coated surfaces. The group of other minerals form a complex group with great variety. Pyrite, fluorite, iron oxides, zinc sulphide and clay are examples of coatings within this group.

The mentioned conditions are generally in agreement with the results reported by Wollenberg, et al (1980), which is based on megascopical classifications, X-ray diffraction analyses and analyses on thin sections.

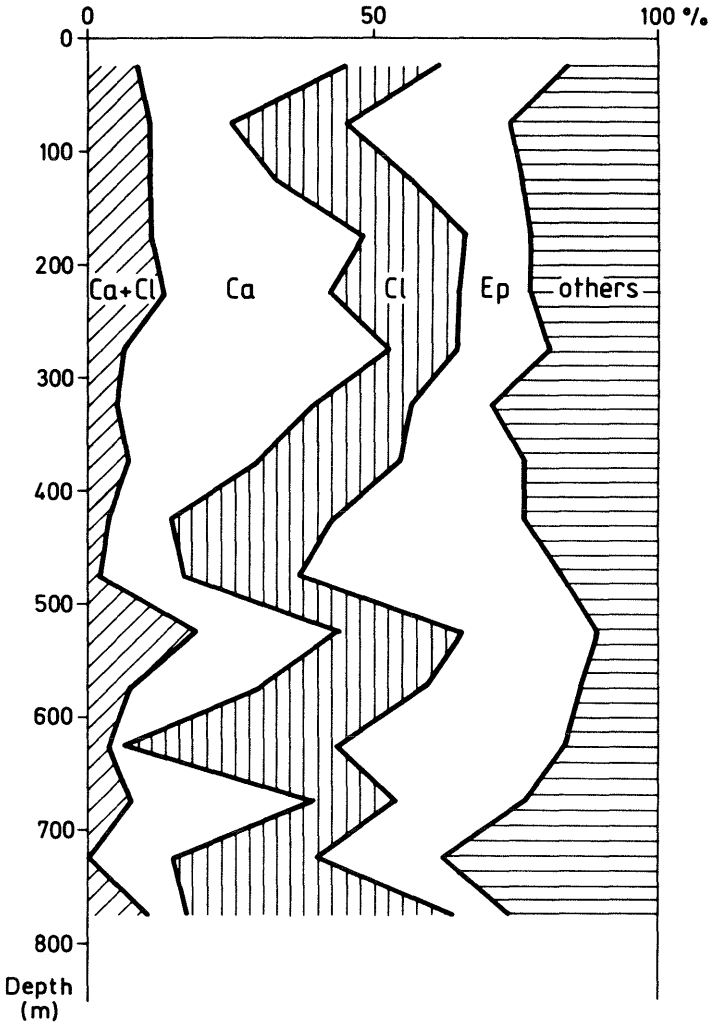

Figure 1.9 Distribution of coating minerals in V2 versus depth.

1.3.5 The Stripa ore

Stripa was, according to old registrations, first mined during 1448-1470 and 1551-1578. After years of no activity mining was again reestablished 1634-1771 (Paulsryd, 1941). In the 1780:s mining started in larger scale, but it was first during the present century that the mining went deep underground and as late as 1930-1960 the deeper parts were mined.

The ore deposits occur mainly as two bodies called the Main and the Parallel ore body respectively. The Main body with a maximum thickness of 16 to 17

meters is folded into the syncline with an undulating eastward pitch. Both the ore bodies are surrounded by the leptite.

The iron-ore is mainly a quartz-banded hematite, but magnetite ore occurs also. The skarn-minerals associated with the ore are mainly actinolite, diopside and epidote. Pyrite occurs locally and is evidently of secondary origin (Geijer, 1938). The iron-ore in the Main ore body has a higher content of Fe than the ore in the Parallel body. In Table 1.5 the general composition of the two ore bodies is given.

Table 1.5. General composition of the two ore bodies at Stripa (Paulsryd, 1941)

Body	Fe %	P %	S %
Main	50	0.007	0.016
Parallel	41	0.009	0.037

The hematite of the ore bands is developed as grains of 0.2-0.6 mm, slightly elongated in the plane of bedding. The porphyroblastic magnetite may reach up to 15 mm, but the normal size is from 0.5 to 5 mm. Most of the magnetite ore in Stripa seems to occur in connection with a secondary enrichment process that resulted in a very rich, coarsely crystalline magnetite ore (Geijer, 1938). Most of the high-grade magnetite occurs within a marked syncline, from which fault zones diverge striking in ENE.

The type of folding and associated faulting movements that is represented by the Stripa deposit is typical of what could be encountered in large

portions of the ore-bearing region of Central Sweden. On the whole the folding of the Stripa deposit has been comparatively small. There is little interior deformation within the ores, in spite of the normally incompetent character of the quartz-banded ores.

The faulting movements that apparently accompanied the folding exhibit a variety of types. One type appear to be accentuations of folds, through slipping along contact planes. Echelon displacements in the different ore bodies belong to this type also. Usually these displacement zones strike E, that is in slight angle to the fold-axis. Another related type is interpretated as due to shearing movements. Movements along well-defined, steeply dipping fault planes are represented by most disturbances of this group in the main ore body. They usually are parallel to the fold axis. Movements along these faults appear to have been in the form of overthrusts and there are, in some cases, indications that the horizontal component is greater than the vertical one (Geijer, 1938).

Later sets of faults, separated in age from those described, are associated by such geological events as the intrusions of basic rocks and of granite aplite. These faults are usually steep dipping and their orientations differ. However, the most common orientation is almost perpendicular to the fold axis and also towards NE. Usually the displacements have a larger vertical than horizontal component. According to Geijer (1938), the vertical component is usually not exceeding a few meters.

1.4 HYDROGEOLOGY

1.4.1 Hydraulic units

The hydraulic conditions of a crystalline rock mass such as the Stripa granite is partly characterized by the existing discontinuities which intersect the rock. The granitic rock matrix is from a practical point of view, almost impervious and the main flow paths are constituted by the fracture system, zones of fractured or crushed rock and other structural discontinuities. As shown in previous sections, there exists a number of discontinuities, some of which are associated with the synclinal structure of the sedimentary sequence and others more independent of it. However, as the dominant tectonization took place before or immediately at the intrusion of the pluton, the granite is intersected only by a few larger fracture zones.

The dominant ruptural deformation is concentrated in the superficial part of the rock, which shows a rather high fracture frequency and a high hydraulic conductivity. This more fractured part of the rock mass extends down to about 250 m depth. Below this level the rock becomes more sparsly fractured, with fractures which are sealed to a great extent. The fracturing continue to decrease and reaches its lowest frequency below the 1100 m level (c.f. Figure 1.5).

In the deep-seated rock mass the water flow seems to be channelled in a few zones of fractured rock, where the zone found in the lowermost part of V1 is an extreme example of these flow paths. At these deep levels it is probable that the discrete fracture flow is of minor importance.

The mine itself is one of the most important structures governing the water flow in the area. It acts as a drain, with a drainage threshold which was successively lowered as the mining continued. During the SAC-program efforts were put into the establishment of the draining effect of the mine. As reported by Gale (1982) piezometric recordings taken at different levels in SBH-1, SBH-2, SBH-3 and DbhV1 show that there is a downward gradient above the excavations. Around the test areas, the groundwater gradients are directed towards the excavations.

1.4.2 Hydraulic conductivity of the rock mass

A great number of hydraulic tests have produced values on the hydraulic conductivity of the Stripa granite. Tests exist from the surface boreholes as well as from subsurface holes in different test sites, from the large scale ventilation test and from the large scale injection test. This huge stock of values provides a good base for determinations of the water flow in the granitic rock mass around the mine. Table 1.6 summarizes the range in results from the SAC-program.

Thus, it is seen that in the surface boreholes the conductivity is at its maximum, about 5 E-8 m/s, while it is 1 E-9 m/s or lower in the tests made down in the mine. The large scale tests, ventilation and injection tests, which both are measures of the gross conductivity gave low values, 1 E-11 and 4 E-11 respectively. Those latter values are probably representative for the rock mass including minor zones of fractured rock.

A number of hydraulic tests were also made in the current program, in V1 of the fractured zone, and

Table 1.6. Hydraulic conductivity of the rock mass

Test type	Conductivity range m/s	Reference
Injection SBH	5 E-11 - 5 E-8	1
Injection RH and HG	1 E-12 - 1 E-9	2
Ventilation test	1 E-11	1
Large scale injection	4 E-11	3

References:
1. Witherspoon, Cook and Gale (1980)
2. Gale (1982)
3. Lundström and Stille (1978)

in V2, N1 and E1 of selected zones. The tests in this program were all made as pressure build-up tests, where the natural water flow into the boreholes was used for the build-up. The test were analysed according to conventional interpretation techniques. The results of the tests made up to now are summarized in Table 1.7.

Table 1.7. Hydraulic conductivity values of different hydraulic units obtained by pressure build-up tests in V1, V2, N1 and E1.

Bh no	Hydraulic conductivity m/s
V1 Fractured zone	7 E-8
V1 Rock mass	5 E-11
V2 Rock mass	1 E-10
E1	5 E-12 - 4 E-8

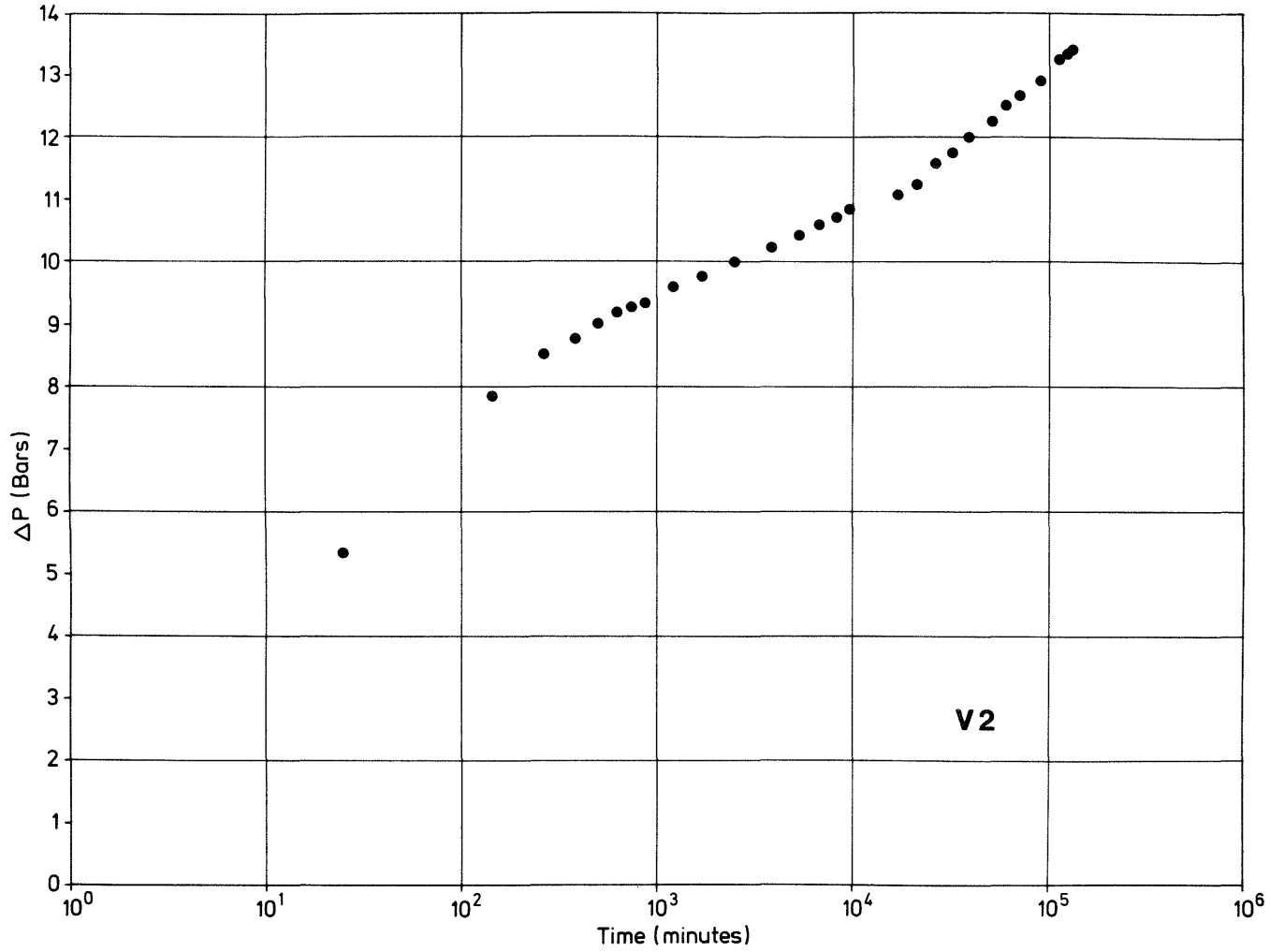

Figure 1.10 Pressure build-up test in V2.

Two zones have been found with relatively high conductivity, one 40 m wide zone in V1 (40 m along the borehole) with a conductivity of 7 E-8 m/s (T = 3 E-6 m^2/s) and one 2 m wide zone in E1 with 4 E-8 m/s (T = 7 E-8 m^2/s). Beside these zones, the conductivity is lower than E-9 m/s.

1.4.3 Hydraulic head

The hydraulic head in the rock is, in principal determined by geological, hydrometeorological and topographical factors. In the current situation it is also, to a very high degree dependent on the geometrical configuration of the mine.

The hydrometeorological conditions in the Stripa area can on an annual basis be described by a mean precipitation of 780 mm, an annual evapotranspiration of 480 mm and a run-off of 300 mm (9 l/s sq.km). The climatic conditions are humid and in the run-off term both the recharge and the discharge of groundwater are included.

The geological factor, which determines the hydraulic conductivity and thus the rate of the groundwater flow, in the bedrock as described in section 1.4.2 points to a rather low conductivity and a low groundwater flow even at high hydraulic gradients. Thus, in combination with the hydrometeorological factor, the conditions are such in the upper part of the bedrock that the groundwater level in general follows the topography.

The hydraulic head has been measured in borehole both from the mine and from the ground surface. The mine itself acts as a sink and its influence on the head is obvious. Measurements of the head are normally made in short sections in boreholes tightly sealed off by packers. When starting such measurements the head was usually in a transient state and the registration had to be carried out under a longer period.

Registrations of hydraulic head in boreholes have been carried out by Olkiewicz, et al (1979), Witherspoon, et al (1980) and Gale (1982). In

Table 1.8 the head from the different registrations are compiled.

Table 1.8. Measurements of hydraulic head in an around the Stripa mine

Borehole	Number of measurements	Head range m a s l	Remarks	Ref
SBH-1	16	-43 - +165		2
SBH-2	4	+125		2
SBH-3	20	+47 - +120		2
Dbh-2	8	-109 - - 24		1
DbhV1	22	-257 - - 80		1
Bp1	1	- 39		
E1	1	-154	not steady state	
N1	1	+ 1		
V1	1	-143	not steady state	
V2	1	-129	not steady state	

1. Olkiewicz, et al 1978
2. Gale 1982

1.4.4 Calculations of groundwater conditions and water inflow to the mine

Based on available data on hydraulic conductivity a preliminary and rougn calculation was made of the groundwater conditions and the groundwater inflow to the mine. The calculation was performed for a vertical plane laid out from the middle of lake Rosvalen, through the mine and further on about 3.5 km towards NNW.In total the section was 7 km in length and 2.6 km in depth. The mine was simulated by as two horizontal drifts, each 1000 m

Table 1.9. Results of numerical calulations of the distance of influence and the groundwater inflow to the mine

Assumptions made regarding the K-value of the rock mass	Horizontal distance for 50 m influence at the mine level of 400 m, in km	Groundwater inflow to the mine in l/min
Case A Hom. condition with K=1. E-9 m/s	0.8	73 l/min
Case B Hom. condition with decreasing K-value	0.45	96 l/min

in length, at the levels 410 m and 290 m respectively in the mine system. The height of the drifts was taken as 70 m.

The calculations were carried out using the finite-element program GEOFEM-G and assuming two-dimensional flow at steady state. The lower and vertical boundaries of the studied plane were set as no flow boundaries. The groundwater head at the upper boundary was given as the ground-surface. At the mine the head was set as the datum level.

As results of the calculations the head distribution around the mine was given together with the inflow to the mine. The calculations were performed in a vertical plane and the total inflow to the mine was estimated by assuming the same inflow per m of mine along the whole mine.

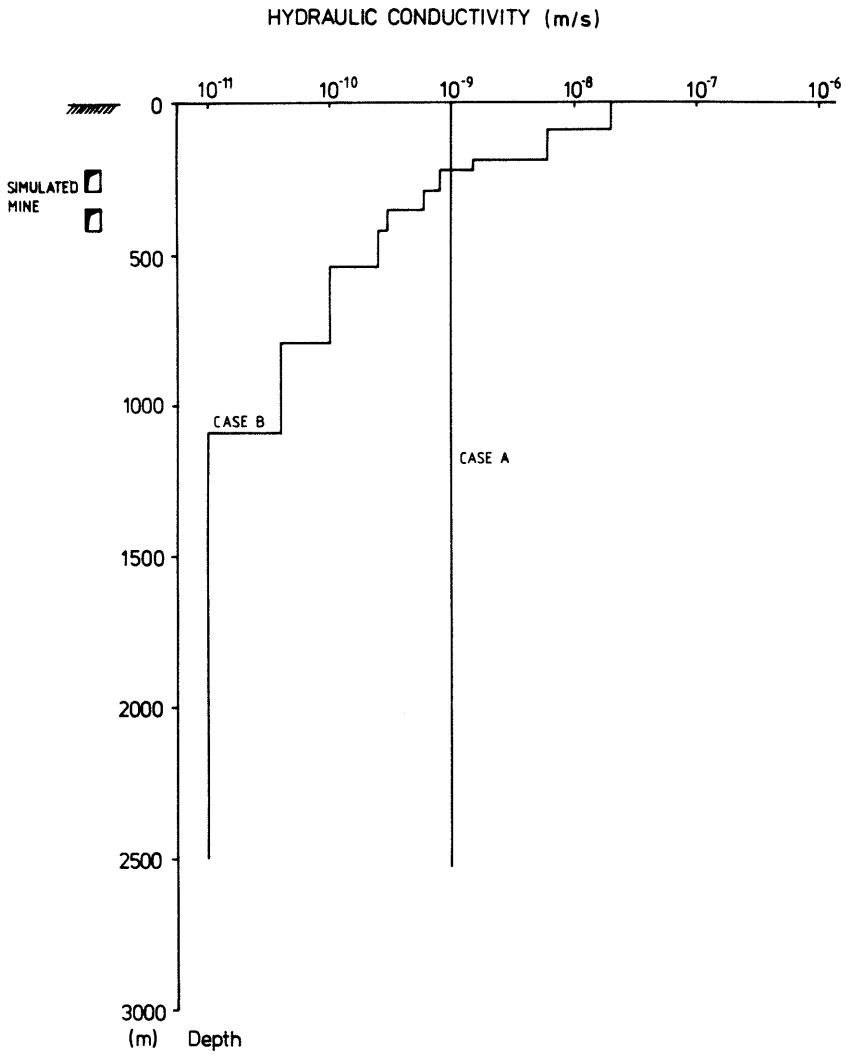

Figure 1.11 Hydraulic conductivity versus depth used in the model calculations.

performed in a vertical plane and the total inflow to the mine was estimated by assuming the same inflow per m of mine along the whole mine.

The hydraulic conductivity of the rock mass was given different values to illustrate different possible conditions in the rock. The conductivity distribution versus depth is given in Figure 1.11. The results of the calculation given as distance of influence on the head and the water inflow are summarized in Table 1.9.

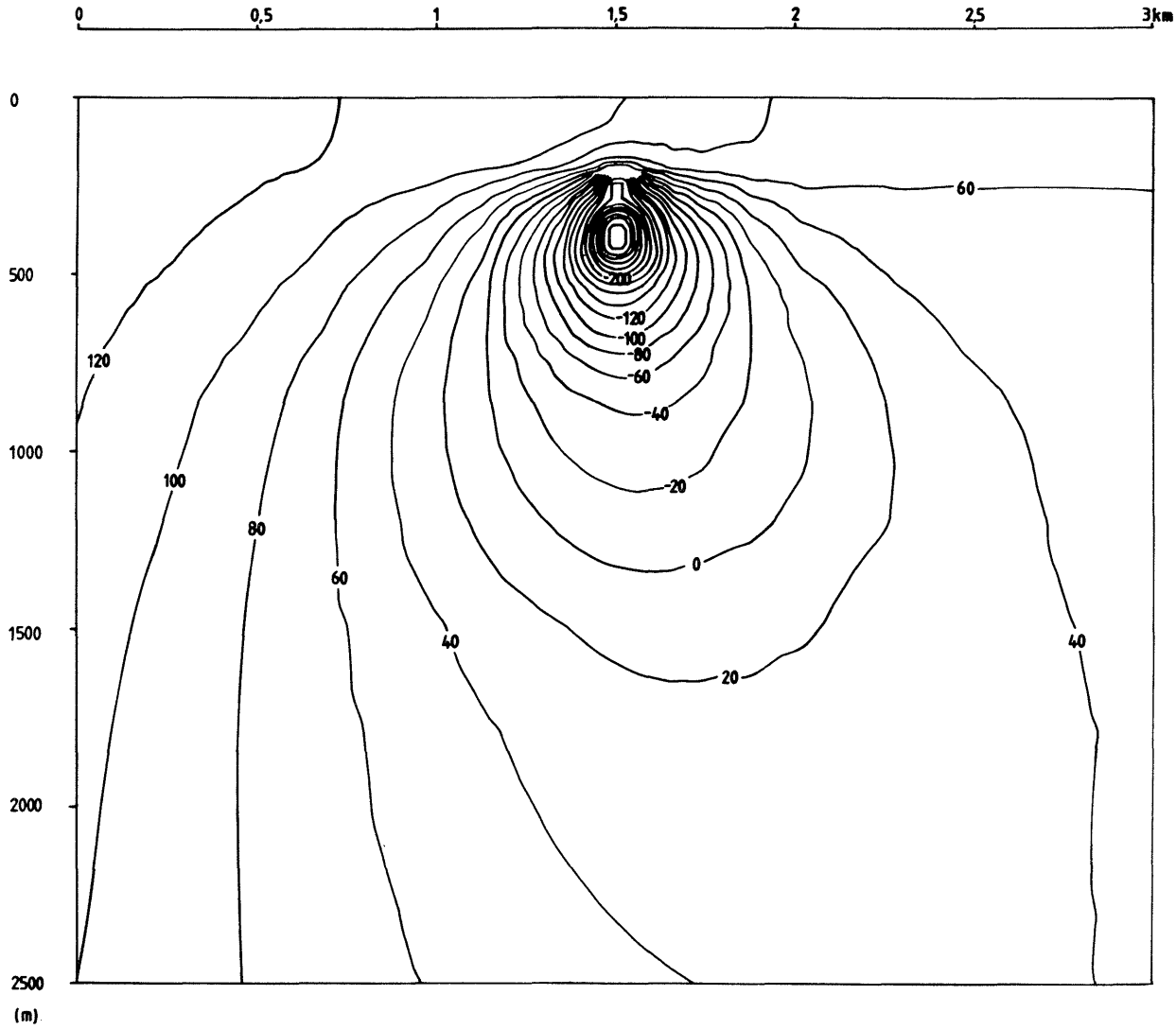

Figure 1.12 Groundwater head around the mine calculated by numerical method, case B.

The latter results based on decreasing conductivity values versus depth (Case B) are more reliable as it is based on actual test results from the area. The groundwater head for this distribution is given in Figure 1.12, where the impact of the mine is clearly visualized.

2 HYDROGEOCHEMICAL INVESTIGATIONS AT THE STRIPA TEST SITE

Little is known about the geochemistry of natural waters deep within crystalline rocks (igneous or metamorphic silicate assemblages). Such information is essential for the safe disposal of high-level radioactive waste for hundreds to thousands of years. Detailed investigations of the deep groundwater chemistry from the Stripa mine are providing valuable information on the origin of saline waters in crystalline rocks. This report presents chemical data collected between January, 1981 and November, 1981. Special sampling techniques for trace elements were initiated in June, 1981 and continued to the present.

2.1 FIELD SAMPLING PROCEDURES

On June 2, 3 and 4, 1981, groundwater samples were collected from drillholes V2, N-1, M-3, R-1(4) and V1 (above and below the single installed packer). These sites were chosen to obtain samples from the deeper portions of the granite (330 to over 800 m) and where there was sufficient flow. A laminar filtered air flow bench was set up at the SGU drilling site (near N1, V1 and E1) to minimize contamination for trace element sampling techniques.

A peristaltic pump was used at each site to collect the water through silicone or tygon tubing from the drillhole to a flow cell arrangement where direct measurements of pH, EMF, temperature and conductivity could be made with little or no air contamination. Measurements of pH were made with glass membrane electrode calibrated against pH 7 and 9 buffers at each site. As a check on accuracy, a pH 10 buffer was measured after the

sample measurement and if the deviation was greater than about 0.05 pH units then the electrode was recalibrated and the sample remeasured. All buffers were thermally equilibrated to the temperature of the flowing drillhole water. A platinum electrode with a calomel reference was used for the EMF (electromotive force) measurements and corrections were made for the half-cell potential from the data of Ives and Janz (1961), to derive the Eh value of the water. ZoBell's solution was used as a check on the EMF measurements (Nordstrom, 1977).

A duplicate set of water samples was collected at each site, during the June field trip, for an interlaboratory comparison of analyses. One set was analyzed by the U.S.G.S. and the other set by S.G.U. (see section 2.2). Each set consisted of a 250 ml teflon bottle for cations and trace metals, a 250 ml polyethylene bottle for nitrate, nitrite, phosphate and ammonia, a 250 ml polyethylene bottle for iron (II, III) and arsenic (III, V), a 1 l glass bottle for mercury, a 50 ml glass for bromide and iodide, a 250 ml polyethylene bottle for anions, a 50 ml glass bottle for dissolved organic carbon (D.O.C.), a 2 l or 1 gallon polyethylene bottle for sulfide, a 125 ml polyethylene bottle for hydrogen and oxygen isotopes and a 1 gallon bottle for sulfur and oxygen isotopes in sulfate. All samples (except some of the isotope samples) were filtered by pumping the water from the same closed line system with the peristaltic pump directly to a precleaned plastic plate filter fitted with a 0.1 micrometer Millipore membrane. The membrane was preleached with at least 1 l of groundwater before collecting samples for analysis. One sample set (81WA202, N1) was unfiltered due to a broken membrane and when this problem was noticed a second filtered sample was collected.

The unfiltered sample was saved for a comparison of the effect of infiltration.

Sample preservation techniques varied according to the particular constituents being analyzed. Preservative reagents were added to the samples inside of a laminar filtered-air flow bench when possible to prevent air-borne particulates from contaminating either the reagents or the samples. Major cations and trace elements collected in teflon bottles were acidified with ultrapure nitric acid to a pH < 1.5. Duplicates for 81WA201, 81WA203, and 81WA206 were also collected in polyethylene containers to compare with collection in teflon containers. These results show excellent agreement.

All splits in different containers (but analyzed by the same lab) agree to < 5 % except for iron.

Samples collected for Fe (II, III) and As (III, V) were acidified with ultrapure hydrochloric acid to a pH < 1.5. Samples collected for dissolved nitrogen species and phosphate were frozen within about 5 hours or less after collection. They were kept frozen until the day of analysis which was within 2 weeks of the sampling dates. Mercury was preserved with the addition of potassium permanganate solution (Avotins and Jenne, 1975), and zinc acetate was added for the preservation of sulfide. Aluminum extractions were made to estimate inorganic monomeric aluminum by the procedure of Kennedy, et al. (1974) and Barnes (1975). These procedures were carried out inside under the laminar air flow bench.

2.2 INTER-LABORATORY COMPARISON OF ANALYTICAL DATA

The duplicate splits of water samples collected during the June field trip were analyzed at the

analytical laboratories of the S.G.U. and the trace element laboratory in Menlo Park, U.S.G.S. The results were compared; certain elements in selected samples which were most discrepant were rechecked and in several instances they were re-analyzed. As an independent check on the accuracy, splits of two standard reference samples from the U.S.G.S. Central Laboratories were analyzed by each laboratory. The final comparison is shown in Appendix 1, with differences that are usually < 5 %. Exceptions are the results for Al, Mg, and K which are trace constituents in these samples (usually < 1 mg/L) and several constituents in sample 81WA203 (Na, Mo, Sr and Ba). A single, final set of values (Table 2.1) for these seven splits was obtained by selecting S.G.U. values for Mg and Al. U.S.G.S. results for K (by AA) and averaging the rest. These selections were based on known biases from analytical techniques and the deviation from standard reference samples. The final selection of values is shown to be of high quality by their charge balances which fall in range of 0.2 to 4 %.

2.3 MONITORING DATA AND ADDITIONAL ANALYSES

Continuous sampling of V1, V2, E1 and N1 is being carried out to monitor chemical variations in the groundwaters which might be caused by mining, drilling, pumping or other man-made perturbations of the hydrologic system. Table 2.2 presents all of the analyses obtained for water samples collected during 1981 except those in Table 2.1. Most of these analyses have been done at the U.S.G.S. Where discrepancies exist between the S.G.U. and U.S.G.S. analyses, charge balance calculations, the general consistency of the data and the inter-laboratory comparison were used as guides to select the more reliable values. Where no logical choice could be made, an average number was chosen.

Table 2.1 Stripa groundwater analyses

Drillhole			V-2	N-1		V-1	R-1	M-3	V-1
Sample Code No.			81WA201	81WA202		81WA203	81WA204	81WA205	81WA206
Sampling Depth			763.7 - 877.7 m.	355.5 m.		764.7 - 856.7 m.	333.1 m.	339.5 - 340.5 m.	364.7 - 765.7 m.
Date Collected			3-6-81	3-6-81		3-6-81	4-6-81	4-6-81	4-6-81
Temperature (°C)			8.0	10.1		10.6	12.0	12.0	10.3
Field (Lab) pH			9.53 (8.69)	8.85 (8.27)		9.31 (7.57)	8.96 (8.51)	8.84 (8.39)	9.73 (8.99)
Conductivity (uS/cm)			960 (1415)	190 (283)		1420 (2230)	215 (286)	210 (291)	510 (710)
Eh (from field emf; mV)			+20 to +79	+13		-56	+57	---	+22
Total Alkalinity (1)			11.5	77		9.25	95	86	18
Charge Balance			0.18	1.2		1.1	1.9	3.9	2.5
Species		Method(2)		Filtered	Unfiltered				
Ca	ppm	S	104	23	22.5	172	15	14	27
Mg	ppm	S	0.11	0.12	0.22	0.19	0.18	0.23	<0.005
Na	ppm	S	180	35.5	35.5	277	49	47	116
K	ppm	AA	0.37	0.12	0.19	1.2	0.10	0.12	0.24
SO_4	ppm	IC	44.5	0.6	----	102	3.2	4.9	11.5
H_2S	ppm(3)	ISE	0.00023	0.026	----	0.0026	----	0.026	----
F	ppm	ISE	3.9	3.2	----	4.6	4.7	5.0	4.6
Cl	ppm	IC	410	45.5	----	630	34	38.5	190
Br	ppm	IC	4.0	0.5	----	6.5	0.3	0.3	2.0
I	ppm	C	0.11	0.015	----	0.16	0.014	0.013	0.061
PO_4	ppm	IC	<0.1	<0.1	----	<0.1	<0.1	<0.1	<0.1
SiO_2	ppm	S	12	12	15	13	12	12	14
B	ppm	S	0.20	0.094	0.10	0.25	0.15	0.18	0.24
NO_2	ppm	IC	<0.005	<0.005	----	<0.005	<0.005	<0.005	<0.005
NO_3	ppm	IC	4.8	0.7	----	7.0	0.5	0.6	2.5
NH_4	ppm	IC	<0.01	<0.01	----	<0.01	<0.01	<0.01	<0.01
Al	ppm	S	<0.005	0.059	0.56	0.008	<0.005	<0.005	0.032
Fe	ppm	F	0.088	0.018	0.16	0.004	0.046	0.010	0.020
Mn	ppm	S	0.009	<0.005	<0.005	<0.005	<0.005	<0.005	0.008
Cu	ppm	S	<0.003	<0.003	0.043	<0.003	<0.003	<0.003	<0.003
Zn	ppm	S	<0.005	<0.005	0.024	<0.005	<0.005	<0.005	<0.005
Hg	ppb	FAA	0.023	----	----	<0.005	----	----	----
Co	ppm	S	<0.005	<0.005	<0.005	<0.005	<0.005	<0.005	<0.005
Ti	ppm	S	0.014	<0.010	<0.010	0.035	<0.010	<0.010	<0.010
Mo	ppm	S	0.051	0.049	0.054	0.027	0.038	0.056	0.050
Li	ppm	AA	0.038	0.019	0.017	0.085	0.020	0.020	0.020
Sr	ppm	S	0.99	0.16	0.17	1.7	0.12	0.14	0.20
Cs	ppm	FE	0.046	0.035	0.066	0.074	0.064	0.047	0.078
Rb	ppm	FE	0.015	0.003	0.003	0.032	<0.002	<0.002	0.009
Ba	ppm	S	0.024	0.003	0.004	0.035	0.006	<0.003	<0.003
DOC	ppm	TCA	4.0	----	----	4.2	4.0	----	1.1

(1) Expressed as mgL^{-1} HCO_3 equivalent.
(2) S = plasma emission spectroscopy (USGS: direct current; SGU: inductively coupled), AA = atomic absorption, F = visible spectrophotometry (ferrozine method), FE = flame emission spectroscopy, ISE = ion-selective electrode, IC = ion chromatography, E = solvent extraction, FAA = flameless atomic absorption, TCA = total carbon analyser, C = colorimetric (Analyses performed by Don Whittemore.).
(3) Values are minimums.
(4) Dissolved organic carbon.
(5) ---- = Not analysed for.
(6) The following elements were found to be below detection limit for all samples (d.l. in ppm): As (0.003), Be (0.002), Bi (0.080), Cd (0.005), Ni (0.004), Pb (0.010), Sb (0.20), Se (0.20), Tl (0.007), V (0.005).

Table 2.2 Stripa groundwater analyses

Drillhole			V-1	V-1	N-1	V-1	V-1	V-1
Sample Code No.			81WA207	81WA208	81WA209	81WA210	81WA211	81WA212
Sampling Depth			766.4 - 862.7	766.4 - 862.7	358.5 - 655.5	766.4 - 862.7	360.7 - 862.7	360.7 - 862.7
Date Collected			13-7-81	19-8-81	19-8-81	8-9-81	11-9-81	21-9-81
Temperature (°C)			10.5	10.6	10.4	10.5	15.5	15.5
Field pH			9.54	9.27	8.91	9.28	9.17	9.10
Conductivity (uS/cm)			1600	1340	190	1420	1580	----
Eh (mV) (1)			+55	+129	-39	+79	----	----
Total Alkalinity (2)			11	13	81	16	19	12
TDS (3) (g/L)			1.12	1.43	0.18	1.28	1.15	1.03
Charge Balance			3.21	2.34	6.44	0.021	0.039	0.29
Species		Method(4)						
Ca	ppm	S	152	170	23	167	146	146
Mg	ppm	S	0.60	0.32	0.57	0.27	0.81	0.55
Na	ppm	S	270	304	37	290	260	248
K	ppm	S	2.6	2.5	0.61	2.5	2.2	2.4
SO_4	ppm	IC	110	95	0.45	105	92	90
H_2S	ppm	ISE	----	----	----	----	----	----
F	ppm	ISE	4.5	4.5	3.5	4.2	4.4	4.5
Cl	ppm	IC	570	700	40	650	575	560
Br	ppm	IC	6.6	6.2	0.42	6.6	5.9	5.9
I	ppm	C	0.16	0.11	0.014	0.16	0.14	0.14
PO_4	ppm	IC	<0.03	<0.02	<0.02	<0.02	<0.02	<0.02
SiO_2	ppm	S	13.7	13.7	11.1	13.0	13.0	13.0
B	ppm	S	0.25	0.24	0.07	0.22	0.21	0.21
NO_2	ppm	IC	<0.005	<0.005	<0.005	<0.005	<0.005	<0.005
NO_3	ppm	IC	<0.10	7.0	<0.2	<0.2	1.4	6.4
NH_4	ppm	IC	0.03	<0.02	<0.02	<0.02	<0.02	<0.02
Al	ppm	S	<0.005	<0.005	0.080	<0.01	<0.01	<0.01
Fe	ppm	S	<0.01	<0.01	0.14	0.01	0.03	<0.01
Mn	ppm	S	<0.01	<0.01	<0.01	<0.005	<0.005	<0.01
Cu	ppm	S	<0.005	<0.005	<0.005	<0.005	<0.005	<0.005
Zn	ppm	S	<0.005	<0.010	<0.010	<0.010	<0.010	0.051
Hg	ppb	FAA	----	----	----	----	----	----
Co	ppm	S	0.009	<0.005	<0.005	<0.005	<0.005	<0.005
Ti	ppm	S	----	----	----	----	----	----
Mo	ppm	S	0.010	0.010	0.050	0.020	0.020	0.010
Li	ppm	S	0.19	0.18	0.020	0.15	0.15	0.15
Sr	ppm	S	2.0	1.8	0.15	2.0	1.8	1.7
Cs	ppm	FE	----	----	----	----	----	----
Rb	ppm	S	0.005	<0.005	<0.005	0.005	0.005	<0.005
Ba	ppm	S	0.040	0.030	0.005	0.030	0.030	0.025
DOC	ppm(5)	TCA	1.6	4.8	1.2	1.0	----	----

(1) Corrected from field EMF using reference electrode potential (see text).
(2) Expressed as mgL^{-1} HCO_3 equivalent.
(3) Total dissolved solids.
(4) S = plasma emission spectroscopy (USGS: direct current; SGU: inductively coupled), AA = atomic absorption, F = visible spectrophotometry (ferrozine method), FE = flame emission spectroscopy, ISE = ion-selective electrode, IC = ion chromatography, E = solvent extraction, FAA = flameless atomic absorption, TCA = total carbon analyser, C = colorimetric (Analyses performed by Don Whittemore.).
(5) Dissolved organic carbon.
(6) ---- = Not analysed for.
(7) The following elements were found to be below detection limit for all samples (d.l. in ppm) : As (0.003), Be (0.002), Bi (0.080), Cd (0.005), Ni (0.004), Pb (0.010), Sb (0.20), Tl (0.007), V (0.005).

Table 2.2 Continued

Drillhole/Site			V-1	N-1	Well #1	Well #2	Stream	E-1	V-2
Sample Code No.			81WA213	81WA214	81WA215	81WA216	81WA217	81WA218	81WA219
Sampling Depth (m)			360.7 - 862.7	358.5 - 655.5	0 - 80	0 - 80	0	358.7 - 655.7	763.7 - 878.7
Date Collected			6-10-81	6-10-81	8-10-81	8-10-81	8-10-81	11-11-81	19-11-81
Temperature (°C)			14.5	11.5	11.2	10.2	10.1	10.5	8.0
Field pH			9.11	8.93	5.11	6.13	6.96	----	9.17
Conductivity (uS/cm)			1650	215	50	82	315	175	----
Eh (mV) (1)			+135	-4	+463	+490	+468	-1	----
Total Alkalinity (2)			11	72	12	20	9	84	28
TDS (3) (g/L)			1.07	0.18	0.03	0.07	0.03	0.18	0.90
Charge Balance			0.67	11.1	9.29	3.28	1.77	22.6	7.15
Species		**Method(4)**							
Ca	ppm	S	146	21	4.0	13	3.5	20	101
Mg	ppm	S	0.57	0.21	1.1	2.5	1.2	0.32	0.29
Na	ppm	S	246	33	3.7	2.5	2.0	45	160
K	ppm	S	2.4	0.38	1.1	1.7	0.83	0.80	1.0
SO_4	ppm	IC	90	0.30	10	12	6.1	6.8	45
H_2S	ppm	ISE	----	----	----	----	----	----	----
F	ppm	ISE	4.1	3.3	0.30	0.22	0.51	3.1	3.4
Cl	ppm	IC	560	51	4.5	14	2.3	25	400
Br	ppm	IC	5.8	0.50	0.014	0.023	0.014	0.155	4.2
I	ppm	C	0.14	0.016	0.002	0.003	0.003	0.006	0.11
PO_4	ppm	IC	<0.02	<0.02	<0.02	<0.02	0.05	<0.02	0.02
SiO_2	ppm	S	13.5	11.8	13.5	10.5	5.35	11.8	11.8
B	ppm	S	0.20	0.084	<0.005	<0.005	<0.005	0.10	0.21
NO_2	ppm	IC	<0.005	<0.005	<0.005	<0.005	<0.005	<0.005	<0.005
NO_3	ppm	IC	7.8	0.40	0.80	4.3	1.3	0.10	3.7
NH_4	ppm	IC	<0.02	0.02	0.04	<0.02	0.03	<0.02	0.04
Al	ppm	S	<0.005	0.033	0.12	0.090	0.055	<0.005	<0.005
Fe	ppm	S	<0.005	0.043	0.042	<0.005	0.13	0.060	0.034
Mn	ppm	S	<0.005	<0.005	0.027	0.010	0.015	0.005	<0.005
Cu	ppm	S	<0.005	<0.005	0.051	<0.005	<0.005	<0.005	<0.005
Zn	ppm	S	0.020	<0.005	0.12	0.027	0.018	0.073	0.069
Hg	ppb	FAA	----	----	----	----	----	----	----
Co	ppm	S	<0.005	0.010	<0.005	<0.005	<0.005	<0.005	<0.005
Ti	ppm	S	----	----	----	----	----	----	----
Mo	ppm	S	0.013	0.046	<0.005	<0.005	<0.005	0.049	0.071
Li	ppm	S	0.15	0.022	<0.005	<0.005	<0.005	0.019	0.073
Sr	ppm	S	1.7	0.16	0.016	0.033	0.011	0.13	1.0
Cs	ppm	FE	----	----	----	----	----	----	----
Rb	ppm	S	0.005	<0.005	<0.005	0.008	0.005	<0.005	0.010
Ba	ppm	S	0.027	<0.003	0.018	0.022	0.011	0.003	0.022
DOC	ppm(5)	TCA	----	----	----	----	----	1.3	----

(1) Corrected from field EMF using reference electrode potential (see text).
(2) Expressed as mgL^{-1} HCO_3 equivalent.
(3) Total dissolved solids.
(4) S = plasma emision spectroscopy (USGS: direct current; SGU: inductively coupled), AA = atomic absorption, F = visible spectrophotometry (ferrozine method), FE = flame emission spectroscopy, ISE = ion-selective electrode, IC = ion chromatography, E = solvent extraction, FAA = flameless atomic absorption, TCA = total carbon analyser, C = colorimetric (Analyses performed by Don Whittemore.).
(5) Dissolved organic carbon.
(6) ---- = Not analysed for.
(7) The following elements were found to be below detection limit for all samples (d.l. in ppm) : As (0.003), Be (0.002), Bi (0.080), Cd (0.005), Ni (0.004), Pb (0.010), Sb (0.20), Tl (0.007), V (0.005).

2.4 GAS SAMPLES

A few gas samples were obtained during the June field trip and the analytical results are shown in Table 2.3. These data are somewhat variable yet they provide information which relates to the origin of the groundwaters. Nitrogen and helium dominate with N_2 composing 78-95 % of the gas and N_2 + He composing 95-97 % of the gas. Gas ratios can be particularly useful in identifying an atmospheric origin for gases dissolved in groundwaters (e.g. Mazor and Wasserburg, 1965; Gunter and Musgrave, 1966; Vidal, et al. 1982). Argon is relatively inert and serves as a useful conservative tracer for normalizing the gas data. Ratios of He/Ar are between those values for air and air-saturated water at 20°C in groundwaters from M3 and R66. In contrast, samples from V1 and V2 are considerably higher in He/Ar than air which indicates He production at depth. These data are consistent with the high ^4He concentrations discussed in chapter 3. Anomalous levels of He in geothermal areas (Mazor and Wasserburg, 1965; Vidal, et al., 1982) have also been correlated with radioactive decay. Ratios of Ar/N2 vary from that of air to considerably less than air. These ratios suggests that an additional non-atmospherie source of nitrogen may be entering the Stripa groundwaters. An organic source is not likely because of the low concentrations of organic matter in the rock and the groundwaters and because of the low CH_4 and CO_2 content. Contamination from packers inflated with N2 may explain one or two of the samples but not all of them. Leakage from fluid inclusions is a possibility since nitrogen is a common fluid in inclusions (Crawford, 1981; Jouret, 1981) although it seems unlikely. It is noteworthy that the samples which give the lowest Ar/N2 ratios relative to air (R66

Table 2.3 Analyses of gas samples

Borehole	VI	M3	R66	V2	VI
Date	4-6-81	4-6-81	4-6-81	4-6-81	10-14-81
Species:					
N_2 %	78.0	92.9	94.6	84.4	79.8
Ar %	0.93	0.95	0.29	0.48	0.71
CH_4 %	0.093	0.35	0.15	0.35	0.108
Hc %	19.2	3.9	1.08	10.9	15.4
O_2 %	0.32	0.32	1.94	1.19	0.56
H_2 %	0.2	(< 20)	(< 20)	(< 20)	(< 50)
CO_2 %(ppm)	0.88	(140)	(320)	(160)	(280)
CO %(ppm)	(< 10)	(< 10)	(< 10)	(< 10)	(< 10)
Total	99.62	98.42	98.06	97.32	96.58
$\frac{(Ar/N_2)sample}{(Ar/N_2)air}$	1.0	0.86	0.26	0.48	0.75

and V2) also contain the highest concentrations of oxygen. If this were air contamination, it is unlikely that the argon concentration would decrease relative to sample V1. Therefore, it would appear that the oxygen might also have a non-atmospheric source. Detectable oxygen concentrations in deep groundwaters is not at all uncommon (Winograd and Robertson, 1982) and the possibility of a radiolytic origin as proposed by Gutsalo (1971) should be considered in light of the high radioactive content of the Stripa granite. Hopefully, nitrogen stable isotope data and more gas analyses will help to resolve these questions.

2.5 TRACE METAL ANALYSES

The sampling, preservation and analysis of major and trace elements show a high degree of reliability both in accuracy and precision. These data will provide a valuable reference set for comparison with future water analyses. The trace element concentrations are generally at or below detection limits, especially for steel-alloying elements, such as Mn, Ni and Cr, and metals which are common contaminants from machinery, such as Cu and Zn. Trace element contamination does not appear to be a major problem in these samples. Mo may be leaching from steel packers, from metal stains or powders in the drillhole or it may be representative of uncontaminated groundwater. We do not have any definitive way of distinguishing these possible sources at this time. We can say, however, that these values for Mo concentrations are similar to those analyzed in other unpolluted subsurface waters.

2.6 MAJOR TRENDS IN GROUNDWATER CHEMISTRY

The analytical data in Tables 2.1 and 2.2 are consistent with the major trends in groundwater chemistry discussed by Fritz, et al (1979, 1980): (a) salinity increases with depth, (b) pH increases with depth, and (c) alkalinity decreases with depth.

The increase in salinity with depth is clearly shown in Figure 2.1 where chloride is plotted as a function of depth for all data from this report and the reports by Fritz, et al (1979, 1980). Since any one drillhole contains many different fractures whose hydrologic connection is un-

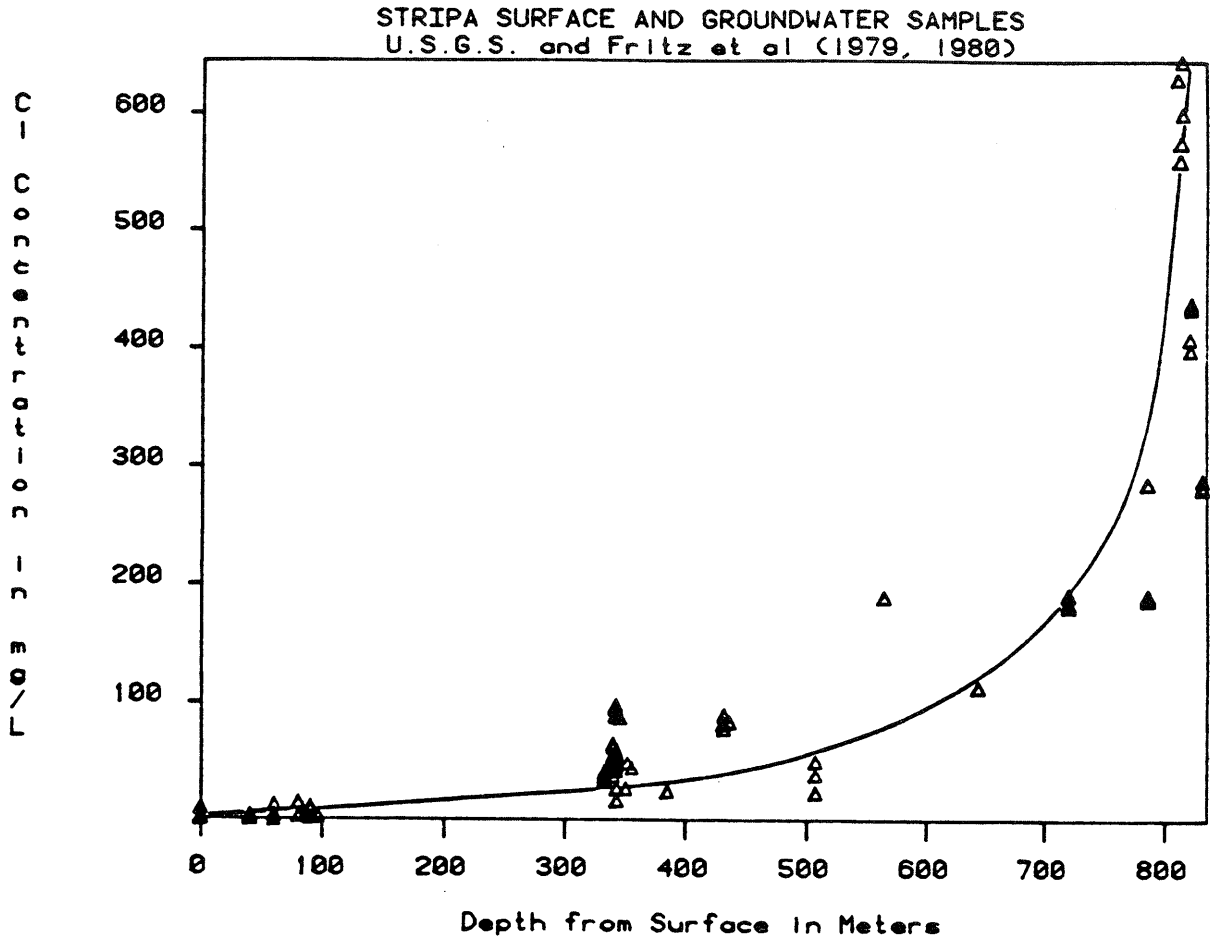

Figure 2.1 Chloride vs depth

certain, it seems more appropriate to pool all of the avaiable data rather than draw any conclusions from a single hole. Also, by pooling the data it can be readily determined whether correlations in the chemical data are independent of the drillhole location. In Figure 2.1 it is apparent that the chloride content of these subsurfaces waters increases exponentially with depth. The dramatic increase in chloride below 600 m shows that a considerable amount of salt is coming into the groundwater from some source.

The increase of pH with depth is shown in Figure 2.2 where values of pH approach 10. The low

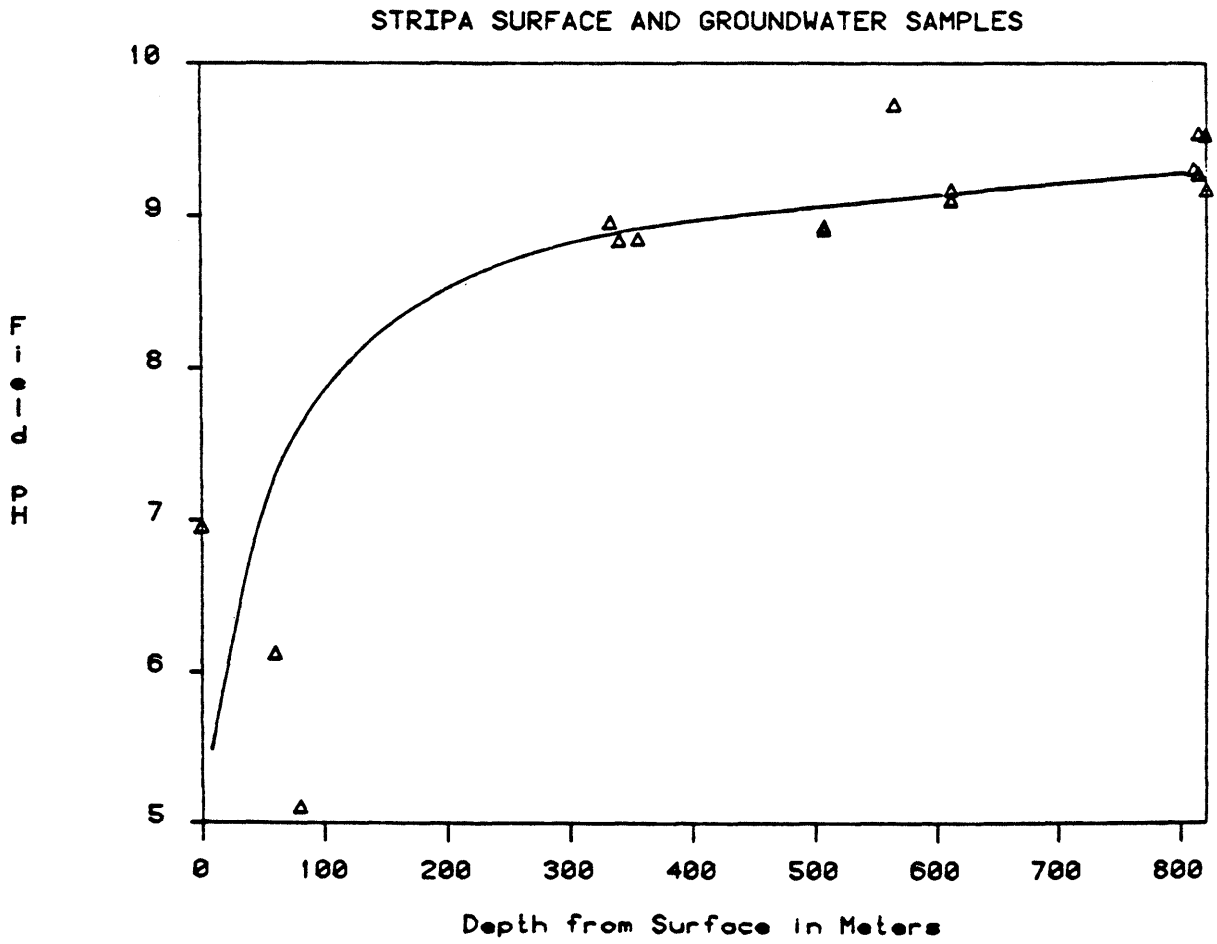

Figure 2.2 pH vs depth

alkalinity in these high pH samples indicates that an increasing proportion of hydroxide is contributing to the alkalinity. These samples are also seen to be greatly undersaturated with respect to CO_2 since their pH drops considerably after being exposed to the air.

The first step towards interpreting these data can be made by comparing constituent concentrations with chloride since chloride is safely assumed to be a chemically conservative tracer. When sodium and calcium are plotted (in meq/L) against chloride (Figure 2.3) the results are two strikingly parallel and linear lines. This graph suggests that sodium, calcium and chloride all

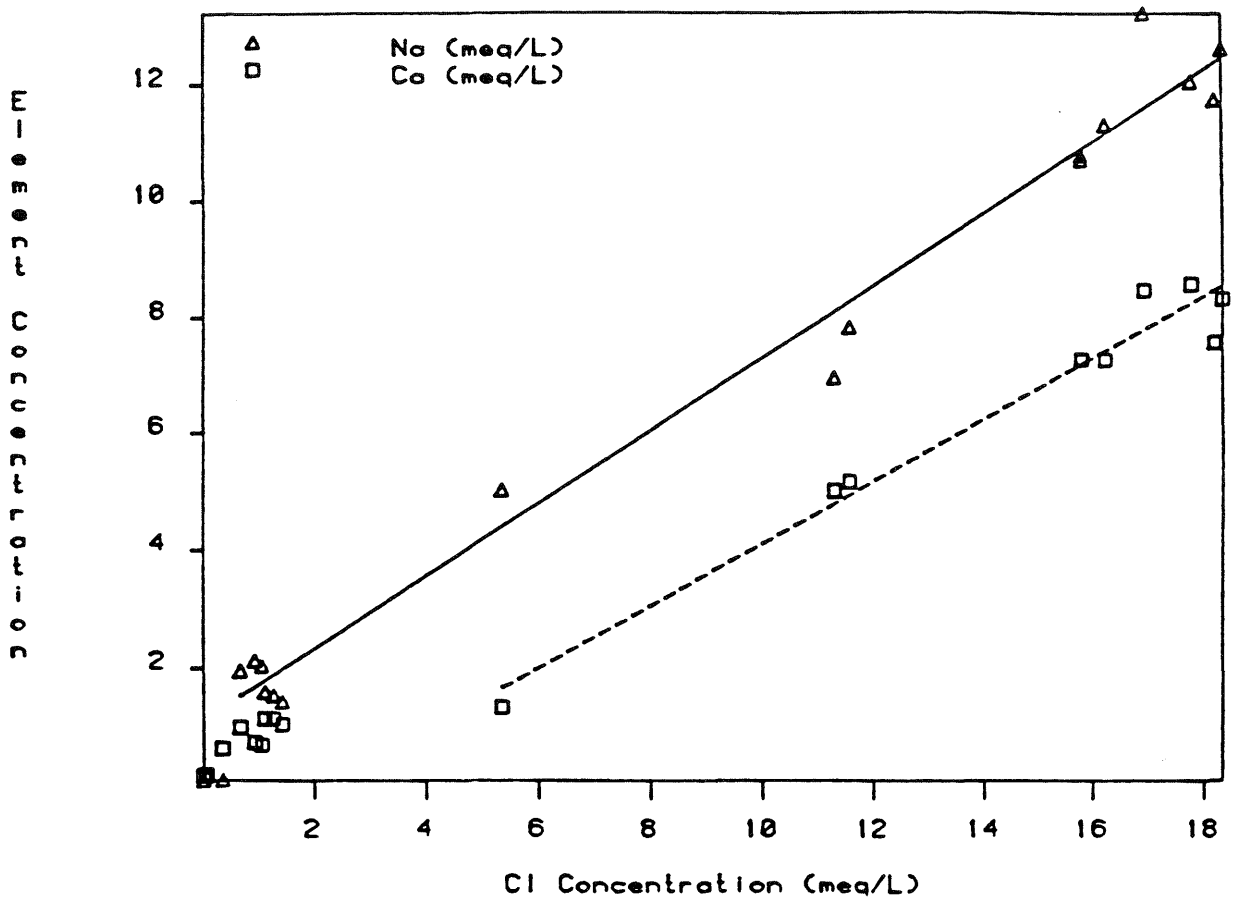

Figure 2.3 Sodium and calcium vs chloride

originate from a single source and the linear trend suggests a simple mixing line. In Figure 2.4 the plots for bromide and strontium are also linear and nearly parallel. Bromide correlates very strongly with chloride in a linear regression (r^2=0.9992), providing the best argument for a single source for the salinity increase at depth. Figure 2.5 shows the linear correlation of barium, rubidium, and iodide with chloride. Nitrate also shows a fairly good linear correlation with chloride (Figure 2.6), but many other constituents are independent of chloride such as fluoride (Figure 2.6), boron (Figure 2.8) and silica (Figure 2.9). Potassium (Figure 2.8) is somewhat independent of chloride, but at the highest chloride concentrations it begins to increase. As shown in Figure 2.7, sulfate tends to increase

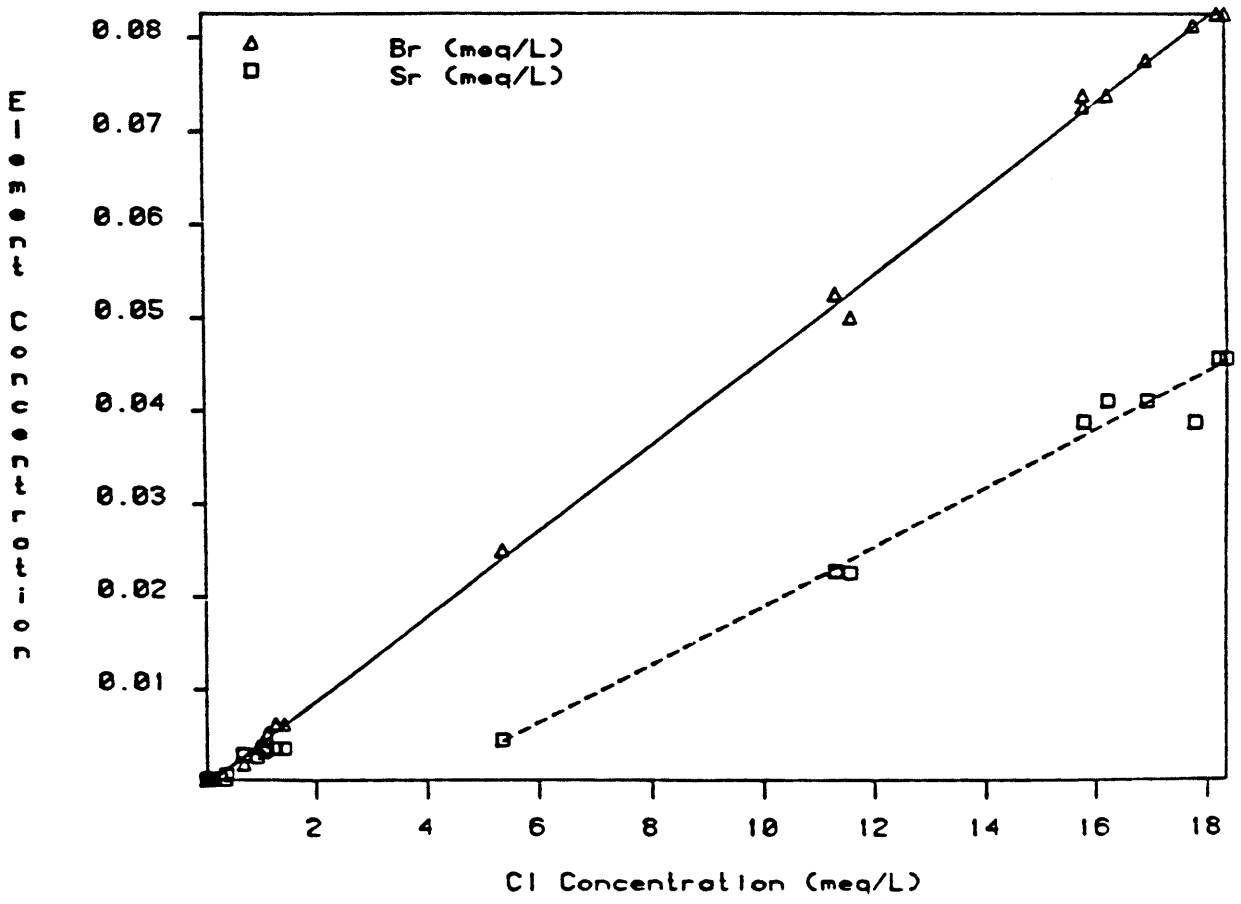

Figure 2.4 Bromide and strontium vs chloride

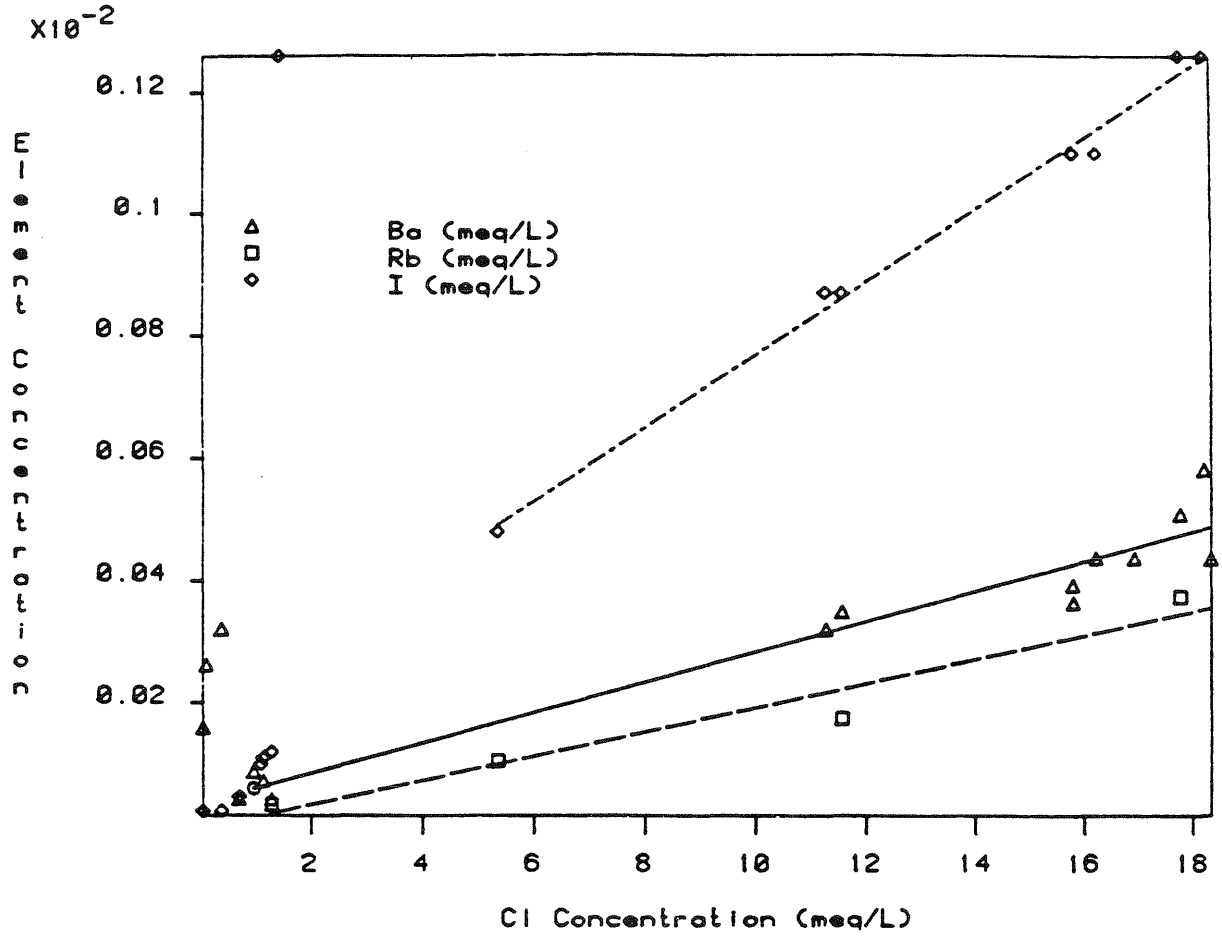

Figure 2.5 Barium, rubidium, and iodide vs chloride

exponentially with chloride while bicarbonate decreases exponentially with chloride. All of these constituents are clearly nonconservative, implying that they undergo chemical reactions during the evolution of the deep groundwaters and are not directly related to the source of salinity described by the conservative constituents. Sulfate is unique among the constituents analyzed in that it increases at a greater rate than chloride.

The chemical data can be summarized by describing the constituents as conservative or non-conservative with respect to chloride. The constituents Na, Li, Rb, Ca, Sr, Ba, Br, and are all conservative and correlate linearly with Cl on a linear-linear plot and many have the same slopes.

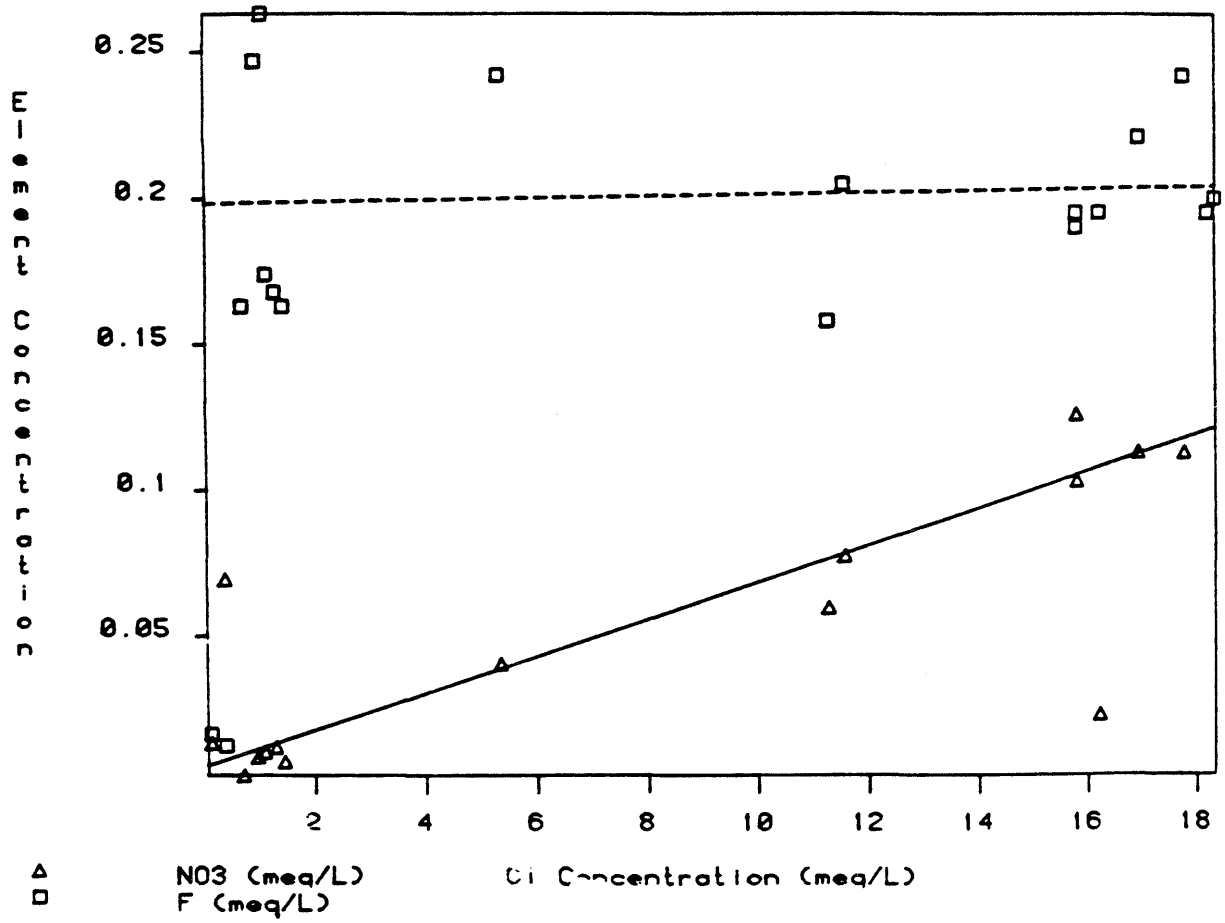

Figure 2.6 Nitrate and fluoride vs chloride

In contrast, the constituents, K, Cs, Mg, HCO_3, F, SO_4, B, Mo, Al, and Fe are non-conservative. Among the non-conservative constituents, all but HCO_3 and SO_4 are nearly constant regardless of Cl concentration. The concentrations of HCO_3 decrease exponentially with chloride, suggesting a removal process such as calcite precipitation, whereas SO_4 concentrations increase exponentially, suggesting an additional input of SO_4 into the groundwater such as pyrite oxidation or gypsum

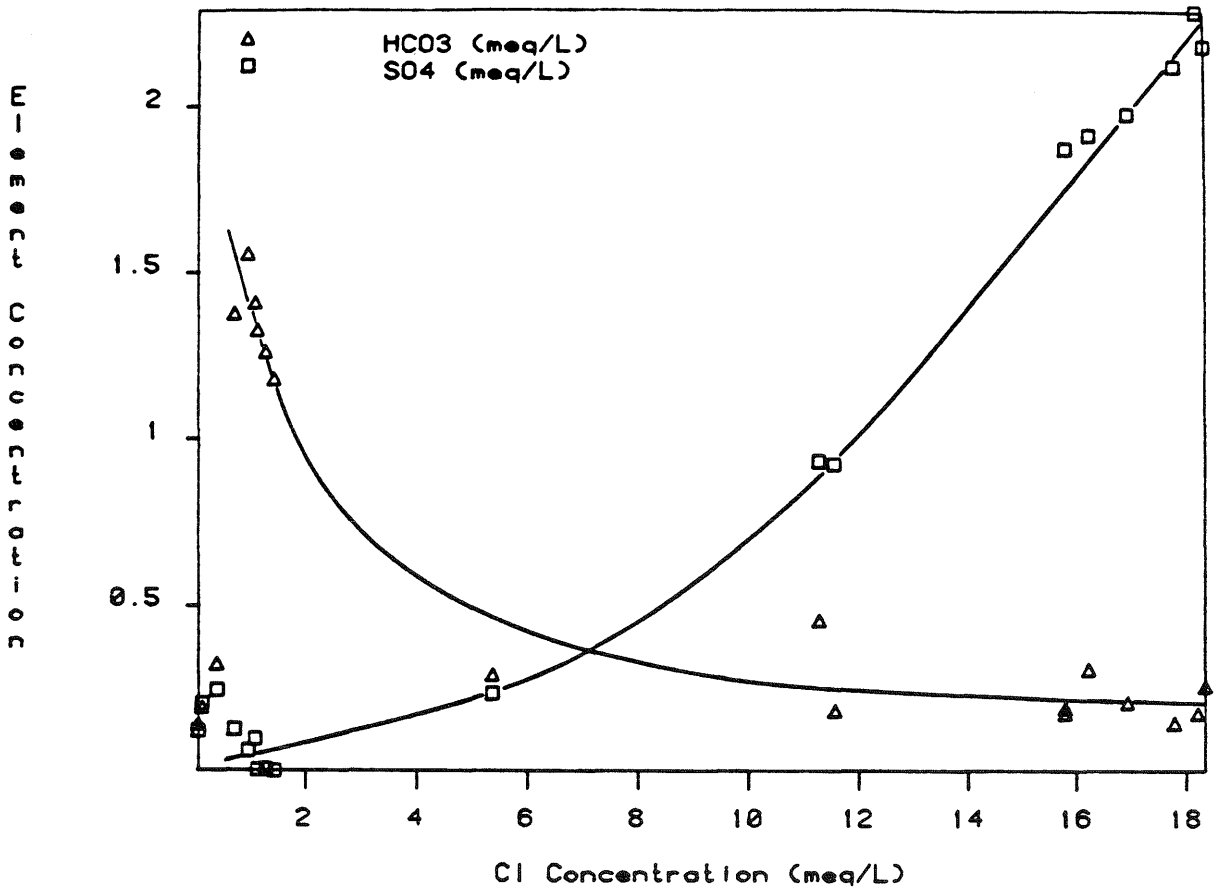

Figure 2.7 Carbonate and sulphate vs. chloride

dissolution. Any interpretation of the groundwater geochemistry at Stripa must include a single source for the conservative solutes and appropriate water-mineral reactions to explain the non-conservative constituents. An interpretation that is consistent with these constraints is offered in Chapter 5.

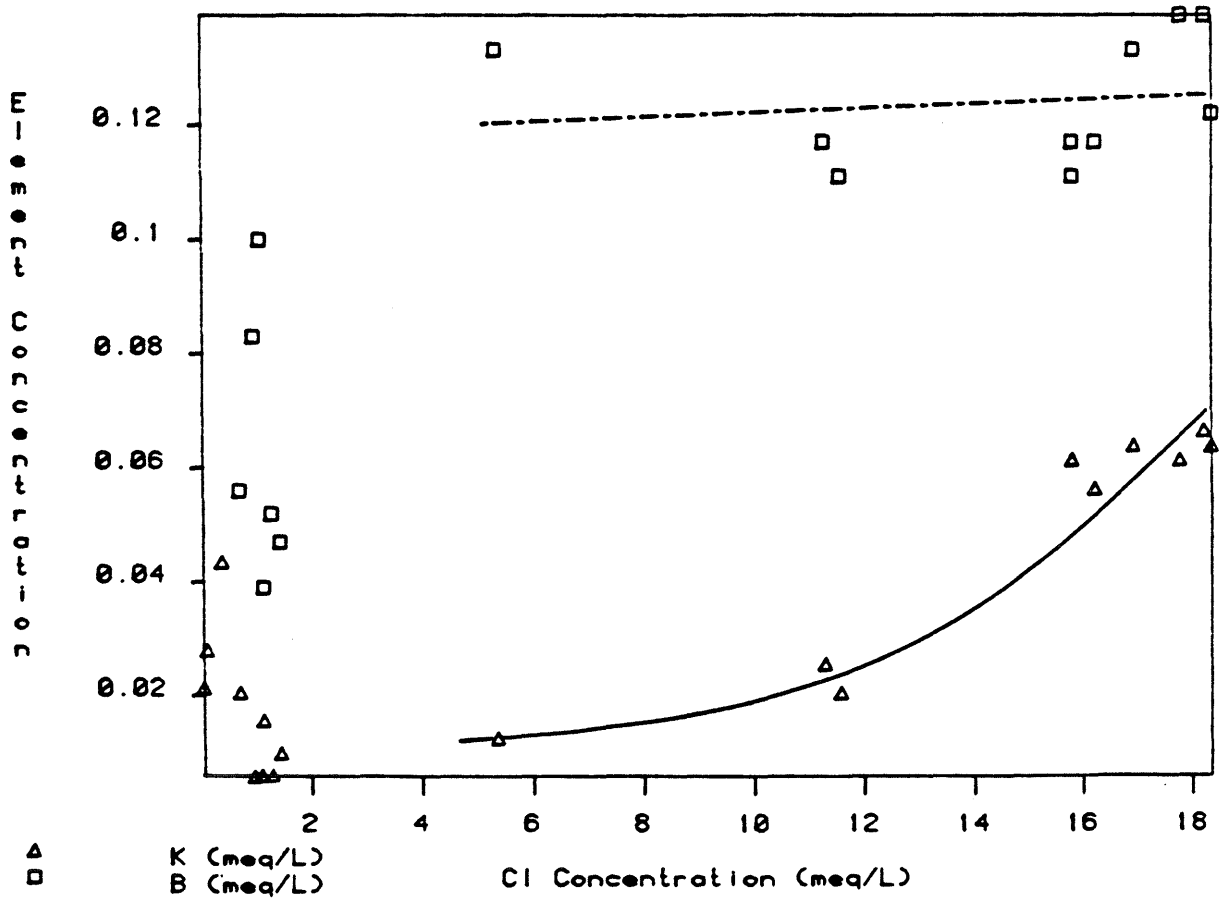

Figure 2.8 Potassium and boron vs chloride

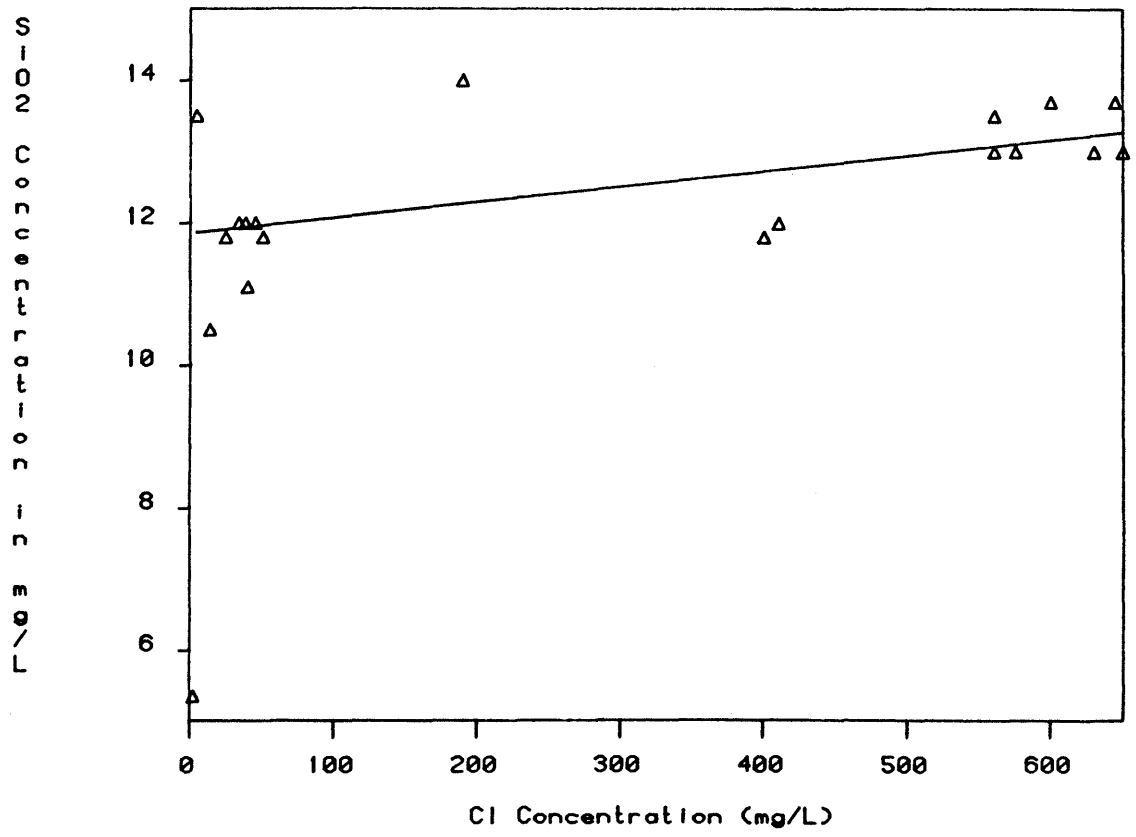

Figure 2.9 Silica vs chloride

3 RADIOELEMENTS AND INERT GASES IN THE STRIPA GROUNDWATERS

The results of radioelement and inert gas measurements which were made during the SKBF/LBL phase of investigations at Stripa have been discussed by Fritz et al (1969) and by Andrews et al (1982). Following on this first phase of investigations, further measurements have been made during 1981/82 on groundwaters from the boreholes M3, E1, N1, V1 and V2 (DBH V1). Although the intervals sampled and flow/shut-in periods for these boreholes have varied, this has enabled the temporal variation of radiochemical parameters to be studied. These results are tabulated for 1981/82 in tables 3.1 - 3.4, and temporal variations since 1977 for boreholes M3 and V2 are shown in Figures 3.1 and 3.2. Figure 3.3 shows the same variations for borehole V1 since drilling in 1981.

Table 3.1 Natural U-contents and $^{234}U/^{238}U$ activity ratios of dissolved uranium in Stripa groundwaters.

Borehole	Sampling Date	Depth Interval	FILTERED SAMPLE U-content µg/kg	FILTERED SAMPLE $^{234}U/^{238}U$ A.R.	FILTERED SAMPLE Analysis No	UNFILTERED SAMPLE U-content µg/kg	UNFILTERED SAMPLE $^{234}U/^{238}U$ A.R.	UNFILTERED SAMPLE Analysis No
V1	15.1.81	92.0 - 94 m	34.76 ± 0.46	2.90 ± 0.04	1450 1F	26.05 ± 0.34	3.17 ± 0.05	1450 1UF
V1	11.6.81	409.7 - 506 m	0.42 ± 0.04	3.96 ± 0.44	1450 2F	0.63 ± 0.04	3.92 ± 0.27	1450 2UF
V1	14.7.81	409.0 - 506 m	0.90 ± 0.13	3.37 ± 0.56	1450 3F	0.57 ± 0.08	5.00 ± 0.77	1450 3UF
V1	8.9.81	409.0 - 506 m	5.36 ± 0.13	3.06 ± 0.08	1450 5F	14.33 ± 0.23	2.87 ± 0.05	1450 5UF
V1	9.9.81	4.0 - 506 m	0.60 ± 0.04	4.91 ± 0.38	1450 6F	0.60 ± 0.04	5.16 ± 0.37	1450 6UF
V1	16.9.81	4.0 - 506 m	0.35 ± 0.05	5.14 ± 0.73	1450 7F	0.30 ± 0.05	5.57 ± 0.91	1450 7UF
V1	21.9.81	4.0 - 506 m	0.36 ± 0.03	4.65 ± 0.49	1450 8F	0.31 ± 0.03	4.74 ± 0.52	1450 8UF
V1	6.10.81	4.0 - 506 m	0.28 ± 0.03	4.52 ± 0.45	1450 9F	0.25 ± 0.03	5.88 ± 0.65	1450 9UF
V2	11.6.81	356.0 - 470 m	0.25 ± 0.06	3.98 ± 1.00	1453 1F	0.22 ± 0.02	4.08 ± 0.44	1453 1UF
V2	19.11.81	356.0 - 471 m	0.14 ± 0.03	3.14 ± 0.72	1453 2F	-	-	-
N1	14.7.81	002 - 300 m	8.46 ± 0.23	3.22 ± 0.10	1454 1F	8.91 ± 0.32	3.35 ± 0.14	1454 1AUF
N1	14.7.81	002 - 300 m	-	-	-	7.76 ± 0.32	3.45 ± 0.16	1454 1BUF
N1	6.10.81	3 - 300 m	1.83 ± 0.08	5.64 ± 0.26	1454 3F	2.43 ± 0.10	4.79 ± 0.22	1454 3UF
M3	12.1.81	-	-	-	-	11.52 ± 0.18	11.00 ± 0.18	1452 1UF
M3	3.6.81	-	18.03 ± 0.49	11.24 ± 0.32	1452 2F	-	-	-
M3	10.6.81	-	-	-	-	10.00 ± 0.19	10.91 ± 0.22	1452 2UF
E1	11.11.81	003 - 300 m	9.50 ± 0.24	4.71 ± 0.13	1455 1F	10.36 ± 0.18	4.51 ± 0.09	1455 1UF
PW1	21.1.81	-	90.4 ± 1.80	3.23 ± 0.07	1451 1F	90.1 ± 1.52	3.19 ± 0.06	1451 1UF

3.1 URANIUM GEOCHEMISTRY

Uranium solution of both ^{238}U and ^{234}U may occur by chemical leaching, and isotope ^{234}U may be dissolved more rapidly than ^{238}U by this process. In addition, ^{234}U may be dissolved as a result of α-recoil of ^{234}Th. The theoretical change of the $^{234}U/^{238}U$ activity ratio may be shown to depend upon the equation (Andrews et al, 1982):

$$AR_t = 1 + (AR_i - 1)e^{-^{234}\lambda t} + \frac{0.235[U]_r \rho SR(1-e^{-^{234}\lambda t})}{[U]_s} \quad (1)$$

where AR_t = $^{234}U/^{238}U$ activity ratio at time t after the groundwater has acquired an initial activity ratio, AR_i, by chemical leach processes in a rock matrix of density ρ and U content, $(U)_r$.

R is the recoil range of ^{234}Th,
S is the internal surface area/unit volume of fluids,
$[U]_s$ is the U-content of the groundwater.

The value of AR_i may either decrease or increase with time, depending upon the values of $[U]_r/[U]_s$ and S. The equation assumes that the groundwater remains a closed system for ^{234}U after the initial leach solution. Figure 3.4 shows the behaviour of a fluid-filled fracture system with a fracture separation of 0.2 mm for two values of $[U]_s$. The activity ratio approaches a steady state value which is dependent upon both $[U]_s$ and S. For this fracture separation, however, significant recoil-induced changes in activity ratio require groundwater residence times greater than 10^4 years. If the uranium is largely contained within microfractures (Nelson et al, 1979) and the recoil-process is dominated by these (fracture

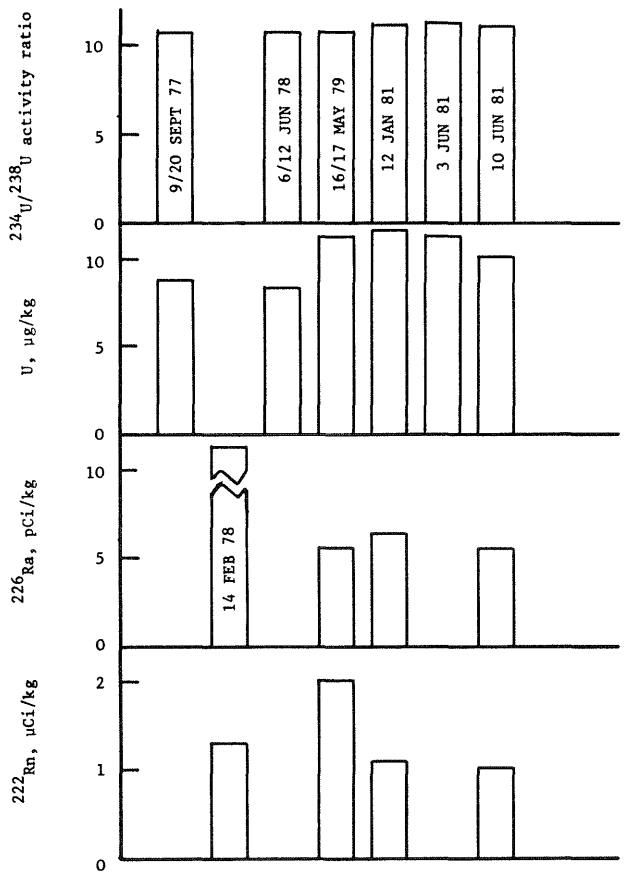

Figure 3.1 Temporal variations in radiochemical parameters for groundwaters from the M3 borehole.

separation 2 µm), then recoil-enhancement of the activity ratio would occur in residence times as short as a few years (Figure 3.4).

The activity ratio of dissolved uranium in the shallow groundwaters from the Stripa area is about 3 and is almost independent of groundwater U-content (Andrews et al, 1982). Although this would suggest that preferential chemical leaching of ^{234}U is the cause of $^{234}U/^{238}U$ activity ratio enhancement, the possibility that it might be the result of α-recoil enhancement within micro-fractures could not be excluded.

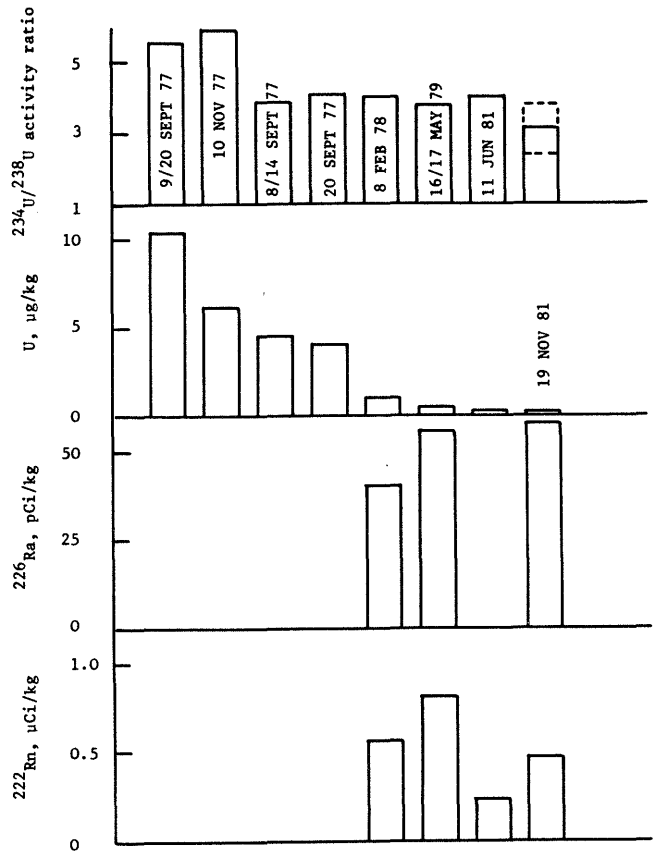

Figure 3.2 Temporal variations in radiochemical parameters f groundwaters from V2 borehole.

Figure 3.1 shows that the activity ratio of dissolved uranium in the M3 groundwater is remarkably constant (~11), but that its U-content is more variable. The behaviour for the V2 groundwater (Figure 3.2) shows that the activity ratio in waters from the lower section of the borehole is constant (~4), but that there has been a progressive decline in U-content. Both of these boreholes have been flowing continuously. A sample obtained from the V1 borehole during a drilling stop (15 January, 1981) had a very high U-content and an activity ratio of about 3. Subsequently, the U-content decreased and the activity ratio increased. Just after a shut-in period (to 8 September

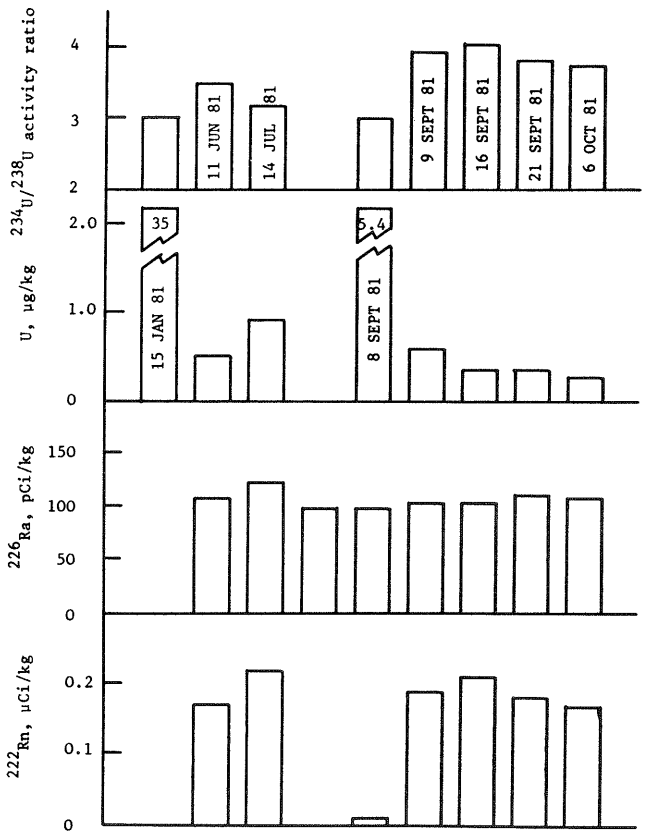

Figure 3.3 Temporal variations in radiochemical parameters for groundwaters from V1 borehole.

1981) this behaviour was reversed, and a subsequent flow showed a trend similar to that for V2. These results show that U solution is subject to flow conditions but that the activity ratio becomes constant under flowing conditions. The value attained is probably dependent upon the U-content of the matrix at the depth of origin of the groundwater. This is presently being investigated.

Since uranium in solution in the Stripa groundwaters never approximates closed system conditions, it is not possible to deduce residence times from activity ratio systematics. It is, however, possible to use U-content and activity

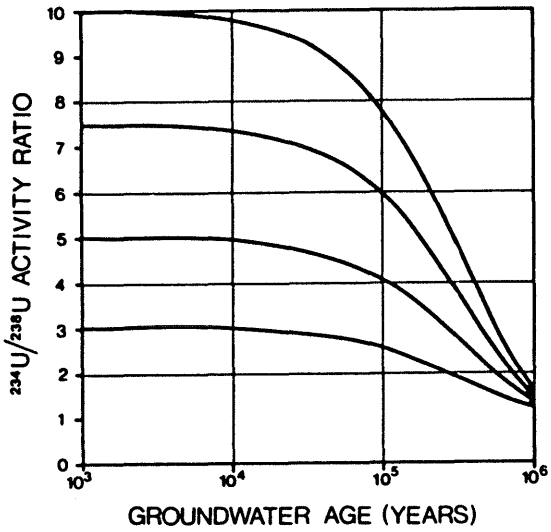

Figure 3.4 $^{234}U/^{238}U$ activity ratio change with age for uranium in groundwater present in a granite with fracture openings of 0.2 cm ($S = 10\ cm^2/cm^3$) and a uniform uranium content of 40 ug/g, calculated from equation 1. The activity ratio/age relationship is shown for various initial activity ratios and for a groundwater uranium content of 10 ug/kg.

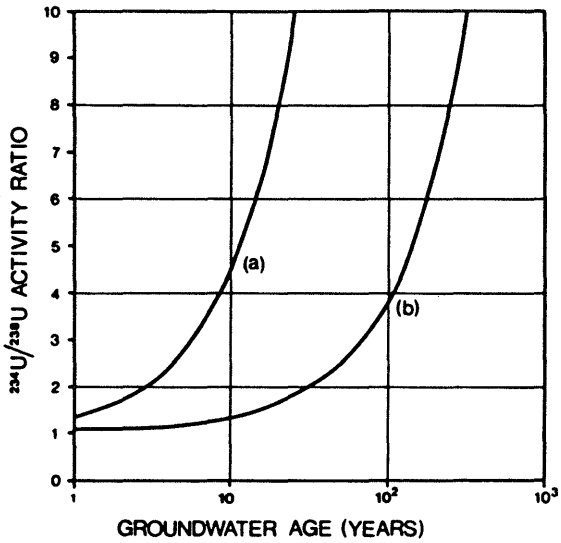

Figure 3.5 $^{234}U/^{238}U$ activity ratio change with age for uranium in groundwater present in the micro-fractures of a granite which has a uanium content of 5,000 ug/g in fracture surfaces, calculated from equation 1. The activity ratios are calculated for (a) fracture openings of 0.5 um ($S = 40{,}000\ cm^2/cm^3$) and (b) fracture openings of 2.0 um ($S = 10{,}000\ cm^2/cm^3$). In each case the groundwater uranium content is 10 ug/kg.

Table 3.2 The ^{222}Rn and ^{226}Ra contents of Stripa groundwaters.

Borehole	Depth Interval	Sampling Date	Analysis No	^{222}Rn pCi kg^{-1}	^{226}Ra pCi kg^{-1}
V1	409 - 506 m	11.6.81	1450 - 2	172250 ± 1400* 123350 ± 1300*	112.2 ± 0.22 128.4 ± 0.53
V1	409 - 506 m	14.7.81	1450 - 3	218350 ± 900 222750 ± 900	134.1 ± 0.33 146.8 ± 1.60
V1	409 - 506 m	19.8.81	1450 - 4	-	101.9 ± 0.15 106.7 ± 0.24
V1	409 - 506 m	8.9.81	1450 - 5	11000 ± 50* 9200 ± 50*	102.1 ± 0.68 95.5 ± 0.85
V1	4 - 506 m	9.9.81	1450 - 6	178200 ± 800 198300 ± 200	125.6 ± 1.02 103.4 ± 0.71
V1	4 - 506 m	16.9.81	1450 - 7	209100 ± 2800 212250 ± 1000	111.2 ± 1.31 104.3 ± 0.92
V1	4 - 506 m	21.9.81	1450 - 8	182200 ± 1500 183750 ± 550	122.5 ± 0.96 120.9 ± 1.36
V1	4 - 506 m	6.10.81	1450 - 9	170600 ± 700 173250 ± 800	120.1 ± 0.63 109.6 ± 0.91
M3		12.1.18	1452 - 1	1111800 ± 1500*	6.88 ± 0.04 5.89 ± 0.04
M3		10.6.81	1452 - 2	847150 ± 3350* 1037650 ± 4000*	5.24 ± 0.05 5.79 ± 0.05
V2		11.6.81	1453 - 1	224800 ± 2000*	-
V2		19.11.81	1453 - 2	500716 ± 600*	56.6 ± 0.53 56.9 ± 0.66
V2	6 - 822 m	22.4.82	1453 - 3	471930 ± 460 453780 ± 450	
N1	3 - 300 m	14.7.81	1454 - 1	1675 ± 9 1900 ± 10	2.28 ± 0.04 2.30 ± 0.02
N1		19.8.81	1454 - 2		2.90 ± 0.03 2.14 ± 0.02 2.47 ± 0.03
N1		6.10.81	1454 - 3	171700 ± 1100 173700 ± 800	3.26 ± 0.03 3.67 ± 0.03
E1	3 - 300 m	11.11.81	1455 - 1	402500 ± 1050 357000 ± 850	5.14 ± 0.04 5.21 ± 0.04
E1	127.5 - 129.5 m	24.3.82	1455 - 2	81820 ± 800 84080 ± 800	- -

* determined by γ - spectroscopy

ratio measurements to identify groundwaters with similar flow paths. V1 + V2 and $M3_2$+ E1 + N1, for example, are significantly different groups. The hydrogeochemistry of uranium would also be of great significance in the assessment of possible actinide migration from stored nuclear wastes.

3.2 THORIUM ISOTOPES

The first few members of the ^{232}Th decay series are:

$$^{232}Th \xrightarrow{\alpha} {}^{228}Ra \xrightarrow{\beta} {}^{228}Ac \xrightarrow{\beta} {}^{228}Th \xrightarrow{\alpha}$$

1.4×10^{10}a 6.7a 6.13h 1.91a

The isotope ^{230}Th (half-life 8 x 10^4a) belongs to the ^{238}U decay series and was found to be absent from all of the groundwaters. ^{232}Th and ^{228}Th are present (table 3.4) and ^{228}Th is generally present in an amount exceeding equilibrium with ^{232}Th. Thorium is generally absent from groundwaters because of the insolubility of its hydroxide. At Stripa, the amounts of ^{232}Th present in the waters are low but significantly above detection limits and a proportion of it may be carried on particulates of colloidal dimensions. ^{228}Th is produced by a α-recoil ejection of ^{228}Ra into solution and this decays to ^{228}Th, transient equilibrium being established after about 35 years. The ^{228}Th content would be identical to the ^{228}Ra content for a constant ^{228}Ra recoil rate.

The alpha-recoil rate for ^{228}Ra and ^{226}Ra may be estimated from the amount of ^{228}Th in solution. The ^{228}Th activity in solution is equal to that of about 30 μg kg^{-1} of ^{232}Th (Table 3.4), that is, to about 7.4 disintegrations $min^{-1}kg^{-1}$. This is

the ^{228}Ra recoil rate* and as the concentrations of U and Th in the Stripa granite are about 40 μg kg^{-1} and 30 μg respectively, the recoil rate for ^{226}Ra is given by:

$$^{226}Ra \text{ recoil rate} = {}^{238}U \text{ series recoil rate}$$
$$= \frac{40 \times 0.7336}{30 \times 0.246} \times 7.4$$
$$= 29.4 \text{ disintegrations } min^{-1}kg^{-1}.$$

This estimate of the ^{226}Ra recoil rate assumes that both U and Th are uniformly distributed in the rock surface. The very high ^{222}Rn contents in the groundwaters and the ready solution of ^{234}U and ^{238}U indicate that the U concentration in the fracture surfaces may be much greater than that of Th. The ^{226}Ra content of the groundwaters exceeds that suggested by the above recoil rate, by a factor of about 10 (see below). This suggests that U is preferentially concentrated close to fracture surfaces.

The number ratio of ^{232}Th to ^{228}Th atoms for radioactive equilibrium is about $10^{10}/1$, so that the mass of ^{228}Th in solution is negligible even though its activity is readily determined. The relatively high activities of ^{228}Th do not exceed solubility limits and this suggests that other high specific activity 4-valent activities could have appreciable mobility in the Stripa groundwaters.

3.3 RADON

The ^{222}Rn contents of the deeper Stripa groundwaters are exceptionally high. The waters

* subject to the ^{228}Th residence time exceeding 8.5 a.

from shallow boreholes (up to 60 m depth) have ^{222}Rn contents of 5 - 20 nCi/kg which is typical of other granitic provinces. For the deep groundwaters, values range from 200 - 2,000 nCi/kg.

The ^{222}Rn content of a groundwater is related to the U-content of the rock, $[U]_r$ ppm, and its porosity, ϕ, by the equation:

$$[Rn] = \frac{0.7336\ \rho\ [U]_r}{2.2\ \phi}\ \text{nCi/kg}$$

where ρ is the rock density; if all the ^{222}Rn generated is dissolved in the water. For porosities of about 1 %, this equation yields ^{222}Rn contents which are comparable to those found in waters from the experimental boreholes. This suggests that most of the ^{222}Rn generated in the rock matrix reaches the water phase. The uranium distribution in the granite must therefore be in close contact with the water phase since dispersion within the rock matrix would require ^{222}Rn to diffuse to the water, which would significantly reduce ^{222}Rn contents by decay.

^{222}Rn contents are generally constant within $\pm$ 10 % for constant flow conditions. For borehole V1, however, there was a large decrease in ^{222}Rn content on restoration of flow after a shut-in period (8 September 1981 - figure 3.3). This may have been caused by decay during static fluid storage within the borehole or its associated fractures.

Provided that groundwater residence times are in excess of 25 days, ^{222}Rn contents of the

experimental boreholes are dependent upon the U-contents of the matrix in the borehole locality and upon its fracture porosity. The matrix for M3, E1 and N1 should be similar since they are at about the same depth. At M3, the high ^{222}Rn contents require a low porosity with frequent tight fractures, whilst at E1 and N1 the porosity may be greater and/or the frequency of fractures less. The high ^{3}H content of E1 waters suggests that the low ^{222}Rn content may be due to infrequent high permeability fractures.

The V1 and V2 boreholes have lower ^{222}Rn contents than at M3, possibly due to decrease of $[U]_r$ with depth.

3.4 RADIUM

^{226}Ra, a member of the ^{238}U decay series, is formed by α-decay of ^{230}Th and can therefore enter solution by the α-recoil process. The ^{226}Ra activity in solution at time t, $^{226}A_t$, is given by the equation:

$$^{226}A_t = {}^{226}A_e(1-e^{-^{226}\gamma t})$$

where $^{226}A_e$ is the ^{226}Ra activity in solution after a steady state has been attained and ^{226}Ra activity is then equal to the ^{226}Ra recoil rate.

The ^{226}Ra recoil rate has been estimated from the ^{228}Th activity in the groundwaters (above), but this is likely to be too low because of preferential U concentration on fracture surfaces. The recoil rate may also be estimated from the ^{222}Rn contents of the groundwaters, since this nuclide is also an α-recoil product. This, however, yields too high values for the recoil rate because of the large contribution that diffusion can make to ^{222}Rn escape from

uraniferous surfaces. The ^{226}Ra contents of the Stripa groundwaters increase with depth and the maximum value observed was for borehole V1, which had ~ 110 pCi kg^{-1} ($\equiv$ 240 disintegrations min^{-1} kg^{-1}). In the absence of any precise estimate of the recoil rate, an assumption that the highest observed ^{226}Ra content corresponds to the steady state may be reasonable. This would place the age of the V1 groundwater 8,000 years.

If the V1 groundwater is at recoil equilibrium, the ages of the V2 and M3 waters are then 1,600 years and 120 years respectively. The shallow

groundwaters from private wells around Stripa have ^{226}Ra contents 1 pCi kg^{-1} and their ages are 12 years on this model.

3.5 RADIOGENIC HELIUM

All of the Stripa minewaters contain large amounts of radiogenic ^{4}He (table 3.3). The groundwater ^{4}He content generally increases with depth in the granite (Figure 3.6) and the shape of this concentration/depth profile is very similar to those calculated for diffusive loss ^{4}He from ^{4}He generating rock with one surface open to the atmosphere (Figure 3.7). This suggests that the ^{4}He content of the water is due to diffusive equilibration between the rock and water phases. The amount of ^{4}He generated within a rock of age t years is given by:

$$[He]_{rock} = \rho t\{1.19\times10^{-13}[U]_r + 2.88\times10^{-14}[Th]_r\}$$

cm^3 STP/cm^3 rock

The time required to generate the ^{4}He concentration observed in the V1/V2 groundwaters for the

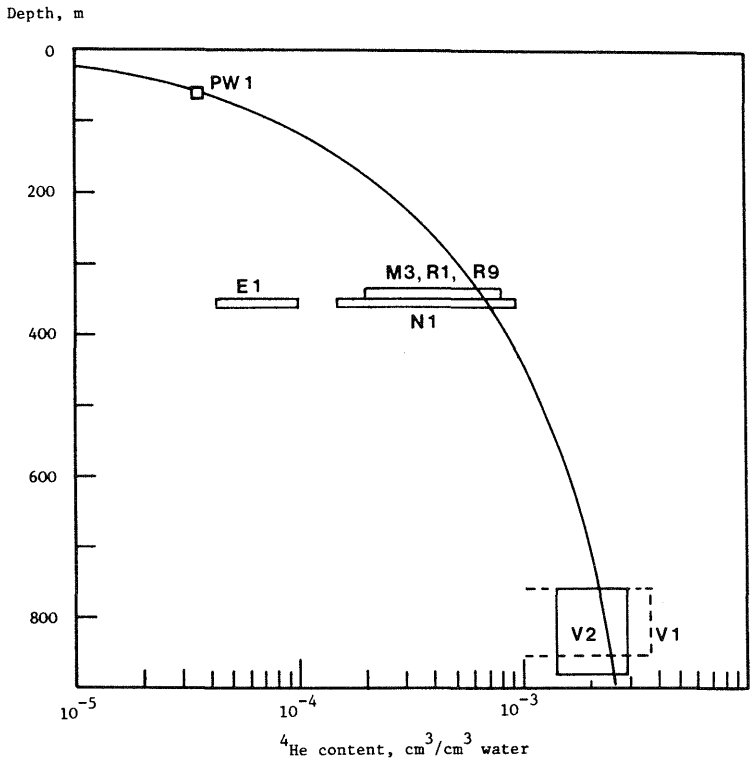

Figure 3.6 The variation of the ^{4}He content of Stripa groundwaters with depth.

radioelement contents typical of the Stripa granite is 170 x 10^6 years, which may be compared with the pre-Cambrian age of the granite.

Some diffusive loss of ^{4}He may have occured from the granites, or groundwater flushing may have removed it. The E1 borehole has an anomalously low ^{4}He content in its groundwater and this suggests that there is a rapid flow of water from shallower depths in this locality. The high ^{3}H content of this water also suggests that it is of recent origin.

3.6 DISSOLVED INERT GASES

The stable inert gas contents of the Stripa minewaters are very variable (table 3) and this suggests that they are frequently contaminated by either excess air or by exsolved gases. All dissolved gases in a groundwater should generally be held in solution at a pressure 3 atmospheres. Exsolution of gases should therefore only occur in

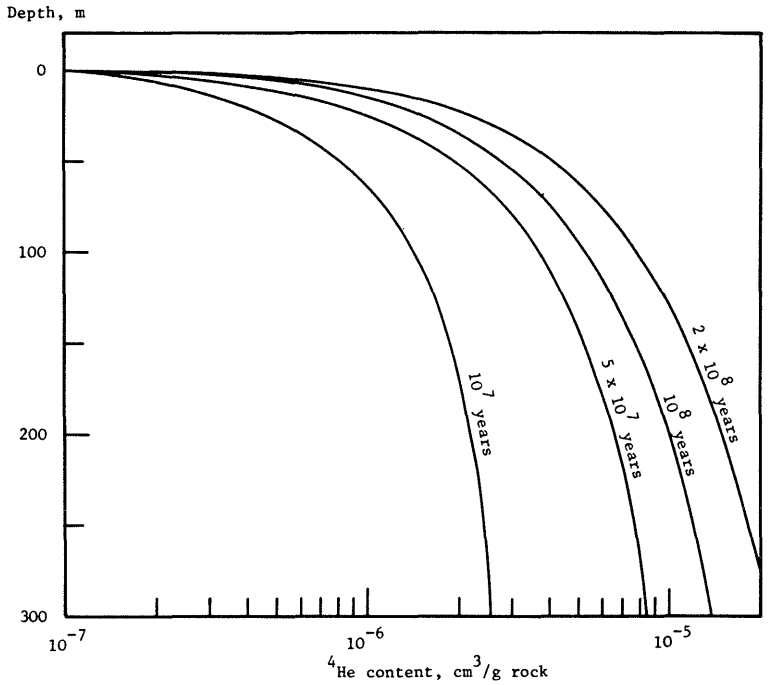

Figure 3.7 The dependence of the radiogenic ^{4}He content on depth and age of rock (For U = 1.5 ppm, Th = 4,5 p and diffusion coefficient = 3.16 x 10^{-3} m^2 a^{-1}.

the uppermost 30 m of water in a borehole. It is thus possible to prevent this exsolution of gases by collecting samples under a pressure head of 30 m. This would enable the amount of any excess air which was introduced in the recharge process to be determined. It is proposed to resample some discharges in this way so that recharge temperatures can be estimated. At the same time, the N_2/Ar ratio will also be determined as a further indicator of the presence of excess air.

3.7 URANIUM SERIES EQUILIBRIA IN THE STRIPA GRANITE

The isotopes ^{238}U, ^{234}U and ^{230}Th are genetically related, being members of the 4n + 2 decay series. Radioactive equilibrium would be established within 1.25 million years as required by the half-lives in the decay sequence:

Table 3.3 Inert gas content of Stripa groundwaters (cm^3 STP/cm^3)

Borehole	Depth Interval	Sampling Date	Analysis No	$^4He \times 10^8$	$Ne \times 10^7$	$Ar \times 10^4$	$Kr \times 10^8$	$Xe \times 10^8$
V1		16.1.81	1450 - 1	21987	11.07	9.78	1.33	-
				21107	11.03	9.20	1.98	0.71
V1		4.6.81	1450 - 2	387403	5.84	8.91	15.39	2.29
				335867	2.72	8.60	14.56	1.58
				103122	3.23	8.62	14.37	3.70
V1	409 - 506 m	14.7.81	1450 - 2	168088	3.30	7.86	13.81	1.70
				133352	2.88	6.96	11.69	1.27
				91911	3.50	6.00	11.35	1.70
V1	409 - 506 m	19.8.81	1450 - 4	371585	4.00	8.33	30.94	-
				160718	3.40	7.58	12.72	1.81
				145270	8.19	7.85	37.52	1.66
V1	409 - 506 m	8.9.81	1450 - 5	299428	-	8.92	27.00	2.06
				297042	1.80	8.16	15.64	1.89
				238388	-	7.68	14.78	1.94
V1	4 - 506 m	9.9.81	1450 - 6	89037	6.07	7.74	14.38	1.87
				168948	-	7.07	13.33	1.77
				154143	3.38	7.20	14.97	1.46
				93301	3.22	6.72	11.79	1.66
V1	4 - 506 m	16.9.81	1450 - 7	88849	2.71	7.17	13.82	1.79
				107998	3.10	7.63	14.27	1.79
				108318	2.66	7.04	14.57	1.63
V1	4 - 506 m	21.9.81	1450 - 8	96958	3.14	7.40	17.98	1.81
				111139	2.82	7.12	-	-
				107574	4.46	8.18	15.43	1.80
M3		12.1.81	1452 - 1	20187	2.77	3.71	1.03	-
				23194	2.69	2.01	-	-
M3		4.6.81	1452 - 2	81967	6.30	7.90	15.15	1.52
				62004	4.85	8.59	17.96	1.91
				32659	3.24	6.08	13.27	1.48
				24479	8.28	7.48	17.54	1.87
V2	356 - 471 m	11.6.81	1453 - 1	288181	-	-	-	-
				257024	-	-	-	-
				171585	4.31	8.10	13.21	1.88
				154769	5.76	9.13	13.77	1.71
				145127	3.83	6.65	-	1.32
V2	356 - 471 m	19.11.81	1453 - 2	148241	10.30	10.00	15.85	0.95
				138565	10.57	9.86	15.54	1.04
V2	6 - 822 m	27.4.82	1453 - 3	115410	3.46	6.86	13.32	1.37
				112454	3.54	7.06	12.63	1.44
				92278	3.04	6.61	12.35	1.44
N1	2 - 300 m	14.7.81	1454 - 1	93614	4.36	6.79	13.06	1.83
				25267	4.13	6.27	11.89	1.31
N1	3 - 300 m	19.8.81	1454 - 2	60917	3.16	5.89	11.47	1.84
				28679	4.42	6.89	13.45	1.54
				15923	3.70	6.09	20.71	1.73
E1	3 - 300 m	11.11.81	1455 - 1	10208	8.87	9.69	-	1.89
				10759	8.65	9.41	16.62	1.92
				5488	6.20	7.83	15.54	1.96
E1	127 - 129.5 m	24.3.82	1455 - 2	5281	2.85	5.29	11.73	1.24
				4374	2.80	5.36	12.01	1.36
				6780	2.85	5.33	11.43	1.32

Table 3.4 ^{222}Th content, $^{230}Th/^{234}U$ ratio and ^{228}Th content of Stripa groundwaters.

Sample number+	Collection date	Description		^{232}Th content µg kg^{-1}	$^{230}Th/^{234}U$	^{228}Th dpm kg^{-1}	^{228}Th equiv. ^{232}Th µg kg^{-1}
1450-2F	11-6-81	VI	409-506 m	0.081 ± 0.027	0.0051	---	---
1450-3F	14-7-81	VI	409-506 m	---	---	6.954	28.27
1450-3U	14-7-81	VI	409-506 m	0.274 ± 0.064	0.0319	---	---
1452-2F	3-6-81	M3		---	---	7.885	32.05
1452-2U	3-6-81	M3		0.113 ± 0.035	0.0013	---	---
1453-1F	11-6-81	V2*	356-470 m	---	---	6.402	26.02
1453-1UF	11-6-81	V2*	356-470 m	>0.071 ± 0.028	0.0221	---	---
1454-1	14-7-81	N1	2-300 m	0.232 ± 0.081	0.0012	---	---

* formerly DBH VI
\+ F = 0.45 µm filtered sample
U = unfiltered sample

^{238}U —α,2ß→ ^{234}U —α→ ^{230}Th —α→

half-life: 4.5×10^9 a; 2.48×10^5 a; 8×10^4 a

The equilibria $^{234}U/^{238}U$, $^{230}Th/^{238}U$ and $^{230}Th/^{234}U$ may therefore be used to determine whether or not closed system conditions for U and Th have persisted within a rock over this time scale.

Samples of the Stripa granite from four locations were crushed to sub-micron size and then dissolved in HF in a Teflon pressurized digestion vessel. U and Th were subsequently separated by anion exchange, electrodeposited on stainless steel and determined by alpha-spectrometry. The natural U and Th contents and the various activity ratios are reported in table 3.5. The U and Th contents of a 12.8 m core from the 330 m level in the Stripa mine were determined (Nelson et al, 1979)by γ-spectrometry. The U-content was 44.0 ± 24.6 µg/g

Table 3.5 γ-Spectrometric determination of the U, Th and K contents of the Stripa granite.

Analysis No.	Borehole	Depth, m	U-content μg g^{-1}	±	Th-content μg g^{-1}	±	Th/U	K-content, %	±
601	N1	22.53- 22.60	42.16	0.25	49.97	0.89	1.19	4.05	0.04
602	N1	282.03-282.11	20.24	0.20	29.00	0.83	1.43	2.98	0.03
603	E1	22.37- 22.43	26.72	0.22	48.88	0.88	1.83	4.34	0.03
604	E1	286.41-286.47	43.35	0.25	50.30	0.89	1.16	4.18	0.04
605	V1	25.51- 25.59	40.83	0.25	59.14	0.91	1.45	3.91	0.04
606	V1	75.45- 75.52	75.17	0.30	55.22	0.90	0.73	4.22	0.04
607	V1	128.44-128.54	39.09	0.24	45.24	0.88	1.16	3.84	0.03
608	V1	186.34-186.41	38.78	0.24	47.17	0.88	1.22	4.05	0.04
609	V1	228.75-228.82	42.89	0.25	47.42	0.88	1.11	3.99	0.04
610	V1	282.47-282.53	48.75	0.26	53.37	0.90	1.09	4.06	0.04
611	V1	330.41-330.49	47.97	0.26	54.38	0.90	1.13	4.16	0.04
612	V1	385.46-385.54	35.40	0.24	52.02	0.89	1.47	4.16	0.03
613	V1	432.29-432.38	42.79	0.25	49.25	0.89	1.15	3.86	0.04
614	V1	498.16-498.25	39.67	0.24	46.22	0.88	1.17	4.27	0.04
615	V1Exc.	-	39.18	0.24	44.86	0.87	1.14	4.05	0.04
		Average (605-615)	44.59	10.38	50.39	4.49	1.21	4.05	0.14
625	V2	00.97- 01.06	42.54	0.24	54.80	0.90	1.29	4.27	0.04
626	V2	55.22- 55.31	43.98	0.24	55.78	0.90	1.27	4.27	0.04
627	V2	106.03-106.13	36.13	0.22	41.59	0.86	1.15	3.67	0.04
628	V2	147.08-147.19	38.79	0.23	45.93	0.87	1.18	3.91	0.04
629	V2	196.04-196.15	40.23	0.23	55.51	0.90	1.38	4.25	0.04
630	V2	249.68-249.78	42.34	0.24	56.98	0.90	1.35	4.36	0.04
631	V2	303.10-303.20	42.34	0.24	57.31	0.90	1.35	4.33	0.04
632	V2	348.52-348.61	42.59	0.24	59.32	0.91	1.39	4.32	0.04
633	V2	400.54-400.64	42.95	0.24	59.86	0.91	1.39	4.23	0.04
634	V2	448.79-448.90	43.13	0.24	56.57	0.90	1.31	4.63	0.04
635	V2	503.84-503.95	45.07	0.24	57.26	0.90	1.27	4.34	0.04
636	V2	548.78-548.86	41.90	0.23	52.95	0.89	1.26	4.21	0.04
637	V2	599.21-599.30	42.53	0.23	52.27	0.89	1.23	4.13	0.04
638	V2	645.11-645.19	44.84	0.24	57.01	0.90	1.27	3.86	0.04
639	V2	701.54-701.66	46.47	0.24	58.06	0.90	1.25	4.30	0.04
640	V2	750.93-751.03	47.89	0.25	60.84	0.91	1.27	4.31	0.04
641	V2	800.14-800.25	47.51	0.25	64.46	0.92	1.36	4.36	0.04
642	V2	817.44-817.53	53.74	0.26	70.30	0.93	1.31	4.09	0.04
		Average (625-642)	43.61	3.72	56.49	6.08	1.29±0.07	4.21	0.21

Note: The errors quoted for individual determinations are 2σ errors based on counting statistics. The errors for the set averages are the standard deviation for the set.

and the Th-content was 30.1 ± 15.2 μg/g. More precise determinations of the U-content (Andrews et-al, 1982), by delayed neutron activation, ranged from 37.3 - 39.9 μg/g for samples from the 330 and 410 mine galleries. The U-contents of the granite samples from the extensometer drift and the V1 excavations (table 3.5) are comparable with those determined by delayed neutron activation, and the Th-contents are within the range found by Nelson et al. The granite from the extensometer drift is in isotopic equilibrium ($^{234}U/^{238}U = {}^{230}Th/^{238}U =$

Table 3.6 Radioelement determinations on Stripa granites.

Sample	U-content µg/g	Th-content µg/g	$^{234}U/^{238}U$	$^{230}Th/^{238}U$ activity ratios	$^{230}Th/^{234}U$
A	19.1 ± 0.8	24.4 ± 0.9	0.74 ± 0.05	1.15 ± 0.04	1.55
	18.5 ± 0.6	27.2 ± 1.9	0.75 ± 0.04	1.27 ± 0.07	1.69
B	24.2 ± 0.7	12.0 ± 0.6	0.98 ± 0.04	0.78 ± 0.03	0.80
	26.1 ± 0.8	15.0 ± 0.7	1.00 ± 0.04	0.94 ± 0.04	0.94
C	38.6 ± 0.9	25.8 ± 1.1	1.00 ± 0.03	1.00 ± 0.03	1.00
	38.2 ± 0.9	24.8 ± 1.2	1.02 ± 0.03	0.91 ± 0.03	0.89
D	36.5 ± 0.8	19.2 ± 1.3	0.99 ± 0.03	0.72 ± 0.03	0.73
	36.0 ± 0.6	16.1 ± 0.9	0.96 ± 0.03	0.61 ± 0.02	0.63

A. Grey granite from outcrop.
B. Pink granite from outcrop.
C. Granite from extensometer drift, 350 m depth.
D. Granite from VI excavation, 350 m depth.

$^{230}Th/^{234}U = 1$) and has therefore been undisturbed over the last 1.25 Ma. That from the Vl excavation, however, is apparently depleted in ^{230}Th. Since Th is not mobile in natural waters, this can only be explained as a consequence of uranium deposition. The effect needs confirmation with other samples.

The grey granite (the most typical of the granites at Stripa) from outcrop has a depleted $^{234}Th/^{234}U$ ratios. This behaviour is expected when uranium is mobilised by groundwaters and when ^{234}U is preferentially mobilised relative to ^{238}U. The pink granite is in U/Th equilibrium and shows no evidence of uranium loss. Its radioelement contents (both U and Th) are much less than those for the granites at depth. The grey granite has a Th-content similar to that for the deeper granites. If it had an original U-content similar to that in the deep granite, the $^{230}Th/^{238}U$ ratio would be about 2

for recent loss uranium and the observed $^{230}Th/^{238}U$ ratio shows that the loss must have occurred over a period in excess of 150,000 years. Alternatively, if the uranium leaching is a recent occurrence, the original U-content of this outcrop granite cannot have exceeded 24 μg/g.

The mobility of uranium series nuclides within the Stripa granites is very significant in relation to actinide mobility in the system and further work is required to fully define the changes which are occurring between outcrop and the deep granites in the mine.

3.8 SUMMARY OF CONCLUSIONS

The Stripa groundwaters are actively disturbing the uranium geochemistry in the granite, primarily as the result of chemical etch processes. Preferential solution of ^{234}U occurs but the amount of dissolved uranium present is very dependent upon the flow regime. Natural thorium is not dissolved by the groundwater, but significant amounts of high specific activity nuclides such as ^{228}Th can enter solution. These findings are very pertinent to the problem of actinide mobility in radioactive waste disposal.

Uranium series methods cannot be applied to groundwater age determination at the Stripa site because of the open-system uranium chemistry.

The ^{226}Ra content of the groundwaters increases with groundwater age and suggests that the V1 groundwater is oldest, and that V2 and M3 waters have residence times of order 2,000 and 100 years respectively.

The radiogenic ^4He contents of the groundwaters are due to diffusive leakage from the granite into water-filled fractures. The ^4He-contents, though high, are less than those calculated for equilibration with the granite and suggest that active groundwater flow is reducing the ^4He-content of the rock by ^4He-transport.

4 STABLE ISOTOPES GEOCHEMISTRY IN GROUNDWATER SYSTEMS FROM STRIPA SITE

4.1 OXYGEN 18 AND DEUTERIUM

4.1.1 Introduction

Several oxygen 18 and deuterium measurements have been performed on Stripa groundwater systems since the beginning of the LBL-KBS project. Basic principles and a discussion of results can be found in Fritz et al, 1979, 1980.

New data obtained in the framework of the Stripa project by several laboratories: University of Waterloo (UW), International Atomic Energy Agency (IAEA), Gesellschaft für Strahlen und Umwelt-forschung MBH München (GSF), Université de Paris-Sud (UPS) are gathered in table 1 together with a summary of data from LBL-KBS project. Some results from UPS which necessitate some more analytical effort will be available in the near future.

4.1.2 Methodological aspects

Stable isotopes analyses are used to distinguish waters from different origins when ^{2}H and ^{18}O contents are conservative. They may be used to study diagenetic and/or reactions with rocks and minerals when ^{2}H and ^{18}O contents are not conservative.

4.1.2.1 Conservative stable isotope contents

This case deals with groundwater systems in which ^{2}H and ^{18}O contents are defined by recharge processes and remain unchanged during groundwater flow. Natural labelling conditions have been extensively and recently reviewed (see e.g Fontes, 1980, IAEA 1981, 1982, 1983). For practical purpose one considers two cases:

- non evaporated waters before or during the recharge:

  - stable isotope content decrease with the number of condensation stages of the initial vapour, i.e. mainly with temperature (altitude effect, seasonal effect, paleoclimatic effect) following a slope of 8 in the $\delta^{2}H$ - $\delta^{18}O$ diagram;

- in evaporated waters before or during the recharge:

  - stable isotpe content increase with the amount of evaporated water, following slope variable but lower than 8 in the $\delta^{2}H$ - $\delta^{18}O$ diagram.

A crucial parameter for the discussion of the origin of a given water is thus the deuterium excess (Dansgaard, 1964):

$$d = \delta^{2}H - 8\ \delta^{18}O \text{ (per mil)}$$

Values of d are generally close to 10 $^{0}/_{oo}$ in present day oceanic precipitation (Craig, 1961; Yurtsever and Gat, 1981) and, depending on the slope, are obviously much lower for evaporated waters.

In our state of knowledge two causes of variation may influence d values in non evaporated precipitation:

- the participation of vapour originated in closed (evaporated) basins under kinetic conditions to the condensing atmospheric vapour.

- a global change in climatic conditions of oceanic vapour formation (paleoclimatic effect).

The former case is noteworthy in the Mediterranean basin (Nir, 1967, Gat and Carmi, 1970) where d reaches + 22 o/oo. The latter case is strongly suspected through values as low as 5 o/oo found in ancient groundwaters e.g. in Sahara deep confined aquifer (Gonfiantini et al, 1974; Fontes, 1981). Direct evidence for d values lower than present and close to + 5 o/oo as well were recently obtained on Antarctic ice core profiles from last glacial age (Jouzel et al com.pers.). In that case the decrease of d values is probably due to an average relative humidity higher than present day ones, indicating cooler conditions over tropical and equatorial oceanic masses.

Deuterium excess investigation appears therefore as a powerful tool for groundwater identification. It is anyway much safer than the study of only ^{2}H or ^{18}O contents. Such a limited study does not allow to characterize the origin of initial vapour and variations may only be due to local conditions of recharge (e.g. exceptional rains or floods) without any significant change in general climatic conditions. However, by definition, deuterium excess vakues cumulate both ^{2}H and ^{18}O analytical errors (1 to 1.5 o/oo). Therefore they require accurate and repeated measurements in order to get the best attainable definition.

4.1.2.2 Non conservative stable isotope contents

Oxygen 18 and/or deuterium contents of groundwaters may not be conservative in some special hydrogeological and chemical situation:

- high temperature environment (geothermal) lead to an exchange between ^{18}O rich minerals from rocks and therefore to an increase of ^{18}O content of waters (see e.g. Painichi and Gonfiantini, 1982); such enrichment persists after cooling;

- environments rich in fluids where CO_2 and H_2S release may represent a significant amount with respect to oxygen and hydrogen atomic content in waters;

These processes lead to significant isotope fraction in heavy isotopes. (Friedman and /O'Neil, 1977). Exchange with gaseous carbon dioxide depleted the water in ^{18}O whereas H_2S exchange produces an increase of ^{2}H content of the water;

- cristallization of clay minerals from weathering solutions of feldspars or micas occurs with an enrichment in oxygen 18 and a depletion in deuterium (see Savin, 1980); the remaining atomic fractions of oxygen and hydrogen in the water may be significantly depleted in ^{18}O and enriched in ^{2}H respectively.

- low temperature isotopic exchange between clay minerals and water will produce the same kind of isotope effect the amount of which will depend on the repsective proportions of atoms in clays and in water; such a process would require dead endpores (stagnant waters), low flows and low permeability rocks.

4.1.3 Discussion and interpretation

Main features observed by Fritz et al, 1979, 1980 are confirmed.

A clear-cut distinction is observed between deep and subsurface groundwaters (Table 4.1 and Figure 4.1).

Subsurface groundwaters from private well (PWI) lie much below meteoric water line. This may reflect the evaporation during the melting of the snow blanket before infiltration. Surface water (Hammarskogsån creek) in draining position and thus integrating shallow aquifer stable isotope content suggests that local and recent infiltration shows an isotopic signature of evaporation.

Deep waters, depleted in heavy isotopes as compared to subsurface waters, lie close to the present day global meteoric water line (MWL). Deep groundwaters are probably not evaporated (if they were evaporated it would mean that local meteoric water line, at infiltration time, would have been much above the global MWL.

Heavy isotope contents of deep groundwaters are rather variable from well to well and within a given well, depending on the respective packer intervals. If one excludes (as an a priori which should be checked) that time variations can occur in a confined aquifer system this suggests either that the system is heterogeneous and delivers water of various origin or, that mixing occurs between, at least, two sources of waters.

The somewhat regular chemical and isotope dependence with depth (Fritz et al, 1980) is in favour of the hypothesis of a two terms mixing.

Table 4.1 Stable isotopes in Stripa groundwaters.

Borehole V_1. V_1 .

DATE	Depth	$\delta^{18}O(H_2O)$ ‰ vs SMOW	$\delta^{2}H(H_2O)$ ‰ vs SMOW	$\delta^{18}O(SO_4^{=})$ ‰ vs SMOW	$\delta^{34}S(SO_4^{=})$ ‰ vs CD	^{3}H T.U.	An.
81/06	409 506	-12.8(1)	-93(1)	+7.80(11)	+12.84(11)	-	UW(1) UPS(11)
"	"	-13.0	-	-	-	-	UW
"	"	-13.0	-	-	-	-	UW
"	"	-12.9	-	-	-	-	UW
"	"	-13.0	-	-	-	-	UW
"	"	-13.0	-	-	-	-	UW
81/07	"	-13.25	-	-	-	-	UPS
81/08	"	-12.5	-89.6	-	-	-	IAEA
"	"	-12.92	-91.7	-	-	-	GSF
81/08 (N_2)	"	-12.91	-92.2	-	-	-	GSF
81/09	"	-12.80	-91.6	-	-	1.1±0.7	GSF
81/11	5 506	-13.08	-	+8.10	+13.96	-	UPS
82/06	5 506	-13.10	-93.0	+7.81	+13.79	-	UPS

Table 4.1 Continued

Borehole V_2.

DATE	Depth	$\delta^{18}O(H_2O)$ ‰ vs SMOW	$\delta^{2}H(H_2O)$ ‰ vs SMOW	$\delta^{18}O(SO_4^{=})$ ‰ vs SMOW	$\delta^{34}S(SO_4^{=})$ ‰ vs CD	^{3}H T.U.	An.
77/78		-11.9 to -13.2	-88.8 to -95.9	-	-	-	UW
78/11	401 428	-	-	-	+20.1	-	UW
79/05	"	-	-	+8.5	+17.4	-	UW
81/06	356 470	-13.6(1)	-97(1)	+7.95(11)	+15.04(11)	-	UW (1) UPS (1
81/06		-13.3	-	-	-	-	UW
81/11	0* 356	-13.19		-	-	-	UPS
81/11	356 471	-12.9	-93.1	-	-	-	IAEA
82/04	6 822	-12.8	-	-	-	-	IAEA
82/04	"	-12.84	-91.9	-	-	1.0±06	GSF

Borehole N_1.

DATE	Depth	$\delta^{18}O(H_2O)$ ‰ vs SMOW	$\delta^{2}H(H_2O)$ ‰ vs SMOW	$\delta^{18}O(SO_4^{=})$ ‰ vs SMOW	$\delta^{34}S(SO_4^{=})$ ‰ vs CD	^{3}H T.U.	An.
81/08	3 300	-12.6	-89.5	-	-	-	IAEA
82/06	"	-12.97	-93.6	+5.27	+27.92	-	UPS
82/06	"	-12.8	-89.0	-	-	-	IAEA

* Sampling depth to be confirmed.

Table 4.1 Continued

Borehole E_1.

E_1.

DATE	Depth	$\delta^{18}O(H_2O)$ ‰ vs SMOW	$\delta^{2}H(H_2O)$ ‰ vs SMOW	$\delta^{18}O(SO_4^{=})$ ‰ vs SMOW	$\delta^{34}S(SO_4^{=})$ ‰ vs CD	^{3}H T.U.	An.
81/06		-12.7	-	-	-	-	UW
81/11	3 300	-12.80		-	-	-	UPS
82/03	127.5 129.5	-12.00	-86.4	-	-	42.6±3.1	GSF
82/06	0 267	-12.66	-90.5	-	-	-	UPS

Borehole M_3.

M_3.

DATE	Depth	$\delta^{18}O(H_2O)$ ‰ vs SMOW	$\delta^{2}H(H_2O)$ ‰ vs SMOW	$\delta^{18}O(SO_4^{=})$ ‰ vs SMOW	$\delta^{34}S(SO_4^{=})$ ‰ vs CD	^{3}H T.U.	An.
77/78		-11.8 to -12.2	-86.4 to -87.9	-	-	-	UW
81/06	3 4	-12.3	-87	-	-	-	UW
81/07	3 10	-12.60		-	-	-	UPS
82/06		-12.32	-87.7	+0.78	+11.28	-	UPS

Borehole R_1.

R_1.

DATE	Depth	$\delta^{18}O(H_2O)$ ‰ vs SMOW	$\delta^{2}H(H_2O)$ ‰ vs SMOW	$\delta^{18}O(SO_4^{=})$ ‰ vs SMOW	$\delta^{34}S(SO_4^{=})$ ‰ vs CD	^{3}H T.U.	An.
77/08		-	-	+8.8	+20.7	-	UW
81/06		-11.9	-8.2	-	-	-	UW

Table 4.1 Continued

Private Well 1 — PW1

DATE	Depth	$\delta^{18}O(H_2O)$ ‰ vs SMOW	$\delta^{2}H(H_2O)$ ‰ vs SMOW	$\delta^{18}O(SO_4^{=})$ ‰ vs SMOW	$\delta^{34}S(SO_4^{=})$ ‰ vs CD	^{3}H T.U.	An.
77/09		-10.8	-81.3	-	-	-	UW
79/05		-	-	-	+7.6	-	UW
82/06		-11.56	-82.5	+4.28	+5.13	-	UPS

Private Well 4 — PW4

DATE	Depth	$\delta^{18}O(H_2O)$ ‰ vs SMOW	$\delta^{2}H(H_2O)$ ‰ vs SMOW	$\delta^{18}O(SO_4^{=})$ ‰ vs SMOW	$\delta^{34}S(SO_4^{=})$ ‰ vs CD	^{3}H T.U.	An.
79/05		-	-	-1.7	+2.8	-	UW
82/06		-12.91	-93.4	+1.02	+3.60	-	UPS

Surface Water. — SW

DATE	Depth	$\delta^{18}O(H_2O)$ ‰ vs SMOW	$\delta^{2}H(H_2O)$ ‰ vs SMOW	$\delta^{18}O(SO_4^{=})$ ‰ vs SMOW	$\delta^{34}S(SO_4^{=})$ ‰ vs CD	^{3}H T.U.	An.
77/09		-9.1	-73.4	-	-	-	UW
82/06		-10.73	-80.8	-	-	-	UPS

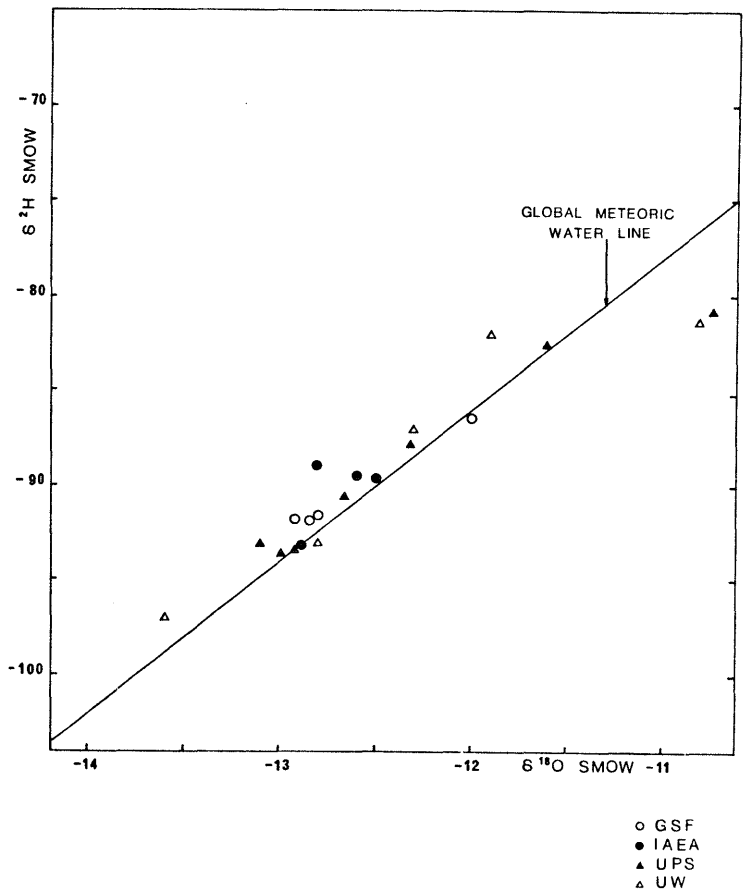

Figure 4.1 Deuterium and oxygen 18 content of waters from Stripa. Symbols refer to Table 1.

Since local and surficial groundwaters are affected by evaporation and do not preserve the initial stable isotope content of precipitation it is difficult to evaluate the isotopic difference between shallow and deep groundwaters.

Extrapolating shallow water values along evaporation lines to the global MWL one may evaluate a maximum value of about 1.5 o/oo for the difference in ^{18}O content. According to common values of the isotopic gradient in altitude this figure would imply a difference of several hundreds of meters between the respective areas of recharge (possibly 500 m).

Fritz et al, 1980, point out that the occurence of such a regional flow is unlikely.

Exceptional pluvial events may also be invoked to account for the difference between shallow and deep water. It is well known that heavy precipitations are significantly depleted in heavy isotopes as compared to average values at a given location. (Yurtsever and Gat, 1981). However, this interpretation implies extreme conditions of the same meteorological regime. In other terms it means that representative points of both subsurface and deep waters lie upon the same local meteoric water line in the δ^2H - $\delta^{18}O$ diagram.

Since present day local MWL is not available one cannot decide whether deep groundwaters are isotopically compatible with present day precipitation.

The deuterium excess of deep waters appears somewhat higher than in surface waters and in precipitation at the global scale. This suggests that deep groundwaters originated under different meteorological conditions from present day oceanic ones. However, care should be taken in such an interpretation because:

- differences remain small (maximum 4 o/oo);

- subsurface water may have not preserved their initial deuterium excess;

analyses were made in various laboratories and systematic deviations may occur;

- H_2S and HS^- occurence have been detected in deep waters and could account for a increase of their ^2H content.

4.1.4 Recommendations

Despite rather large number of analyses has been made on the Stripa system, conclusions remain highly hypothetical and it is still not possible to decide whether deep waters have really a paleo-waters isotopic signature.

Reasons for that are:

- the lack of reference on present day precipitations and infiltration (shallow groundwaters);

- the lack of statistical values for the definition of the deuterium excess in each single well

It is suggested to collect and analyze oxygen 18 and deuterium contents:

a) of monthly samples of precipitations on some (three or four) selected stations at different altitudes over one year in order to draw the present day regional range of variations of heavy isotope content and relative deuterium excess;

b) of selected supplementary surficial samples (about 15) of groundwater in order to obtain a precise evaluation of the heavy isotope content of the recharge;

c) of time seried (monthly) sampling of the deep boreholes in order to correlate variations at depth with ionic contents and investigate mixing processes and possible exchange reactions involving H_2S.

For internal coherence of data it would be appropriate to organize an analytical inter-comparison between the laboratories involved in the program and to make repeated measurements in order to improve the definition of deuterium excess values. Furthermore the obtention of values of time variations of deuterium excess in arctic ice could be possible encouraged for comparison purpose with deep water in Stripa.

4.2 STABLE ISOTOPE CONTENT (^{34}S, ^{18}O) OF SULPHUR COMPOUNDS

4.2.1 Introduction

Sulphur cycle (s) in the Stripa groundwater system displays a special interest due to:

- the relatively large amount of SO_4^{2-} content in the system and its variations (0.5 to 500 ppm);

- the increase in SO_4^{2-} with depth and TDS;

- the occurence of both reduced and oxidized forms of aqueous sulphur correlated to a large range of redox conditions (highly oxidizing in subsurface waters and reducing in deep waters);

- the identification of solid sulphides, possibly pyrite, in the rock matrix.

In order to investigate the origin of sulphur and processes which lead to its variations a detailed isotopic study was planned in the Stripa project. A preliminary investigation on stable isotope content of aqueous sulphate was conducted in the framework of the LBL/KBS project (Fritz and Baker, unpublished data).

Because the isotopic cycles of sulphur are rather complicated, the discussion of available data is preceded by a review of basic information dealing with natural isotopic variations of sulphur compounds.

4.2.2 Variations of stable isotpes contents of sulphur compounds

4.2.2.1 Isotopes effects

Defination. Sulphur compounds are involved in numerous reactions (chemical and biological which are generally isotope partitioning. Isotopes fractionation affect also ^{18}O contents of oxidized compounds (chiefly sulphate).

Sulphur 34 and/or oxygen 18 distribution between two compounds 1 and 2 of geochemical cycles of sulphur is expressed according to the noteworthy general otations valid for all environmental isotopes (see Friedman and O'Neil, 1977):

$$\alpha = R_2^1 \quad \text{and} \quad \varepsilon = (a-1)\ 1000 \simeq 1000\ \ln\alpha \simeq \delta_1 - \delta_2$$

$$\text{where } R = \frac{^{34}S}{^{32}S} \text{ or } \frac{^{18}O}{^{16}O} \text{ and } \delta = \frac{R_{sample}}{R_{standard}} - 1 \quad 1000$$

Standards reporting heavy isotope contents are:

- canyon Diablo (CD) for ^{34}S: troilite (high temperature FeS) from a meteorite;

- Standard Mean Ocian Water (SMOW) for ^{18}O.

Equilibrium (thermodynamic) isotope effect are generally very high for sulphur compounds especially at low temperatures (see Friedman and O'Neil, 1977). However, because of technical

problems and low reaction rates low temperature measurements remain unfrequent and corresponding values are generally deduced from extrapolation of high temperature experiments or from theoretical calculations.

In the specific case of elements like which sulphur enter into metabolic cycles another type of isotope effect may occur under the influence of biocatalysts which increase preferentially rates of chemical as well as of isotopic reactions. In these conditions isotope effects are no longer equilibrium but kinetic fractionations.

Generally kinetic isotope fractionations are not only temperature dependent (as equilibrium fractionation) but depend also upon environmental conditions. Values for kinetic isotope effect are thus rather defined within ranges of variations than as precised values.

As a general rule biochemical catalysts involve preferentially common i.e. light isotopes giving rise to a heavy isotope concentration in the unmetabolized fraction.

Reservoir effects (open and closed systems). When a reaction involve two components, one of which containing a negligible amount of a given isotope with respect to the other one, the isotopic difference between the two products is equal to the enrichment factor at any time. This is for instance the case for ^{18}O enrichment between calcite and water during precipitation. The process occurs in open system.

However, in the case of sulphur system all isotopic reactions affect the heavy isotope content of both reactants and products. Processes

occur in closed system. Closed system process are described by the Rayleigh's equation:

$$\delta - \delta_o \simeq 0\varepsilon\ nf$$

in which the isotopic enrichment $\delta - \delta_o$ of the reactant is correlated to the logarithm of the remaining fraction f through the isotopic enrichment factor ε.

A special treatment of the closed system is necessary when both reactant and product remain homogeneized within the same reservoir. In that case the observed isotopic difference Δ between product p and reactant r is (see e.g. Fritz and Fontes, 1980):

$$\Delta = \delta_r - \delta_p = -\frac{\varepsilon \ln f}{(1 - f)}$$

This may be the case when suphate and H_2S are involved in redox processes in groundwaters.

As expected from the numerous steps of its geochemical cycles, the isotopic cycle of sulphur compounds in lithosphere and hydrosphere is highly complex. For simplification purpose it will be retained here under that sulphur is mainly represented under two chemical forms:

- reduced: gaseous and aqueous H_2S, agueous HS^- and solid sulphides (e.g. pyrite).
- oxidized: aqueous SO_4^{2-} and evaporites (chiefly gypsum and anhydrite).

4.2.2.2 Reduced species of sulphur

Due to the occurence of kinetic and reservoir effects in their formation a large range of ^{34}S contents is observed in natural sulphides.

For instance sedimentary pyrites may show ^{34}S values from - 50 to 70 per mill (see Krouse, 1980). However sedimentary sulphides are generally depleted in ^{34}S with respect to coexisting sulphates. When formed at high temperatures from primordial (mantle) sulphur, volcanic H_2S rains generally close to the standard troilite and shows isotopic composition nearby zero or slightly negative.

Because reducing conditions are not frequent in groundwater systems and because the solutility of sulphur reduced species is low, the most frequent form of dissolved sulphur is sulphate.

4.2.2.3 Sulphates (Figure 4.2)

Ocean and rain-out. Oceanic masses provide the main reservoir of sulphate. Because of a steady state process between input (river) and outputs (precipitation and reduction) the isotopic composition of the oceanic sulphate is very homogeneous:

$$\delta^{18}O\ (SO_4^{2-}) = +\ 9.5 \text{ vs SMOW}$$

$$\delta^{34}S\ (SO_4^{2-}) = +\ 20.0 \text{ vs C.D.}$$

Meteoric sulphates from oceanic rains and aerosols (unpolluted by industrial dusts and smokes) show similar values (Mizutani and Rafter, 1969 c; Rightmire et al, 1974).

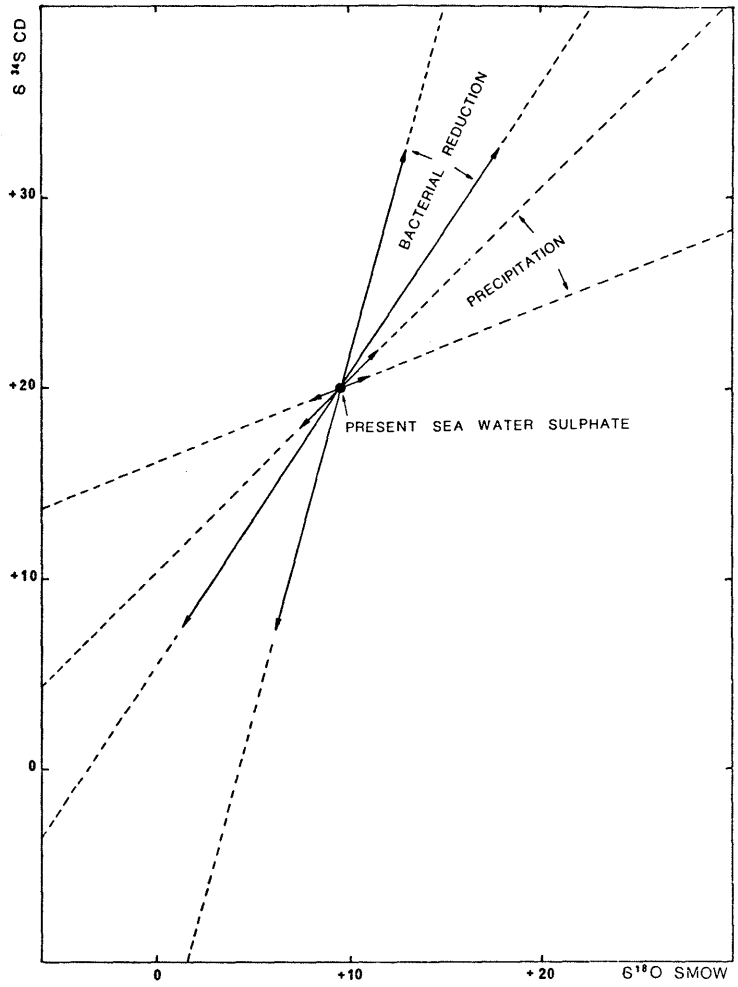

Figure 4.2 Sulphur 34 and oxygen 18 evolution of present day aqueous oceanic sulphate during crystallization of sulphate and sulphate reduction. Solid arrows: one stage process.

Solid sulphate. When a sulphate precipitates and isotopic fractionation occurs:

δ (solid sulphate) = δ (aqueous sulphate) + ε_p
where ε_p states for the isotopic enrichment factor during precipitation (FRITZ and FONTES, 1980).

Experimental and field values for ε_p fall in the following ranges (for gypsum and anadrite precipitation):

3.0 ε_p ($^{18}0$) 4°/oo (Lloyd, 1968; Fontes and Schwarcz, unpublished data; Pierre, 1982).

1.4 $\varepsilon_p(^{34}S)$ 3.4 °/oo (Thode and Monster, 1965; Pierre, 1982).

Obviously after precipitation took place the remaining aqueous sulphate is depleted in heavy isotopes and further precipitation stages lead to solid sulphate depleted in ^{34}S and ^{18}O with respect to initial aqueous SO_4^{2-}. Complex (Mg, K) marine sulphates show ^{34}S content lower than ocean average (Nielsen and Ricke, 1964).

Sulphate reduction. Reduction processes hardly occur at low temperatures except if sulphate reducing bacteria are present in the environment (e.g. Desulfovibrio desulfuricans. Kinetic enrichments and steady state conditions become predominent. As seen before products from biosynthesis are depleted in heavy isotopes.

When a bulk of sulphate is reduced the remaining part of SO_4^{2-} is enriched in heavy isotopes:

δ (aqueous sulphate) = $\delta(H_2S$ gaseous) + ε_r (eq) with values of about 80 °/oo at 30°C (see Friedman and O'Neil, 1977).

The equilibrium enrichment appears therefore much higher than kinetic values.

The behaviour of oxygen isotopes in reduction processes can only be investigated indirectly since water - the resulting oxygen bearing compound in the reaction - is mixed with environmental water. However, the remaining aqueous SO_4^{2-} becomes enriched in ^{18}O by about 1/4 of the ^{34}S enrichment (Rafter and Mizutani, 1967: Mizutani and Rafter, 1969). One can thus admit that typical values of ε_r(kin) for ^{18}O are close to +6,0 °/oo.

However, because rates of kinetic reactions are generally specific of a given environment, values of ε_r(kin) may exhibit a large range of variations. Mizutani and Rafter report values of the ratio $\varepsilon^{34}S$ (kin) / $\varepsilon^{18}O$ (kin) ranging between -7,8 abd + 23,5. In reducing evaporitic ponds Zak et al (1980) and Pierre (1982) found values close to +1,5 for this ratio.

Sulpide and H_2S oxydation. - Sulphur isotope behaviour. Reduced sulphur is quickly transformed into S^0, SO_3^{2-} and finally SO_4^{2-} when groundwater circulation reaches an oxidizing zones and/or mixes with superficial waters saturated with oxygen.

Beside inorganic processes, oxidation may occur through biological (bacterial) activity (Thiobacillus thiooxydans).

Further experimental data are still needed about isotope fractionation occuring during oxidation. It is generally admitted (see Krouse, 1980; Pearson and Rightmire, 1980) that the pure chemical process is not fractionating whereas slight depletion in ^{34}S may occur through bacterial formation of SO_4^{2-} (Kaplan and Rittenbergg, 1964).

- Oxygen isotope behaviour. The atoms of oxygen which participate to sulphate ion formation from H_2S (or HS^- and S^{2-}) may have several origins. It has been shown by Lloyd (1967, 1968) and by Mizutani and Rafter (1969 a, 1969 b) that part of the oxygen involved in the process comes from environmental water and part from dissolved (molecular) oxygen:

$$S + H_2O + O \leftarrow SO_3 + H_2$$

$$SO_3^{2-} + \frac{1}{2} O_2 \rightleftarrows SO_4^{2-}$$

According to Lloyd (1968) the isotopic balance requires that a proportion of 1/3 of oxygen atomes be supplied by the water and 2/3 by dissolved oxygen. The incorporation of water oxygen into the sulphur bond would occur without fractionation. The admixture of dissolved oxygen is isotope fractionating:

$\delta^{18}O$ (dissolved oxygen) = $\delta^{18}O$ (binding oxygen) + ε_{ox}. The isotope enrichment factor ε_{ox} is 8,7 °/oo (Lloyd, 1968).

In that case the oxygen 18 content of a sulphate ion formed through sulphide or H_2S oxidation becomes

$$\delta^{18}O\ (SO_4^{2-}) = \frac{2}{3}\ \delta^{18}O\ (\text{environ. } H_2O) + \frac{1}{3}\ [\delta^{18}O\ (\text{dissol. } O_2) - \varepsilon_{ox}]$$

If dissolved oxygen is of atmospheric origin and not modified by organic processes one has $\delta^{18}O$ (ox) = +23,5 °/oo (Kroopnick and Craig, 1972). Thus:

$$\delta^{18}O\ (SO_4^{2-} = 0{,}66\ \delta^{18}O\ (\text{environ. } H_2O +$$

$$+ 0{,}33\ (23{,}5 - 8{,}7)$$

$$\delta^{18}O\ (SO_4^{2-}) = 0{,}66\ \delta^{18}O + 4{,}9$$

This leads to sulphate ion with a $\delta^{18}O$ close to + 5 if oxidation takes place in sea water ($\delta^{18}O$ = 0) and to -3,7 in water with an ^{18}O content of - 13 °/oo (Stripa deep water).

However this picture may be modified if dissolved oxygen is partially used for metabolic processes respiration. In that case an oxygen enrichment occurs in the remaining fraction of initial dissolved oxygen of atmospheric origin. The kinetic isotope enrichment factor $\varepsilon_{resp.}$ is important and probably close to 20 °/oo (21 °/oo according to Kroopnick, 1972; Kroopnick and Craig, 1976)

$$\delta^{18}O \text{ (dissolved } O_2) = \delta^{18}O \text{ (respired } O_2) + \varepsilon_{resp.}$$

The heavy isotope content of the remaining fraction f of dissolved oxygen is then given by:

$$\delta(\text{remaining}) - \delta \text{ (initial)} = - \varepsilon_{resp} \ln f$$

If for instance 1/4 of the total dissolved oxygen is consumed before sulphide oxidation takes place $\delta^{18}O$ of the remaining oxygen is increased by about 6 per mill. The ^{18}O content of the resulting sulphate becomes +6,9 in seawater and - 1,7 in water with $\delta^{18}O$ = -13 per mill.

According to Cortecci (1973) the proportions of atmospheric and water oxygen participating to the constitution of the sulphate ion would approach stoichiometric proportions:

$$\delta^{18}O \ (SO_4^{2-}) \text{ oxidation} = \frac{2\delta^{18}O(SO_2) + \delta^{18}O(O_2) + \delta^{18}O(H_2O)}{4}$$

in which SO_2 (or SO_3^{2-}) is formed equally from atmospheric and water oxygens.

In that case:

$$\delta^{18}O\ (SO_4^{2-})\ \text{oxidation} = \frac{2[\delta(O_2) - 8{,}7 + \delta(H_2O)]/2 + \delta(O_2) + \delta(H_2O)}{4}$$

i.e. + 9,6 and + 3.1 in waters with $\delta^{18}O = 0$ and -13 °/oo respectively.

More data are still needed in the field of sulphate production through oxidation of reduced sulphur. Nevertheless one can admit for practical uses that oxidation processes generally preserve ^{34}S contents of the initial reduced sulphur and produces ^{18}O contents much lower than that of evaporites.

Oxygen isotope equilibrium between sulphate and water. It has been known for a long time (Lloyd, 1967; Longinelli and Craig, 1967) that SO_4^{2-} ion from the oceanic reservoir is, from far, not in equilibrium with sea water.

This is probably due to the extremely slow rate of reaction of the S-O bond with water at neutral pH. Values for this reaction rate has been experimentally determined by Lloyd (1968) for different pH values in the temperature range 298 to 721 K. From these values Pearson and Rightmire (1980) draw the following relationship between half-reaction time $t_{1/2}$, temperature T in K and pH:

$$\log t_{1/2}(\text{hours}) = 2.15\ \frac{10^3}{T} + 0.44\ \text{pH} - 3.09$$

which theorectically could provide a geochronometer since the distance to equilibrium is time dependent.

However care should be taken in any attempt to use this formula for time estimations in groundwater systems, because:

(a) experiments were performed over limited ranges of time (some months) and low temperature runs were thus conducted at very low pH; therefore extrapolations to conditions of normal environmental and to long periods (e.g.millenia) would be risky since no error estimate is available;

b) pH dependence was not discussed in terms of activity ratios of $H_2SO_3^-$ to SO_4^{2-} respectively easily and hardly exchangeable with H_2O;

c) the possible influence of micro environmental conditions (catalystes or inhibitors) on the isotope exchange reaction has not been investigated;

d) as seen before much faster isotopic reactions than equilibration may interfere in the SO_4^{2-} - H_2O system, namely biochemical reduction or oxidation;

e) equilibrium values for isotope fractionation effects between sulphate ions and water are still under discussion.

Furthermore it must be reminded that the residence time of any aqueous compound is not necessarily that of the groundwater in which it is dissolved.

4.2.3 Sampling and analyses

Because of the highly variable SO_4^{2-} content (from less than 1 to about 100 ppm) of Stripa waters the amount of collected water varied from 2 to 60 liters.

When necessary (well N 1) the water sample is treated by pure HCl in order to remove H_2S and HS^- whose further oxidation may modify the stable isotope content of aqueous SO_4^{2-}. In the case of surface water, precipitation of sulphate on a 25 l sample was unsuccessful.

Samples were treated with a solution of baryum chloride in order to precipitate SO_4^{2-} as baryum sulphate. Baryum carbonate is then removed by H^+ addition and a further precipitation step is made. The final baryum sulphate rinsed and dried, is allowed to react with pure graphite at about 1 000°C under vacuum and carbon monoxide is converted into CO_2 according to the classical technique. An aliquote of BaS produced through the reduction is dissolved and converted into Ag_2S and oxidized in oxygen at torch temperature. Oxygen and sulphur isotope contents are then determined through CO_2 and SO_2 analyses on a VG Micromass 602 D mass spectrometer. Uncertainties are $\pm$ 0.2 on both measurements.

A sample of 250 ml of water is also collected for SO_4^{2-} determination and ^{18}O measurement in the water. Results appear on Table 4.11 and Figure 4.3.

4.2.4 Interpretations

4.2.4.1 Aqueous sulphate in subsurface waters

Representative points (three measurements) fall within a heavy isotope range which is intermediate

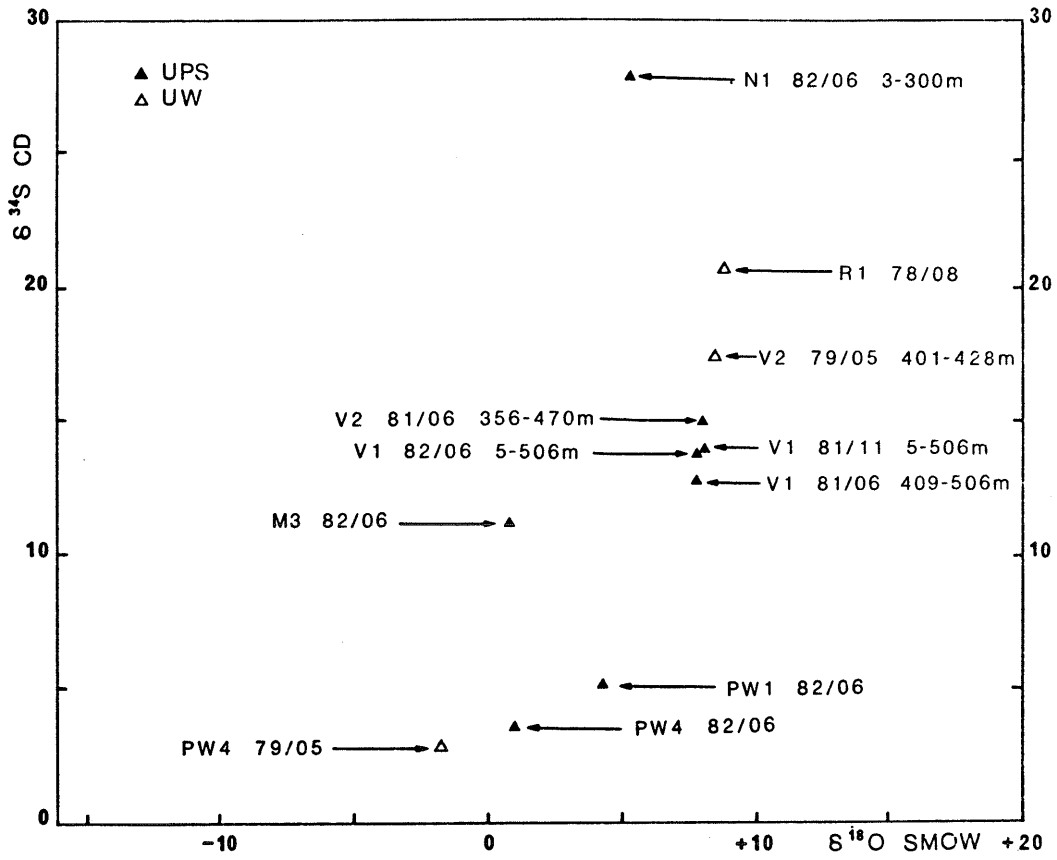

Fig. a Sulphur 34 and oxygen 18 contents of aqueous sulphates with respective well number, dates, exploited intervals.

FIG. 3

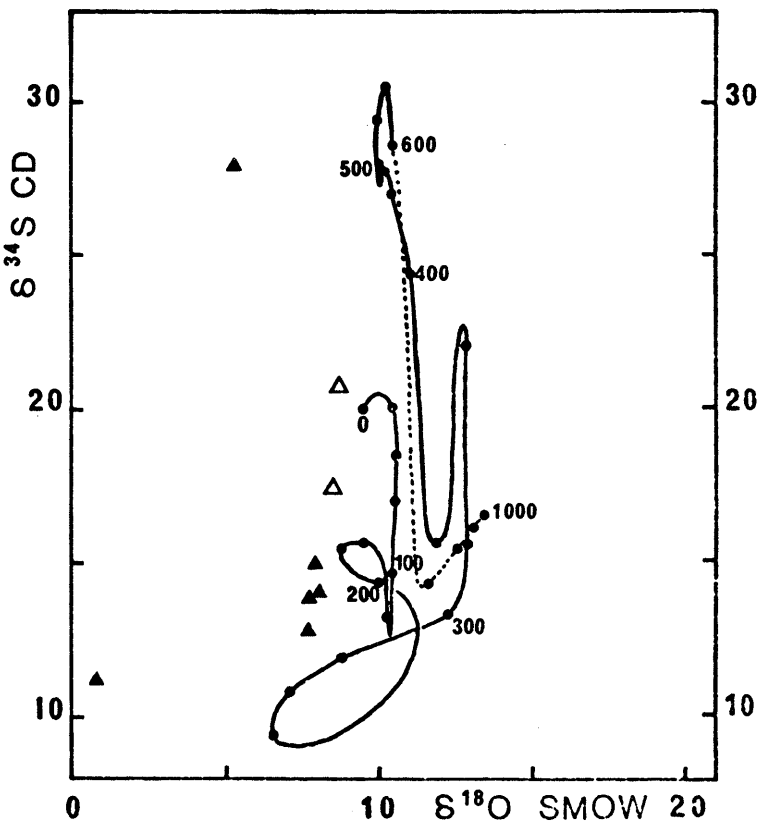

Fig. b Same as a with time curve evolution of aqueous oceanic sulphate (numbers refer to ages in 10^6 a).
From Claypool et al. 1980, corrected for isotopic effects during crystallization.

between marine sulphate (sea spray) and sulphates resulting from oxidation of reduced species of sulphur. Such types of values were also observed in New Zealand (Mizutani and Rafter, 1969 c), in Italy (Cortecci and Longinelli, 1970) and attributed to a mixture of sea spray and sulphates produced through oxidation of HS^- (or S^{2-}) bearing fuels. We adopt this interpretation for Stripa subsurface waters. Sample PWI is probably affected by a secondary enrichment in heavy isotopes due to a partial reduction of the SO_4^{2-} bulk facilitated through water stagnation (the same well shows a low deuterium excess which indicates an evaporation effect).

Subsurface aqueous sulphates do not seem to have any connection with deep water sulphates.

4.2.4.2 Aqueous sulphate in deep waters

Sedimentary origin of the sulphate source. In the $\delta^{34}S$ - $\delta^{18}O$ diagram (Figure 4.3) most of the points fall close to the range of sedimentary, i.e. sea water derived sulphates.

This may be due to:

1) a true sedimentary origin;

2) a succession of geochemical processes which could have given such a heavy isotope content starting from a reduced sulphur species.

Hypothesis 2 would, for instance, imply (among other possibilities) the following geochemical pathways:

a) a dissolution of a fossil evaporite with a ^{34}S content close to + 10 (Permian);

b) a reduction of this sulphate proceeding until completion and thus giving rise without enrichment or depletion to a sulphur 34 content of + 10 °/oo.

c) an oxidation of this reduced sulphur by dissolved oxygen considerably enriched in heavy isotopes by an intense respiration process. For insance the consumption of about 85 % of atmospheric oxygen ($\delta^{18}O$ = + 23.5 °/oo) dissolved in the water is required before oxidation, in order to obtain a sulphate with an ^{18}O content of +9 °/oo within deep water from Stripa.

Condition a) may be easily satisfied in northern Europe. Condition b) requires that reduction products remain homogeneized after completion of the reaction. This means a non circulating flow and is more difficult to expect in this system. Condition c) implies a transfer from the reducing to an oxidizing reservoir where a high aerobiological activity, i.e. a continuous supply of oxygen, takes place.

This schema appears somewhat complicated (despite it represents one of the most simple pathway to reach the observed heavy isotope contents through redox processes). It appears also in contradiction with the respective balances of molecular oxygen and carbon within the environment: the alkalinity is much lower than the sulphate content in V1 and V2 (Nordstrom, this report). This suggests that SO_4^{2-} occurence can hardly be due to H_2S or HS^- oxidation in water with high organic activity.

We will thus consider the hypothesis of a source of original sedimentary sulphate to explain the heavy isotope content to account for the heavy isotope contents found in the Stripa deep groundwater system.

Age of the sedimentary sulphate. Sedimentary sulphates of Stripa groundwaters may have several origins corresponding to various ages:

a) recent sea water intrusions;

b) leaching of Permian evaporites;

c) quaternary baltic sea contribute.

Because present day marine sulphate appears richer in ^{34}S than all but two and richer in ^{18}O than all Stripa sulphates, hypothesis a) will be discarded.

Leaching of evaporites would involve Permian deposits since Zechstein evaporites have heavy isotope contents (corrected for isotopic fractionation due to precipitation, see 2.3.2) very close to those observed in sulphates from V1. Since V1 shows the major sulphate content of the system its heavy isotope content could have been preserved from significant further modification due to partial reduction. However no Permian deposits are recorded from that part om Sweden (H. Norlander, personal com., 1982). Thus hypothesis b) of a direct source of dissolved sulphate through the leaching of local Permian evaporites can not be adopted. Another possible source of sulphate in the Stripa system is the Baltic sea. Measurements of ^{34}S and ^{18}O contents of Baltic sea sulphates are planned in the Stripa project but samples are not yet available. A ^{34}S content of +18.3 is reported by Yeremenjo and Pankina, 1971, for Baltic sea dissolved SO_4^{2-}. Further investigation including oxygen 18 measurements is needed to enquire whether this value, lower than average oceanic content, is due to industrial activities or to a supply of Permian leached sulphates. Gypsum, anhydrite and complex sulphate salts of

Permian age are strongly represented in Northern Germany and Poland. Rivers from the catchment area of the Southern shore of the Baltic may drain diluted solutions of these sulphates. Baltic sea water intrusions would have brought these sulphate to the Stripa groundwater system. This hypothesis would reconciliate the occurence of sulphates having a Permian like fingerprint in local groundwaters with the lack of deposits from that age in the vicinity.

The question then arises upon when these infiltrations could have occured and whether it took place before or after the last glacial period (assuming that no infiltration occured during glacial times). This enhances the interest of putting more efforts on transit time estimations. Stable isotope contents of V2 which appears somewhat higher than those of V1, may be due to a partial reduction of a small amount of the initial sulphate by bacteria. This may account for the much smaller ratio SO_4^{2-}/Cl^- in V_2 than in V1.

For samples very depleted in sulphate like N_1, M_3 and R_1, the heavy isotope content may either be due to a partial reduction (R_1) or to an oxidation of reduced sulphur (M_3). A very pronounced partial reduction could also account for the very high ^{34}S of N_1 whose ^{18}O content remains to confirm and to explain.

4.2.5 Conclusions and recommendations

Despite of its complexity it appears from these preliminary investigations that stable isotope geochemistry of sulphur compounds may offer a powerful tool for groundwater studies (origin of

salts and waters, processes, and, possibly, periods of infiltration and mineralization).

The same kind of time seried study as for deuterium and oxygen 18 may be proposed for deep waters. It must be completed by Baltic sea profiles (including possibly pore waters from deep sea sediments) and investigations of some sulphates from coastal aquifers.

5 CONCEPTUAL FRAMEWORK FOR THE CHEMICAL PROCESSES IN THE STRIPA GROUNDWATERS

5.1 INTRODUCTION AND BACKGROUND

This investigation is concerned with the characterization of groundwater chemistry in crystalline rock, specifically granitic and gneissic formations, in order to assess the risks involved with radioactive waste disposal in this type of geologic environment. The groundwaters at the Stripa site have been sampled at depths approaching 900 m from a granitic intrusion which is in contact with a large body of leptite, a high-grade metamorphic which is similar in mineralogy to the granite. Previous analyses and interpretations of the Stripa groundwaters have been reported by Fritz, et al. (1979, 1980). In addition, several other studies have focused on the groundwater chemistry in igneous and metamorphic rocks including Feth, et al. (1964), Garrels (1967), Garrels and Mackenzie (1967), Paces (1972, 1973, 1974), Jacks (1973, 1978), and Barnes et al. (1981). Unfortunately, most of these other studies are only partially applicable to the Stripa groundwaters because of the difference in chemistry which is related to the greater depth and different environment of the Stripa groundwaters.

The deep Stripa groundwaters differ in chemistry from previous groundwater studies in several obvious respects: (1) the Mg concentrations are much lower, (2) the K concentrations are lower and (3) the alkalinities are lower for comparable Cl concentrations. For example, the HCO_3/ Cl weight ratios for deep Stripa groundwaters range .01-1.0, whereas other studies fall in the range 1-45. One important advantage of the present investigation

is the availability of trace element analyses, especially Br, I, Mg, and B which are essential to the interpretation. The chemical data are extensive enough to narrow the posssible interpretations

5.2 pH AND THE CARBONATE EQUILIBRIUM

The rapid decrease of alkalinity with increasing Cl (Figure 2.7, Chapter 2) follows the inverse of the pattern of increasing pH with depth (Figure 2.2). Fritz, et al. (1979, 1980) have shown that at a depth of about 100 m calcite saturation is reached and all deeper waters show slight supersaturation. It is wellknown that CO_2 in the soil zone is 10-500 times greater than the atmosphere and that this increase in carbonic acid readily attacks primary minerals such as feldspars, thereby releasing Ca to the groundwater. When saturation is reached with respect to calcite, then continued addition of Ca from a saline source would remove carbonate alkalinity by the precipitation of calcite. The markedly decreasing alkalinity with depth and the consistent calcite super-saturation would support this viewpoint. WATEQ2 computations for calcite solubility equilibrium continue to show slight supersaturation for all of the deep groundwaters. The precipitation of calcite at great depth seems to be driven by increased Ca concentrations which is correlated with the increase in salinity with depth. The explanation for the origin of this salinity is one of the most elusive aspects of interpreting the Stripa groundwaters. The pH increase with depth cannot be caused by calcite precipitation and therefore silicate hydrolysis must be considered as a sink for protons.

5.3 THE SOURCE OF SALINITY

The origin of the salinity in the deep Stripa groundwaters can be interpreted by comparing the chemical data with recognized sources of salinity in deep groundwaters. As mentioned in Chapter 2, any interpretation must include an explanation for the distribution of ions between conservative and non-conservative. Furthermore, only a single source is required for the conservative ions which make up most of the salinity. Known or hypothesized sources of salinity in unpolluted groundwaters can be tabulated as follows:

1 Sea water (low temperature origin)
   (a) Recent: coastal sea water intrusion
   (b) Ancient: formation waters, oil-field brines, etc

2 Hydrothermal fluids (high temperature origin)
   (a) Geothermal: hot springs, geysers
   (b) Metamorphic: associated with areas of active metamorphism
   (c) Magmatic: associated with areas of active magmatism
   (d) Fluid inclusions: leakage into groundwater regime

The following arguments suggest that the Stripa groundwaters are gaining their salinity from the leakage (or dissolution) of fluid inclusion and/or grain boundary salts that are an integral part of the granitic and metamorphic rocks. This interpretation is not new, but it has never before been demonstrated.

It will first be shown that the Stripa waters are not likely to be of sea water origin. Sea water intrusion into subsurface waters will maintain the

Br/Cl ratio of sea water (0.0034) and the relative amounts of some of the major ions, such as Ca/Mg (0.30), will not change greatly. The Br/Cl ratio for all samples collected from V1, V2 and N1 average 0.0104 (±0.0005) and the Ca/Mg ratio is more than two orders of magnitude higher than sea water.

Sea water that has evolved over thousands of years can change significantly in chemical composition. The only type of saline water that sometimes has a similar Br/Cl ratio as the Stripa waters are oil-field waters. However, the geology at Stripa is quite far removed from that of an oil-field water in a sedimentary basin environment. More importantly, the Mg/Cl ratios are much lower and the Ca/Mg ratios are much higher in Stripa waters than oil-field waters. Thus, even evolved ancient sea water has little in common with the saline waters from Stripa.

Hydrothermal fluids seem an unlikely source of salinity at Stripa because there is no indication of any thermal activity anywhere near the site. In fact, the geothermal gradient is rather low (15°C/km). To compare the Stripa groundwaters with other saline waters which are typical of both high and low temperature origins, a plot of Ca/Mg ratio vs. Br/Cl ratio is shown in Figure 5.1. "Oil field waters" are from the deep sedimentary basin of the Texas Gulf Coast (Kharaka, et al. 1977), "geo-thermal" waters are from the Wairakei and Broad-lands areas, New Zealand (Ellis and Mahon, 1977), "metamorphic" waters are from the west coast of the United States (Barnes, 1970) and "Sierra springs" are from the Sierra Nevada granitic batholith which are issuing from areas of active metamorphism (Barnes, et al., 1981). For all of these types of saline waters, the deep Stripa

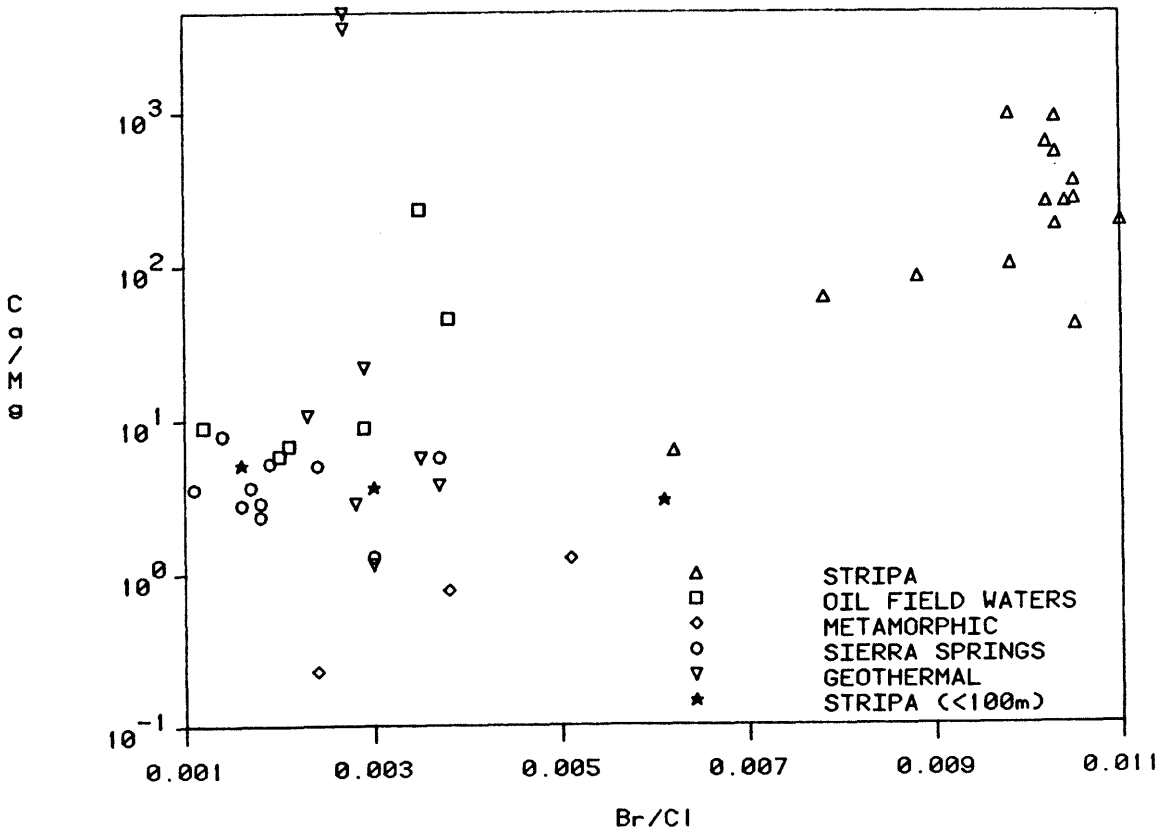

Figure 5.1 Ca/Mg-ratio vs. Br/Cl-ratio for different groundwaters.

groundwaters are clearly in a separate class having very little in common with saline waters of both high temperature and low temperature origins.

There are, however, several chemical geothermometers which can be used to determine whether the solutes are derived from a high temperature or low temperature source. The silica geothermometer (Fournier and Rowe, 1966) is based on increased solubility of silica at high temperatures. Unfortunately, if appreciable cooling has taken place, the precipitation of amorphous silica invalidates the use of this geothermometer. The silica concentrations at Stripa are quite low and

indicative of low temperature processes. Either the water has a low temperature origin, or the silica has reequilibrated at low temperatures and no longer preserves a record of the last thermal event. Since that last thermal event was probably several millions of years ago, it is most likely that the silica geothermometer is of no use. Ratios of Na/K and Na/K/Ca have been shown to be reasonable indicators of temperature (Truesdell, 1975; Ellis and Mahon, 1977). The Na/K geothermometer gives a temperature of -10° which is indicative of high Ca concentrations. These results invalidate the use of this geothermometer (see Truesdell, 1975). Alternatively, the Na/K/Ca geothermometer gives a temperature of 61°. This temperature would suggest a moderately elevated temperature of origin.

Another clue to the original temperature of the source fluid is the Mg concentration. During the shallow groundwater weathering of magnesium silicate minerals by carbon dioxide, Mg concentrations are typically 1-20 mg/l. Ellis (1971), Ellis and Mahon (1977) and Fournier and Potter (1979) have pointed out that Mg concentrations decrease markedly with increasing temperature. The log $(Mg)/(H^+)^2$ is a good indicator of high temperature origins and the Stripa waters indicate a temperature of 250° using the data of Ellis (1971) for a typical water from the lower part of drillhole V1. Averaging the analyses for all of the deepest samples from V1 and V2 and comparing this to the element ratio plots of Fournier and Potter (1979), the results are: for Ca/Mg a temperature of 520°C, for Na/Mg a temperature of 113°C, and for K/Mg a temperature of 46°C. The plot of Mg vs. Cl in Figure 5.2 shows that the Stripa waters do compare well with geothermal waters in their range of magnesium concentrations. They do not compare

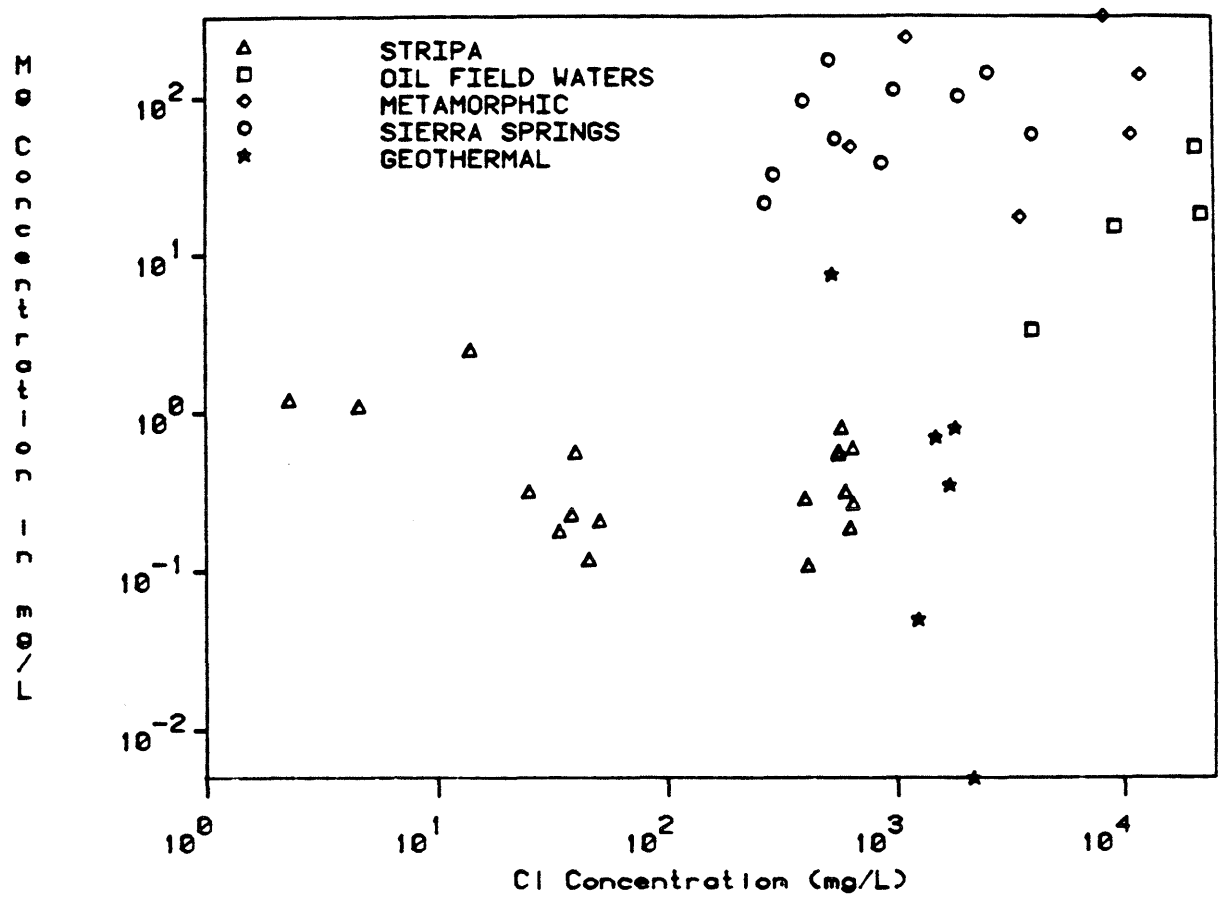

Figure 5.2 Mg vs. Cl for different groundwaters.

well with other saline waters. These facts suggest a high temperature origin for saline source. Since no thermal anomalies are present today, the possibility of leaching fluid inclusions from the crystalline rock must be considered. These fluid inclusions would be frozen-in memories of the last metamorphic event. Figure 5.3, which plots B concentrations vs. alkalinity, also shows a striking separation of the Stripa waters from other types. If it is assumed that most of the available B is either (a) easily lost by volatization to the earth's surface during metamorphism or (b) incorporated into insoluble minerals such as tourmaline, then the B content of

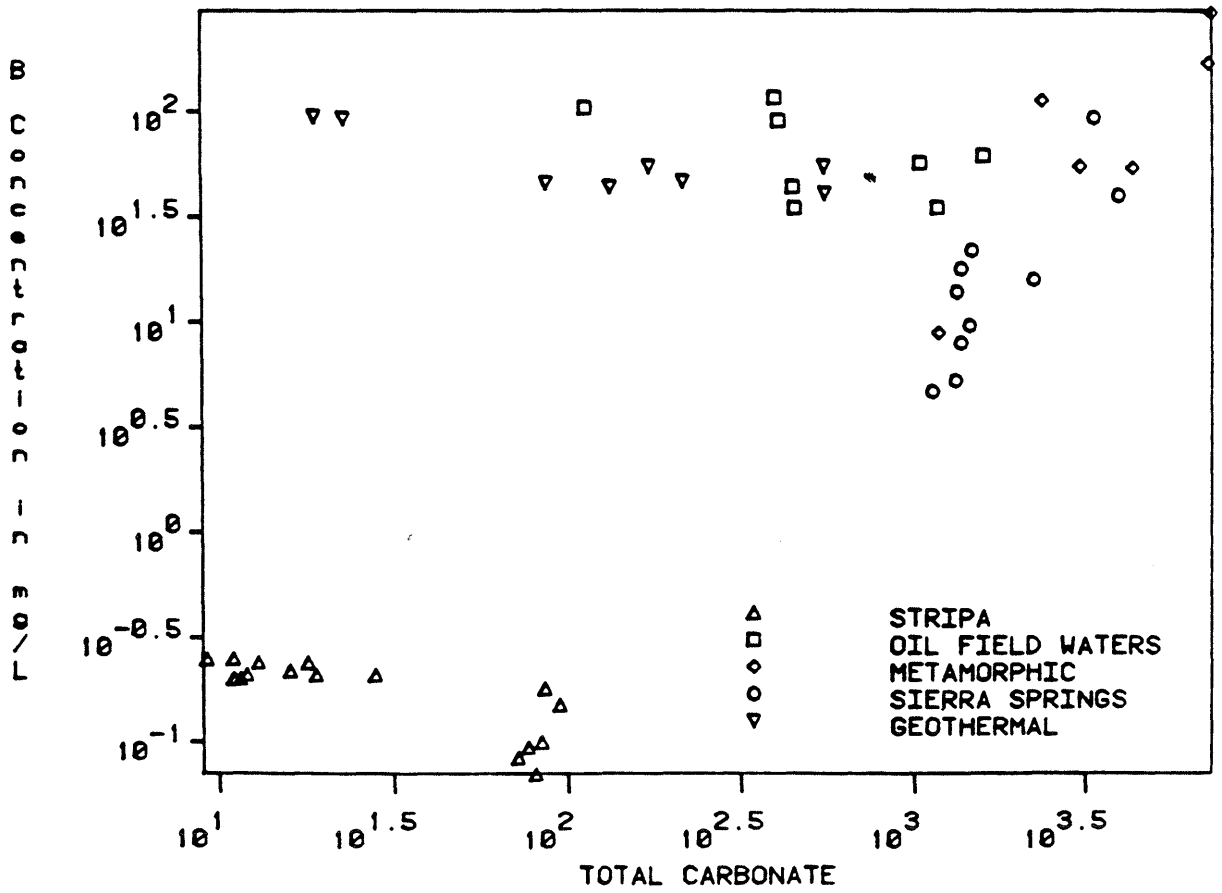

Figure 5.3 Boron vs. carbonate for different groundwaters.

any residual fluids in the rock should be very low. This separation could explain the high B of many thermal waters and the low B content of the Stripa waters if they represent leaching of fluid inclusions.

To test the hypothesis that the Stripa granite might be the source of the salinity, nine samples of V1 and V2 drillcores were leached for fluid inclusions according to the procedures of Roedder, et al. (1963) and Hall and Friedman (1963).

Preliminary analyses have just been obtained which confirm the granite as the source of the salinity.

Fifteen leaches from the nine samples give an average Br/Cl ratio of 0.0101±0.0015 compared to the average of 0.0104±0.0005 from V1, V2 and N1 water samples. Groundwaters from E1 give a lower Br/Cl ratio which is consistent with shallow groundwaters not deep groundwaters. Thus, the Br/Cl ratio gives additional evidence to the ^{4}He and ^{3}H data indicating higher permeabilities in E1.

Evidence suggests that crystalline rocks can provide significant quantities of salinity to deep groundwaters. This interpretation is not new (e.g. see Garrels, 1967; Gambell and Fischer, 1966), but it is the first time groundwater salinity has been shown to come from the leaching of fluid inclusions in crystalline rocks. It suggests that the deeper one drills in igneous - metamorphic rocks, the higher the salinity will become. Consequently, the corrodability of radioactive waste containers increases. Some optimal depth (maybe 500-600 m) may be reached by looking at the decrease in permeability relative to the increase in chloride concentration.

5.4 NON-CONSERVATIVE CONSTITUENTS

Most of the non-conservative ion concentrations can be explained by common water-mineral reactions. For example, the solubility of fluorite limits the concentration of fluoride. This limit has been shown to be very effective in geothermal waters (Mahon, 1964; Ellis and Mahon, 1964, 1967; Nordstrom and Jenne, 1977) and in low temperature groundwaters (Handa, 1975; Jacks, 1978). WATEQ2 calculations consistently give saturated to supersaturated conditions for fluorite solubility equilibrium in the Stripa groundwaters, suggesting that fluorite is actively precipitating. This

process would keep the fluoride concentrations at the constant value seen in Figure 2.6.

As mentioned previously, calcite precipitation in a closed system would be effective in decreasing the HCO_3 concentrations and this process was described by Jacks (1978). The increase in sulfate requires an additional input from either the oxidation of pyrite or the dissolution of anhydrite or gypsum. Pyrite oxidation is highly unlikely because the acidity produced would cause the pH to be well below the values of 9-10 measured for the drillholes. Dissolution of anhydrite (or gypsum) is possible but none has yet been observed in the fractures or the granite, whereas pyrite is abundant. It is also possible that with more analyses at higher chloride concentrations it will give a good linear correlation with chloride. The average SO_4/Cl ratio from fluid inclusion leaching is about 3 but highly variable from sample to sample. The average SO_4/Cl for the high salinity groundwater samples is 0.1 which suggests that some sulfate may be removed by precipitation after leaching of fluid inclusions if this is the source. Further work is needed to understand the behavior of sulfate in these waters. Potassium behaves somewhat like sulfate and is postulated to simply be present in lower concentrations in the fluid inclusions than sodium; therefore it is not seen to correlate with chloride until the higher concentrations are reached.

Silica is at approximate equilibrium with the solubility of chalcedony, a microcrystalline silica of mineral. It would be reasonable to assume that this equilibrium had been achieved except that at pH values of 9.5-10.0 the dissolved silica should increase to 20-30 mg/L due to silica hydrolysis. Since it doesn't, we must assume some other control on the solubility, perhaps by aluminosilicates.

REFERENCES

Chapter 1

Carlsson, L. and Olsson, T., 1981: Hydrogeological investigations in boreholes. Summary of defined programs. Stripa Project 81-01, 1-26.

Carlsson, L., Olsson, T. and Stejskal, V., 1981: Core-logs of borehole V1 down to 505 m. Stripa Project 81-05, 28 pp.

Carlsson, L., Olsson, T. and Stejskal, V., 1982: Core-logs of the subhorizontal boreholes N1 and E1. Stripa Project 82-04, 44 pp.

Carlsson, L., Egerth, T., Olsson, T. and Westlund, B., 1982: Core-logs of the vertical borehole V2. Stripa Project 82-05, 40 pp.

Gale, J. E., 1982: Hydrogeologic characteristics of the Stripa site. Univ. Waterloo Res. Inst. Rep. 003C, 60 pp.

Geijer, P., 1938: Stripa odalsfälts geologi. SGU, Ser Ca 28.

Heier, K. F. and Rogers, J. J. W., 1963: Radiometric determinations of thorium, uranium and potassium in basalts and in two magmatic differentiations series. Geochim. Cosmochim. Acta, Vol. 27, pp 137-154.

Koark, H. J. and Lundström, I., 1979: Berggrundskartan Lindesberg SV. SGU Ser Af 126.

Landström, O., Larsson, S-Å, Lind, G. and Malmqvist, O., 1980: Geothermal investigations in the Bohusgranite area in Sweden. Technophysics, (in press).

Lundström, L. and Stille, H., 1978: Large scale permeability test of granite in the Stripa mine and thermal conductivity test. LBL-7052, SAC-02, 33 pp.

Olkiewicz, A., Hansson, K., Almn, K.-E. and Gidlund, G., 1978: Geologisk och hydrologisk dokumentation av Stripa försöksstation. SKBF/KBS Tech. Rep. 63, 37 pp.

Olkiewicz, A., Gale, J. E., Thorpe, R. and Paulsson, B., 1979: The geology and fracture system at Stripa. LBL-8907, SAC-21.

Paulsryd, B., 1941: Oremapping in the Stripa Mine. Ställbergs Grufe AB

Welin, E., 1964: Pitchblende-bearing vein fillings in the Stripa and Blanka iron ores. Transactions Geological Society of Sweden, Vol. 86, pp. 215-270.

Witherspoon, P. A., Cook, N. G. and Gale, J. E., 1980: Progress with field investigations at Stripa. LBL-10559, SAC-27, 50 pp.

Wollenberg, H., Flexser, S. and Andersson, L., 1982: Petrology and radiogeology of the Stripa pluton, LBL-11654.

Chapter 2 and 5

Avotins, P. and Jenne, E. A., 1975: The time stability of dissolved mercury in water samples II. Chemical stabilization. J. Environ. Qual. 4, 515-519.

Barnes, I., 1970: Metamorphic waters from the Pacific tectonic belt of the west coast of the United States, Science 168, 973-975.

Barnes, I., Kistler, R. W., Mariner, R. H. and Presser, T. S., 1981: Geochemical evidence on the nature of the basement rocks of the Sierra Nevada, California, U.S. Geol. Survey Water-Supply Paper 2181, 13 pp.

Barnes, R. B., 1975: The determination of specific forms of aluminum in natural water, Chem. Geol. 15, 177-191.

Crawford, M. L., 1981: Fluid inclusions in metamorphic rocks-low and medium grade, Mineral Assoc. Canada Short Course Handbook, Vol. 6, Fluid Inclusions: Applications to Petrology, L. S., Hollister and M. L., Crawford, eds., 157-181.

Ellis, A. J. and Mahon, W. A. J., 1964: Natural hydrothermal systems and experimental hotwater/rock interactions. Part 11. Geochim. Cosmochim. Acta 31, 519-538.

Ellis, A.J. and Mahon, W. A. H. 1967: Natural hydrothermal systems and experimental hotwater/rock interactions, Geochim. Cosmochim. Acta 28, 1323-1357.

Ellis, A. J., 1971: Magnesium ion concentrations in the presence of magnesium chlorite, calcite, carbon dioxide, quartz. Am. J. Sci. 271, 481-489.

Ellis, A. J. and Mahon, W. A. J., 1977: Chemistry and Geothermal Systems. Academic Press. N.Y., 392 pp.

Feth, J. H., Roberson, C. E., and Polzer, W. L. 1964: Sources of mineral constituents in water from granitic rocks Sierra Nevada California and Nevada, U.S. Geol. Survey Water-Supply Paper 1535-I, 170 pp.

Fournier, R. O. and Rowe, J. J.1966: Estimation of underground temperatures from the silica content of water from hot springs and wet stream wells. Am. J. Sci. 264, 685-687.

Fournier, R. O. and Potter, R. W. 1979:: Magnesium correction to the Na-K-Ca chemical geothermometer. Geochim. Cosmochim. Acta 43, 1543-1550.

Fritz, P., Barker, J. F. and Gale, J. E. 1979: Geochemistry and isotope hydrology of groundwaters in the Stripa Granite: Results and preliminary interpretation, LBL-8285, SAC-12, 105 pp.

Gutsalo, L. K., 1971: Radiolysis of water as a source of free oxygen in the subsurface hydrosphere, Geokhimya 12, 1473-1481 (Geochem. Int. 8, 897).

Hall, W. E. and Friedman, I., 1963: Composition of fluid inclusions, Cave in-Rock fluorite district, Illinois, and Upper Mississippi Valley zinc-lead district, Econ. Geol. 5(, 886-911.

Handa, B. K., 1975: Geochemistry and genesis of fluoride-containing ground waters in India, Groundwater 13, 275-281.

Ives, D. J. G. and Janz, G. J., eds. 1961: Reference Electrodes Theory and Practice, Academic Press, N.Y., 651 pp.

Jacks, G., 1963: Chemistry of some ground waters in igneous rocks, Nordic Hydrol. 4, 207-236.

Jacks, G., 1978: Ground water chemistry at depth in granites and gneisses, KBS Tech. Rept. 88, 28 pp.

Kennedy, V. C., Wellweger, G. W. and Jones, B. F., 1974: Filter pore-size effects on the analysis of Al, Fe, Mn, and Ti in water. Water Resour. Res. 10, 785-790.

Kharaka, Y. K., Callender, E. and Carothers, W. W., 1977: Geochemistry of geopressured geothermal waters from the Texas gulf coast. Proc. of The Third Geopressured Geothermal Energy Conf., John Meriwether, ed., Vol. 1, 121-165.

Mahon, W. A. J., 1964: Fluorine in the natural thermal waters of New Zealand, N.Z.J. Sci. 7, 3-28.

Mazor, E. and Wsserburg, G. T., 1965: Helium, neon, argon, krypton and xenon in gas emanations from Yellowstone and Lassen volcanic National Parks. Geochim. Cosmochim. Acta 29, 443-454.

Nordstrom, D. K., 1977: Thermochemical redox equilibria of ZoBell's solution. Geochim. Cosmochim. Acta 41, 1835-1841.

Nordstrom, D. K. and Jenne, E. A., 1977: Fluorite solubility equilibria in selected geothermal waters. Geochim. Cosmochim. Acta 41, 175-188.

Paces, T., 1972: Chemical characteristics and equilibration in natural water-felsic rock-CO system. Geochim. Cosmochim. Acta 36, 217-240.

Paces, T.,1973: Steady-state kinetics and equilibrium between ground water and granitic rock. Geochim. Cosmochim. Acta 37, 2641-2663.

Paces, T., 1974: Geochemical behaviour of calcium in ground water-granitic rock system. Vestn. Ustred. Ustavu Geol. 49, 215-218.

Roedder, E., Ingram, B. and Hall, W. E., 1963: Studies of fluid inclusions III: Extraction and quantitative analysis of inclusions in the milligram range. Econ. Geol. 58, 353-374.

Touret, T., 1981: Fluid inclusions in high grade metamorphic rocks. Mineral. Assoc. Canada Shoirt Course Handbook, Vol. 6, Fluid Inclusions: Applications to Petrology, L. S. Hollister and M. L. Crawford, eds., 182-208.

Truesdell, A. H., 1975: Geochemical techniques in exploration. Proc. U.N. Symp. Develop. Use. Geothermal Resources, 2nd, San Francisco, California, May 1, liii-lxxix.

Vidal, F. V., Welhan, T. and Vidal, V. M. V. 1982: Stable isotopes of helium, nitrogen and carbon in a coastal submarine hydrothermal system, T. Volcan. Geotherm. Res. 12, 101-110.

Winograd, I. T. and Robertson, F. N., 1982: Deep oxygenated ground water: anomaly or common occurrence? Science 216, 1227-1230.

Chapter 3

Andrews, J. N., Giles, I. S., Kay, R. L.F., Lee, D. J., Osmond, J. K., Coward, J. B., Fritz, P., Barker, J. F. and Gale, J.: Radioelements, radiogenic helium and age relationships for groundwaters from the granites at Stripa, Sweden. Geochim. Cosmochim. Acta (1982) in press.

Andrews, J. N. and Kay, R. L. F.: The evolution of enhanced $^{234}U/^{238}U$ activity ratios for dissolved uranium and groundwater dating. Fourth Int. Conf. Geochronology, Cosmochronology and Isotope Geology, Denver, U.S.A. (1978).

Langmuir, D.: Uranium solution-mineral equilibria at low temperatures with applications to sedimentary ore deposits. Geochim. Cosmochim. Acta 42, (1978) 547.

Nelson, P., Paulsson, B., Rachiele, R., Andersson, L., Schrauf, T., Hustralid, W., Duran, D. and Magnusson, K. A., 1979: Preliminary report on the geophysical and mechanical borehole measurement at Stripa. Report LBL-8280, Lawrence Berkeley Laboratory, University of California.

Chapter 4

Claypool, G. E., Holser, H. T., Kaplan, I. R., Sakai, H. and Zak, I., 1980: The age curve of sulfur and oxygen isotope in marine sulfate and their mutual interpretation. Chem. Geology, 28, 99-260.

Cortecci, G., 1973: Oxygene-isotope variation in sulfate ions in the water of some Italian lakes. Geochim. Cosmochim. Acta 37, 1541-1542.

Craig, H., 1961: Isotopic variations in meteoric waters. Science 133, 1702-1703.

Dansgaard, W., 1964: Stable isotopes in precipitation. Tellus 16, 436-467.

Fontes, J. C., 1981: Paleowaters. In: Stable Isotope Hydrology. Deuterium and Oxygen 18 in the Water Cycle. Technical Reports Series n°210. IAEA, Vienna, 273-302.

Friedman, I. and O'Neil, J. R., 1977: Compilation of stable isotope fractionation factors of geochemical interest In: M. Fleischer Ed. Data of Geochemistry. U.S. Geol. Surv., Brof. Paper, 440-KK:1-12 (6th ed.).

Fritz, P., Barker, J. F. and Gale, J. E., 1979: Geochemistry and isotope hydrology of groundwaters in the Stripa granite. Results and preliminary interpretation. LBL-8285, SAC-12, 105 pp.

Fritz, P., Barker, J. F., Gale, J. E., Witherspoon, P. A., Andrews, J. N., Kay, R. L. F., Lee, D. J., Cowart, J. B., Osmond, J. K. and Payne, B. R., 1980: Geochemical and Isotopic investigations at the Stripa test site (Sweden). In: Underground Disposal of Radioactive Wastes, Vol. II, IAEA, Vienna, 341-366.

Fritz, P. and Fontes, J. C., 1980: Handbook of Environmental Isotope Geochemistry. Vol. I, Elsevier, Amsterdam.

Gonfiantini, R., Conrad, G., Fontes, J. C., Sauzay, G. and Payne, B. R., 1974: Etude isotopique de la nappe du continental Intercalaire et de ses relations avec les autres nappes du Sahara septentrional. In: Isotope Techniques in Groundwater Hydrology, Vol. I, IAEA, Vienna, 227.

Harrisson. A. G. and Thode, H. G., 1957: The kinetic isotope effect in the chemical reduction of sulfate. Trans. Favaday Soc., 53, 1648-1651.

I.A.E.A., 1982: The role of isotope tecxhniques in hydrogeology. Assessment of potential sites for the disposal of high-level wastes. IlA.E.A. Vienna. In press.

I.A.E.A., 1983: Guidebook on nuclear techniques in hydrology. I.A.E.A., Vienna. In press.

Kaplan, I. R. and Rittenberg, S. C., 1964: Microbiological fractionation of sulfur isotopes, J. Gen. Microbiol., 34, 159-212.

Kemp, A. L. W. and Thode, H. G., 1968: The mechanism of the bacterial reduction of sulphate and of sulphite isotope fractionation studies. Geochim. Cosmochim. Acta, 32, 71-91.

Kroopnick, P. M. and Craig, H., 1972: Atmospheric oxygen: Isotopic composition and solubility fractionation. Science, 175, 54-55.

Kroopnick, P. M. and Craig, H., 1976: Oxygen isotope fractionation in dissolved osygen in the deep sea. Earth Planetary Sci. Letters, 32, 375-388.

Krouse, H. R., 1980: Solphur isotopes in our environmental Isotope Geochemistry. Vol. 1. Elsevier, Amsterdam: 435-471.

Lloyd, R. M., 1967: Osygen 18 composition of oceanic sulfate. Science, 156, 1228-1231.

Lloyd, R. M., 1968: Oxygen isotope behaviour in the sulphate-water system. Jour. Geoph. Res., 73, 6099-6110.

Mizutani, Y, and Rafter, T. A., 1969 (a): Oxygen isotopic composition of sulfates, 3.3. Oxygen isotopic fractionation in the bisulfate-water system. N.Z.J. Sci., 12, 54-59.

Mizutani, Y. and Rafter, T. A., 1969: Oxygen isotopic composition of sulphates, 4. Bacterial sulphate and the oxydation of sulphur. N.Z.J. Sci., 12, 60-68.

Mizutani, Y. and Rafter, T. A., 1969 (c): Oxygen isotopic composition of sulphates, 5. Isotopic composition of sulfate in rain water, Gracefiels, New Zealand. N.Z.J. Sci., 12, 69-80.

Nielsen, H. and Ricke, W., 1964: Schwefel-Isotopenverhältnisse von Evaporiten aus Deutschland; ein Beitvag zur Kenntnis von ^{34}S in Meerwasser-Sulfat. Geochim. Cosmochim. Acta, 28, 577-591.

Nir, A., 1967: Development of isotope methods applied to groundwater hydrology. Am. Geophys. Union. Monograph 11, 109_116.

Panichi, C. and Gonfiantini, R., 1981: Geothermal waters. In: Stable Isotope Hydrology. Deuterium and Oxygen 18 in the Water Cycle. Technical Reports Series n°210. I.A.E.A., Vienna, 241-272.

Pearson, F. J. Jr., Rightmire, C. T., 1980: Sulphur and oxygen isotopes in aqueous sulphur compounds. In: P. Fritz and J. C. Fontes (Eds). Handbook of Environmental Isotope Geochemistry. Vol. 1. Elsevier, Amsterdam, 227-258.

Pierre, C., 1982: Teneurs en isotopes stables (^{18}O, ^{2}H, ^{13}C, ^{34}S) et conditions de génèse des évaporites marines: application à quelques milieux actuels et au Messinien de la Méditerranée. Thèse Doct. Sc. Nat. Université de Paris-Sud, Orsay, 266p.

Rafter, T. A. and Mizutani, Y., 1967: Oxygen isotope composition of sulfates, 2: Preliminary results on oxygen isotopic variation in sulfates and relationship of their environment and to their ^{34}S values. N.Z.J. Sci., 10, 816.

Rees, C. E., 1973: A steady state model for sulphur isotope fractionation in bacterial reduction processes. Geochim. Cosmochim. Acta, 37, 1141-1162.

Rightmire, C. T., Pearson, F. J. Jr., Back, W., Rye, R. O. and Handshaw, B. B., 1974: Distribution of sulphur isotopes of sulphates in groundwaters from the principal artesian aquifer of Florida and the Edwards aquifer of Texas. U.S.A. In: Isotope Techniques in Groundwater Hydrology. Vol. 2, I.A.E.A., Vienna, 191-207.

Sakai, H., 1968: Isotopic troperties of sulphur compounds in hydrothermal processes. Geochem. J., 2, 29-49.

Savin, S. M., 1980: Osygen and hydrogen isotope effects in low temperature mineral-water interactions. In: P. Fritz and J. C. Fontes (Eds.). Handbook of Environmental Isotope Geochemistry. Vol. 1. Elsevier, Amsterdam, 234-328.

Thode, H. G. and Monster, J., 1965: Solphur-isotope geochemistry of petroleum, evaporites and ancient seas. In: A. Young and J. E. Galley (Eds). Fluid in Subsurface Environments. Am. Assoc. Pet. Geol. Mem., 4, 367-377.

Yurtsever, Y. and Gat, J. R., Atmospheric waters. In: Stable Isotope Hydrology. Deuterium and Oxygen 18 in the Water Cycle. Technical Reports Series n°210. I.A.E.A., Vienna, 103-142.

Zak, I., Sakai, H. and Kaplan, I. R., 1980: Factors controlling the $^{18}O/^{16}O$ and $^{34}S/^{32}S$ isotope ratios of ocean sulfates, evaporites and interstitial sulfates from modern deep sea sediments. In: Isotope Marine Chemistry. Uchida Rokakuho, Tokyo, 339-373.

APPENDIX I

INTERLABORATORY COMPARISON

Stripa Groundwater Analyses: Interlaboratory Comparison.

Drillhole		R-1		M-3		V-1	
Sample Code No.		81WA204		81WA205		81WA206	
Sampling Depth		333.1 m		339.5 - 340.5 m.		364.7 - 764.7 m.	
Date Collected		4-6-81		4-6-81		4-6-81	
Temperature (°C)		12.0		12.0		10.3	
Field (Lab) pH		8.96 (8.51)		8.84 (8.39)		9.73 (8.99)	
Conductivity (uS/cm)		215 (286)		210 (291)		510 (710)	
Eh (from field emf: mV)		+57		---		+22	
Laboratory		USGS	SGU	USGS	SGU	USGS	SGU
Total Alkalinity(1)		95	95	86	86	17	19
Carbonate Alkalinity(1)		88	---	79	---	10	---
Charge Balance		2.1	18	1.4	6.2	6.2	2.9
Species	Method(2)						
Ca ppm	S	15	13	14	14	28	26
Mg ppm	S	0.27	0.18	0.24	0.23	0.065	<0.005
Na ppm	S	49	40	48	46	116	116
K ppm	S	<0.30	0.22	<0.30	0.23	<0.30	0.49
	AA	0.10	----	0.12	----	0.24	----
SO_4 ppm	IC	3.2	3.5	4.9	4.9	11	12
H_2S ppm(3)	ISE	----	----	0.026	----	----	----
F ppm	IC	----	5.1	----	5.3	----	4.9
	ISE	4.7	----	5.0	----	4.6	----
Cl ppm	IC	34	35	38	39	190	200
Br ppm	IC	0.3	----	0.3	----	2.0	----
I ppm	C	0.014	----	0.013	----	0.061	----
PO_4 ppm	IC	----	<0.1	----	<0.1	----	<0.1
SiO_2 ppm	S	12	12	12	12	14	14
B ppm	S	0.15	0.16	0.17	0.18	0.24	0.24
NO_2 ppm	IC	----	<0.005	----	<0.005	----	<0.005
NO_3 ppm	IC	----	0.5	----	0.6	----	2.5
NH_4 ppm	IC	----	<0.01	----	<0.01	----	<0.01
Al ppm	S	<0.010	<0.005	<0.010	<0.005	0.034	0.032
	E	<0.010	----	<0.010	----	0.020	----
Fe ppm	S	0.038	0.042	<0.015	0.006	----	0.012
	F	0.046	----	0.010	----	0.020	----
Mn ppm	S	<0.010	<0.005	<0.010	<0.005	<0.010	0.008
Cu ppm	S	<0.003	<0.005	<0.003	<0.005	<0.003	<0.005
Zn ppm	S	<0.006	<0.005	<0.006	<0.005	<0.006	<0.005
Hg ppb	FAA	----	----	----	----	----	----
Co ppm	S	<0.005	<0.005	<0.005	0.014	<0.005	<0.005
Ti ppm	S	<0.010	----	<0.010	----	<0.010	----
Mo ppm	S	0.038	0.045	0.052	0.059	0.045	0.054
Li ppm	S	<0.10	0.024	<0.10	0.023	<0.10	0.030
	AA	0.020	----	0.020	----	0.020	----
Sr ppm	S	0.12	0.11	0.14	0.13	0.21	0.18
Cs ppm	FE	0.064	----	0.047	----	0.078	----
Rb ppm	S	<0.030	<0.005	<0.030	<0.005	<0.030	<0.005
	FE	<0.002	----	<0.002	----	0.009	----
Ba ppm	S	<0.005	0.006	<0.005	<0.003	<0.005	<0.003
DOC ppm	TCA	----	4.0	----	----	----	1.1

(1) Expressed as mgL^{-1} HCO_3 equivalent.
(2) S = plasma emission spectroscopy (USGS: direct current; SGU: inductively coupled), AA = atomic absorption, F = visible spectrophotometry (ferrozine method), FE = flame emission spectroscopy, ISE = ion-selective electrode, IC = ion chromatography, E = solvent extraction, FAA = flameless atomic absorption, C = colorimetric (Analyses performed by Don Whittemore.).
(3) Values are minimums.
(4) Dissolved organic carbon.
(5) ---- = Not analysed for.
(6) The following elements were found to be below detection limit for all samples (d.l. in ppm) : As (0.003), Be (0.002), Bi (0.080), Cd (0.005), Cr (0.003), Ni (0.004), Pb (0.010), Sb (0.20), Se (0.20), Tl (0.007), V (0.005).

Stripa Groundwater Analyses: Interlaboratory Comparison.

Drillhole		V-2		N-1		V-1	
Sample Code No.		81WA201		81WA202		81WA203	
Sampling Depth		763.7 - 877.7 m.		355.5 m.		764.7 - 856.7 m.	
Date Collected		3-6-81		3-6-81		3-6-81	
Temperature (°C)		8.0		10.1		10.6	
Field (Lab) pH		9.53 (8.69)		8.85 (8.27)		9.31 (7.57)	
Conductivity (uS/cm)		960 (1415)		190 (283)		1420 (2230)	
Eh (from field emf: mV)		+20 to +79		+13		-56	
Laboratory		USGS	SGU	USGS	SGU	USGS	SGU
Total Alkalinity(1)		11	12	77	77	8.5	10
Carbonate Alkalinity(1)		8.1	--	70	--	3.1	--
Charge Balance		6.7	5.3	3.3	5.1	1.3	1.8
Species	Method(2)			Filtered Unfiltered	Filtered Unfiltered		
Ca ppm	S	110	98	24 23	22 22	173	170
Mg ppm	S	0.15	0.11	0.20 0.22	0.12 0.22	0.28	0.19
Na ppm	S	184	176	37 36	34 35	266	287
K ppm	S	0.42	0.80	<0.30 0.39	0.23 0.75	1.4	2.4
	AA	0.37	----	0.12 0.19	---- ----	1.2	----
SO_4 ppm	IC	44	45	0.5 ----	0.7 ----	100	103
H_2S ppm(3)	ISE	0.00023	----	0.026 ----	---- ----	0.0026	----
F ppm	IC	----	3.8	---- ----	3.4 ----	----	4.6
	ISE	3.9	----	3.2 ----	---- ----	4.6	----
Cl ppm	IC	400	420	46 ----	45 ----	620	640
Br ppm	IC	4.0	----	0.5 ----	---- ----	6.5	----
I ppm	C	0.11	----	0.015 ----	---- ----	0.16	----
PO_4 ppm	IC	----	<0.1	---- ----	<0.1 ----	----	<0.1
SiO_2 ppm	S	12	12	12 16	12 14	13	13
B ppm	S	0.20	0.20	0.093 0.099	0.095 0.10	0.24	0.25
NO_2 ppm	IC	----	<0.005	---- ----	<0.005 ----	----	<0.005
NO_3 ppm	IC	----	4.8	---- ----	0.7 ----	----	7.0
NH_4 ppm	IC	----	<0.01	---- ----	<0.01 ----	----	<0.01
Al ppm	S	<0.010	<0.005	0.083 0.75	0.059 0.56	0.024	0.008
	E	0.010	----	---- 0.2	---- ----	0.02	----
Fe ppm	S	0.075	0.073	<0.015 0.18	0.022 0.18	----	<0.005
	F	0.088	----	0.018 0.16	---- ----	0.004	----
Mn ppm	S	<0.010	0.009	<0.010 <0.010	<0.005 <0.005	<0.010	<0.005
Cu ppm	S	<0.003	<0.005	<0.003 0.046	<0.005 0.040	<0.003	<0.005
Zn ppm	S	<0.006	<0.005	<0.006 0.026	<0.005 0.021	<0.006	<0.005
Hg ppb	FAA	0.023	----	---- ----	---- ----	<0.005	----
Co ppm	S	<0.005	<0.005	<0.005 <0.005	0.006 0.010	<0.005	<0.005
Ti ppm	S	0.014	----	<0.010 <0.010	---- ----	0.035	----
Mo ppm	S	0.049	0.053	0.044 0.047	0.054 0.060	0.035	0.020
Li ppm	S	<0.10	0.071	<0.10 <0.10	0.022 0.030	0.18	0.19
	AA	0.038	----	0.019 0.017	---- ----	0.085	----
Sr ppm	S	1.1	0.88	0.17 0.17	0.15 0.16	1.9	1.5
Cs ppm	FE	0.046	----	0.035 0.066	---- ----	0.074	----
Rb ppm	S	<0.030	<0.005	<0.030 <0.030	0.007 <0.005	<0.030	0.007
	FE	0.015	----	0.003 0.003	---- ----	0.032	----
Ba ppm	S	0.025	0.023	<0.005 <0.005	0.003 0.004	0.040	0.030
DOC ppm	TCA	----	4.0	---- ----	---- ----	----	4.2

(1) Expressed as mgL^{-1} HCO_3 equivalent.
(2) S = plasma emission spectroscopy (USGS: direct current; SGU: inductively coupled), AA = atomic absorption, F = visible spectrophotometry (ferrozine method), FE = flame emission spectroscopy, ISE = ion-selective electrode, IC = ion chromatography, E = solvent extraction, FAA = flameless atomic absorption, TCA = total carbon analyser, C = colorimetric (Analyses performed by Don Whittemore.).
(3) Values are minimums.
(4) Dissolved organic carbon.
(5) ---- = Not analysed for.
(6) The following elements were found to be below detection limit for all samples (d.l. in ppm) : As (0.003), Be (0.002), Bi (0.080), Cd (0.005), Cr (0.003), Ni (0.004), Pb (0.010), Sb (0.20), Se (0.20), Tl (0.007), V (0.005).

STRIPA PROJECT - PREVIOUSLY PUBLISHED REPORTS

1980

TR 81-01 "Summary of defined programs"
L Carlsson and T Olsson
Geological Survey of Sweden, Uppsala, Sweden

I Neretnieks
Royal Institute of Technology, Stockholm
Sweden

R Pusch
University of Luleå, Sweden

1981

TR 81-02 "Annual Report 1980"
Swedish Nuclear Fuel Supply Co/Division KBS
Stockholm, Sweden, 1981

IR 81-03 "Migration in a single fracture.
Preliminary experiments in Stripa".
Harald Abelin, Ivars Neretnieks
Royal Institute of Technology
Stockholm, Sweden, April 1981

IR 81-04 "Equipment for hydraulic testing"
Lars Jacobsson, Henrik Norlander
Ställbergs Grufve AB
Stripa, Sweden, July 1981

IR 81-05 Part I "Core-logs of borehole Vl down to 505 m"
L Carlsson, V Stejskal
Geological Survey of Sweden, Uppsala, Sweden

T Olsson
K-Konsult, Stockholm, Sweden

Part II "Measurement of triaxial rock stresses in borehole Vl"
L Strindell, M Andersson
Swedish State Power Board, Stockholm, Sweden
July 1981

1982

TR 82-01 "Annual Report 1981"
Swedish Nuclear Fuel Supply Co/Division KBS,
Stockholm, Sweden, February 1982

IR 82-02 "Buffer Mass Test - Data Acquisition and Data Processing Systems"
B Hagvall
University of Luleå, Sweden, August 1982

IR 82-03 "Buffer Mass Test - Software for the Data Acquisition System"
B Hagvall
University of Luleå, Sweden, August 1982

IR 82-04 "Core-logs of the Subhorizontal Boreholes N1 and E1"
L Carlsson, V Stejskal
Geological Survey of Sweden, Uppsala, Sweden

T Olsson
K-Konsult, Engineers and Architects,
Stockholm, Sweden, August 1982

IR 82-05 "Core-logs of the Vertical Borehole V2"
L Carlsson T Eggert B Westlund
Geological Survey of Sweden, Uppsala, Sweden

T Olsson
K-Konsult, Engineers and Architects,
Stockholm, Sweden, August 1982

IR 82-06 "Buffer Mass Test - Buffer Materials"
R Pusch, L Börgesson
University of Luleå, Sweden

J Nilsson
AB Jacobson & Widmark, Luleå, Sweden
August 1982

IR 82-07 "Buffer Mass Test - Rock Drilling and Civil Engineering"
R Pusch
University of Luleå, Sweden

J Nilsson
AB Jacobson & Widmark, Luleå, Sweden
Sept 1982

IR 82-08 "Buffer Mass Test - Predictions of the behaviour of the bentonite-based buffer materials"
L Börgesson
University of Luleå, Sweden
August 1982